PB-228 166

SOME ASPECTS OF ORTHOKINETIC FLOCCULATION

Gordon M. Fair, et al

Harvard University
Cambridge, Massachusetts

9 January 1963

DISTRIBUTED BY:

NTIS
National Technical Information Service
U. S. DEPARTMENT OF COMMERCE
5285 Port Royal Road, Springfield Va. 22151

PB 228 166

Progress Report

U.S.P.H.S. Grant WP-00024

Some Aspects of Orthokinetic Flocculation

Gordon M. Fair, Professor of Sanitary Engineering
and
Robert S. Gemmell, Research Assistant

Division of Engineering and Applied Physics

Harvard University

Period Covered

October 1, 1960 to September 30, 1962

January 9, 1963

Reproduced by
NATIONAL TECHNICAL
INFORMATION SERVICE
U S Department of Commerce
Springfield VA 22151

SUMMARY

Progress Report on U.S.P.H.S. Research Grant WP-00024

Some Aspects of Orthokinetic Flocculation

This report covers experimental work on chemical flocculation that has been in progress since the start of the project on October 1, 1960. The material presented falls into four categories: (1) a review of available literature on flocculation; (2) presentation of a simple mathematical model of flocculation; (3) discussion of results of chemical floc growth studies (including the design of appropriate apparatus); and (4) a report on color and turbidity removal by flocs. Studies of the effect of fluid agitation on biological flocculation have been initiated, but the work has not progressed sufficiently to warrant inclusion at this time.

Generally speaking, the flocculator design parameter Gt, being the non-dimensional product of the temporal mean velocity gradient G and the period of flocculation t, is shown to depend on the number of particles initially present in the system and, hence, on the coagulant dosage used. That it should have an optimal value, or even optimal range of values, which is widely applicable for chemical coagulation of water is, therefore, placed in question. There are reasons to believe that other factors must be considered. Nevertheless, the observed patterns of floc growth indicate that careful investigation of flocculation should provide many insights necessary for optimizing, in an economic sense, the design of coagulation processes.

ACKNOWLEDGMENT

The computations reported in Chapter 3 were done in part at the Computation Center of the Massachusetts Institute of Technology, Cambridge, Massachusetts. Some preliminary investigations on the topics reported here were done by the junior author while he was supported, in part, by a traineeship (59-451) from the Public Health Service.

TABLE OF CONTENTS

Page

SUMMARY ii

ACKNOWLEDGMENT iii

LIST OF FIGURES vii

LIST OF TABLES xi

SYNOPSIS xii

Chapter 1 INTRODUCTION

Surface Chemistry of Colloids 1-3
Flocculation Mechanisms 1-3
Biological Flocculation 1-4
Shift to Chemical Systems 1-5
Idealized Concept of Coagulation 1-5
Approach Used in This Thesis 1-7

Chapter 2 LITERATURE REVIEW

Physical Chemistry of Coagulation 2-1
  Colloid Destabilization 2-1
  Formation of Precipitates 2-4
Kinetics of Flocculation 2-6
  Perikinetic Flocculation 2-6
  Orthokinetic Flocculation 2-13
Application of Orthokinetic Flocculation Concepts to Water Treatment 2-17
  Early Investigations 2-17
  Contributions by Camp 2-21
  Recent Studies 2-26
Summary 2-31

Chapter 3 PARTICLE SIZE STUDIES: MATHEMATICAL MODELS

General Computation Techniques 3-1
Perikinetic Flocculation 3-5
Orthokinetic Flocculation of Monodisperse Systems 3-6
  Breakup 3-6
  Input Variables 3-8
  Selective Contacts 3-12
  Initially Polydisperse Systems 3-12
Summary and Conclusions 3-14

Chapter 4 DESIGN AND CONSTRUCTION OF SHEAR GRADIENT APPARATUS

Hydrodynamics of Flow between Rotating Cylinders......... 4-2
  Equation of Motion.................................... 4-2
  Experimental Confirmation 4-5
  Stability of Flow in Ritchie Apparatus................ 4-7
Design of Test Cells.................................... 4-9
  First Apparatus....................................... 4-9
  Operational Deficiencies.............................. 4-14
  Modified Test Cell.................................... 4-15

Chapter 5 FLOC GROWTH STUDIES

Measurement of Floc Size................................ 5-1
Alternative Size Measures............................... 5-4
Experimental Procedure.................................. 5-4
Experiments Conducted................................... 5-7
Analysis of Floc Pictures....... 5-8
Discussion of Results................................... 5-10
  Flocculation at Different G Values.................... 5-10
  Comparison with Computer Results...................... 5-13
  Effect of Coagulant Dose.............................. 5-15
  Coagulation of Color.................................. 5-16
Conclusions... 5-16

Chapter 6 REMOVAL OF COLOR BY COAGULATION

Experimental Procedures................................. 6-1
  Artificially Colored Water............................ 6-1
  Experimental Technique................................ 6-3
Experimental Results.................................... 6-5
  Coagulation with Iron................................. 6-5
  Coagulation with Alum................................. 6-6
  Color Removal by Preformed Floc....................... 6-8
  Coagulation of Naturally Colored Water................ 6-9
  Coagulation of Turbid Water........................... 6-10
Discussion of Results................................... 6-11

Chapter 7 SUMMARY AND RECOMMENDATIONS

The Smoluchowski Equation for Orthokinetic Flocculation.. 7-1
Results Obtained by a Computer Program.................. 7-2
Kinetics of Flocculation................................ 7-4
Design Criteria... 7-4
Shear Apparatus and Flocculation Measurement............ 7-5
Comparison of Experiment and Mathematical Model......... 7-7
Dosage and Color........................... 7-7
Recommendations for Future Research..................... 7-8

Page

APPENDIX A Notation.................................... A-1

APPENDIX B Bibliography................................ B-1

APPENDIX C Computer Program for Flocculation Equations. C-1

Program Flow Sheets...................... C-2
List of Input Variables.................. C-4
Actual Program in Fortran Mnemonics...... C-6
Sample of Program Output................. C-15

LIST OF FIGURES

Figure	Title	Page
2-1	Change in Number of Particles of Stated Size during Perikinetic Flocculation..................	2-33
2-2	Effect of Heterodispersion on Contact Opportunity in Perikinetic Flocculation.....................	2-33
2-3	Definition Sketches for Orthokinetic Flocculation	2-34
2-4	Momentum Induced Departure of Particle from Streamline..	2-35
3-1	Perikinetic Flocculation: Decrease in Total Number of Particles...............................	3-17
3-2	Perikinetic Flocculation: Increase in Mean Size.	3-18
3-3	Perikinetic Flocculation: Linearizing Plot for Second-Order Decrease in Total Number of Particles	3-18
3-4	Perikinetic Flocculation: Particle Size Distributions for Selected Values of Time..............	3-19
3-5	Orthokinetic Flocculation: Effect of Conjunction and Breakup on Total Number of Particles.........	3-20
3-6	Orthokinetic Flocculation: Effect of Conjunction and Breakup on Floc Growth........................	3-21
3-7	Orthokinetic Flocculation: Particle Size Distributions Obtained with Breakup 1....................	3-22
3-8	Orthokinetic Flocculation: Particle Size Distributions Obtained with Breakup 3..................	3-23
3-9	Orthokinetic Flocculation: Effect of Input Variables on Total Number of Particles...............	3-24
3-10	Orthokinetic Flocculation: Effect of Input Variables on Floc Growth............................	3-25
3-11	Orthokinetic Flocculation: Effect of Selective Combinations on Total Number of Particles........	3-26
3-12	Orthokinetic Flocculation: Effect of Limited Contact Opportunity on Floc Growth..............	3-27

Figure	Title	Page
3-13	Orthokinetic Flocculation: Particle Size Distributions Obtained with Limited Contact Opportunity	3-28
3-14	Orthokinetic Flocculation: Effect of Polydispersion on Floc Growth..................................	3-29
4-1	Shear Apparatus Design Chart......................	4-20
4-2	Schematic Diagram of First Shear Apparatus.......	4-21
4-3	Two Views of First Shear Apparatus...............	4-22
4-4	Velocity Parameter as a Function of Position in Annulus for First Shear Apparatus................	4-23
4-5	Variation in Shear Gradient across Annulus of First Shear Apparatus............................	4-24
4-6	Variation in Centripetal Acceleration Parameter within Annulus of First Shear Apparatus..........	4-24
4-7	Second Shear Apparatus............................	4-25
4-8	Modified Shear Apparatus Design Chart............	4-26
5-1	Typical Floc Pictures, $G = 3.2\ sec^{-1}$, $Fe_2(SO_4)_3 = 1.6x10^{-4}$ mols/liter	5-20
5-2	Typical Floc Pictures, $G = 6.8\ sec^{-1}$, $Fe_2(SO_4)_3 = 1.6x10^{-4}$ mols/liter.................	5-22
5-3	Typical Floc Pictures, $G = 3.2\ sec^{-1}$, $Fe_2(SO_4)_3 = 6.4x10^{-4}$ mols/liter.................	5-23
5-4	Typical Floc Pictures, $G = 3.2\ sec^{-1}$, $Fe_2(SO_4)_3 = 7.5x10^{-4}$ mols/l, Coffee = 38 mg/l...	5-25
5-5	Variation in Mean Floc Size during Flocculation..	5-27
5-6	Dependence of Mean Floc Size on Value of Gt......	5-27
5-7	Variation in Mean Floc Size during Flocculation..	5-28
5-8	Effect of Mean Velocity Gradient on Shear-Controlled sizing of Floc......................	5-29
5-9	Variation in Floc Size Distribution during Flocculation, $G = 3.2\ sec^{-1}$	5-30

Figure	Title	Page
5-10	Variation in Floc Size Distribution during Flocculation, G = 6.8 sec^{-1}......................	5-31
5-11	Orthokinetic Flocculation with Breakup 4: Floc Growth for Untruncated and Truncated Distributions	5-32
5-12	Orthokinetic Flocculation with Breakup 4: Variation in Particle Size Distribution..........	5-33
5-13	Orthokinetic Flocculation with Breakup 4: Variation in Particle Size Distribution..........	5-34
5-14	Effect of Higher Coagulant Dose on Floc Growth at G = 3.2 sec^{-1}	5-35
5-15	Coagulation of Colored Water: Variation in Mean Floc Size during Flocculation at G = 3.2 sec^{-1} ..	5-36
6-1	Spectra of Instant Coffee Solution and Charles River Water at Different pH Values...............	6-13
6-2	Effect of pH on Absorbence of Instant Coffee Solution..	6-14
6-3	Time Stability of Coffee Color at Different pH Values......................................	6-15
6-4	Color Calibration Curves for Instant Coffee at pH = 10.2 and Chloroplatinate Solution...........	6-16
6-5	Effect of G on Rate of Color Removal. Coagulation of Coffee with Ferric Sulfate...................	6-17
6-6	Effect of G on Rate of Color Removal. Flocculation of Ferric Sulfate Alone.......................	6-18
6-7	Effect of G on Rate of Color Removal. Coagulation of Coffee with Alum............................	6-19
6-8	Effect of G on Rate of Color Removal. Coagulation of Coffee with Alum............................	6-19
6-9	Effect of G on Rate of Color Removal. Coagulation of Coffee with Alum Using Second Shear Gradient Apparatus......................................	6-20

Figure	Title	Page
6-10	Effect of G on Rate of Color Removal by Preformed Flocs...	6-21
6-11	Absorbence of Charles River Water upon Dilution..	6-22
6-12	Effect of G on Rate of Color Removal. Coagulation of Naturally Colored Water.......................	6-23
6-13	Absorbence of Turbid Water upon Dilution.........	6-23
6-14	Effect of G on Rate of Turbidity Removal.........	6-24

LIST OF TABLES

Page

Table 2-1 2-25

Dependence of Floc Quality on G and Gt Values Calculated from Data by Leipold.

Table 3-1 3-11

Constancy of the Parameter B = (XKK)(N_0)(T) as Determined from Computer Results.

Table 3-2 3-13

Initial Particle Size Distributions for Orthokinetic Flocculation of Polydisperse Sols

SYNOPSIS

A theoretical base for the effect of fluid velocity gradients on rate of flocculation was laid in 1916 by von Smoluchowski[*] in his equation for orthokinetic flocculation of colloids. Although interest in this equation was revived by Camp's studies[†] of 1943, the equation itself has not found as much use in the management of flocculation processes as it deserves, chiefly because it cannot be solved analytically.

A review of von Smoluchowski's work and that of his successors in this field leads to the conclusion that, in its present form, the equation is an oversimplified mathematical model of flocculation. Nevertheless, the equation does give being to a number of parameters that are of major importance in flocculation performance and is useful for that reason. Moreover, the relative simplicity of its form permits its ready incorporation in a fundamental, even though preliminary, model of floc growth patterns that are traced by chemical coagulation of colored and turbid waters.

Since von Smoluchowski's equation cannot be solved analytically for the relationship between velocity gradient and rate of floc growth, it was one of the purposes of this thesis to obtain numerical solutions for it by means of a high-speed digital computer. For computational purposes, the equation was modified so as to narrow the range of particle sizes that had to be considered. At the same time, a similar

---

[*] von Smoluchowski, M., Drei Vorträge über Diffusion, Brownsche Molekularbewegung und Koagulation von Kolloidteilchen, Physik.Z., 17, 1916, p.557.

[†] Camp, T. R., and Stein, P. C., Velocity Gradients and Internal Work in Fluid Motion, Jour.Bos. Soc. Civil Engrs., 30, 1943, p. 219

modification of von Smoluchowski's equation for perikinetic flocculation was also programmed, primarily for the sake of comparing the results of the modified perikinetic equation with the analytic solution available for its unmodified prototype. Agreement was good, indicating that the modifications introduced did not impair seriously the workings of the formulation.

The computer program was designed to provide information on mean floc size and floc size distribution at designated times in the course of flocculation. Based on the assumption that the particles were spherical, the size measures - diameter, area, and volume - were expressed in units of their respective values for a particle of unit volume, and the relative importance of the following groups of factors affecting the flocculation model were determined: (1) the variables in the von Smoluchowski equation; (2) the mechanism that establishes a floc-size maximum; (3) the restriction of particle contacts in ratio to floc size; and (4) the assumed initial distribution function of particle size.

For an initially monodisperse sol, computations showed that the product of parameters reflecting the velocity gradient, the half-time of flocculation, and the number of particles present at the start of flocculation remains essentially constant. In chemical coagulation, the initial number of particles is a function of coagulant dosage. Hence, the rate at which flocculation in chemical coagulation proceeds, as measured by the half-time of flocculation, must be inversely dependent on the coagulant dose and on the mean velocity gradient. For different floc size limits introduced into the computations, growth patterns proved to be colinear during early flocculation and to depart thence later on only to become asymptotic to their imposed steady-state sizes.

Four procedures of floc breakup or maximum size control were examined computationally. In the first, conjunctions of particles larger than the maximum were automatically returned to their immediately preceding individuality. In the remaining three procedures, oversized conjunctures were split into two, three, or four substantially equisized components. When this was done, floc growth patterns once again proved to be quite similar, except that the steady-state mean size was found to decrease in the order in which the procedures have just been listed. Examination of computed particle size distributions, too, showed that flocs accumulate at size levels depending on the type of imposed breakup. Patterns of floc growth were affected only slightly by the form of imposed distribution graphs for initial particle sizes. However, increased contact opportunity accompanying polydispersion did hasten the rate at which flocculation proceeded.

For comparison of actual floc growth with anticipated theoretical growth, suitable apparatus and techniques for observing and measuring floc growth under controlled conditions of velocity distribution or shear were developed. In the test cell designed, coaxial cylinders enclosed the flocculating liquid in the annulus between them and provided wanted conditions of flow when the outer cylinder was turned at selected rates.

Progress of floc growth was recorded photographically; short-duration flash-lighting was used to "stop" floc motion; and size measurements were made on magnified images of the flocs. The measure of choice was the projected area of floc. To avoid errors in judgment, this was approximated by forming the product of the longest dimension of the floc and the greatest width of the floc perpendicular to the chosen axis.

Growth patterns of floc were recorded for constant mean velocity gradients G of 3.2, 6.8, and 9.3 sec^{-1}. In general, experimental patterns at different G values were quite similar but by no means equal. Observed mean floc size rose sharply at the beginning of flocculation, passed through a mode or maximum, and fell less sharply to an apparently steady-state value. For the coagulant doses used, the modal time, t, expressed in seconds, ranged from 1,500 to 11,000. However, the prominence of the mode was shown to increase with truncation of the floc-size distribution as larger and larger flocs only were included in calculations of the mean. When smaller and smaller floc sizes were added, the curve flattened out. In one instance, the mode vanished altogether. Inverse proportionality between the modal mean floc size and the G value pointed to a reciprocal relationship between fluid shear and shear-controlled sizing.

When the experimental results of this thesis were compared with the results synthesized by the mathematical models, it was discovered that the model in which flocs are assumed to break up into four nearly equi-sized particles appears to simulate the experimental growth patterns with reasonable success. However, a maximum could not be created without truncating* the size distribution of the model. Moreover, the degree of truncation was found to determine the height of the maximum. The synthetic and experimental size distributions resembled one another and so gave added evidence of successful simulation. In agreement with theory, bigger coagulant doses produced rates of growth more or less in keeping with the coagulant concentration.

When water was colored with instant coffee, the rate of floc growth was found to be retarded. Most of the color or turbidity ultimately removed by floc was bound to it within the first five or ten minutes of flocculation. Initial rates of color uptake were somewhat larger at high G values, but final differences in color removal were small. Although the color uptake was not confined exclusively to a 30 sec rapid-mix period, the first few minutes of flocculation saw most of the "ultimate" binding of color to flocs. This lends support to the theory that the primary purpose of flocculation is to promote floc growth and thereby to facilitate sequent separation of flocs from the treated water.

The studies reported in this thesis are exploratory, and many aspects of the work deserve further elaboration and substantiation. Most important among them appear to be the following: (1) determination of the factors controlling floc destruction; (2) description of the dynamics of particle interaction in a moving viscous fluid; (3) elaboration of the mathematical model to include flocculation of non-spherical from

---

* Computations performed after this thesis was written indicate that truncation is not necessary if the breakup procedure and input variables are properly adjusted.

p xv

particles, as well as the formation of spherical and non-spherical agglomerations with or without included water; and (4) definition of the kinetics of floc nucleation and of color or turbidity uptake.

Chapter 1

INTRODUCTION

The term flocculation is widely used to describe the agglomeration of finely divided or colloidal particles suspended in a fluid. The resulting aggregates are called flocs. If they are sufficiently large and heavy, they are no longer kept in suspension by convective currents; instead they settle. Where suspended and normally non-settling material is to be removed from a fluid, therefore, flocculation followed by sedimentation offers an important means of fluid clarification or phase separation. Where, on the other hand, a colloidal suspension is to be kept intact, care must be exercised to prevent flocculation. Whichever purpose is to be served, a knowledge of the factors that govern flocculation is essential.

The removal of colloidal or pseudo-colloidal matters from water is a frequent objective of sanitary engineering practice. Two types of matters may have to be removed(1)*: colloidal suspensions naturally present in the water before treatment and colloidal suspensions issuing from the treatment itself. In natural waters, the colloids vary from clays and organic color (probably humic acid derivatives) to proteins; in chemically coagulated waters, the colloids are commonly hydrous metal oxides by themselves or in conjunction with natural colloids. The importance of separating fine particles or colloids from water depends on the use the water is to serve.

Color or turbidity is removed from domestic water supplies primarily for esthetic[ƒ] reasons, but some benefits may accrue also from their absence in subsequent stages of treatment. For example, such materials often exhibit

---

[*] All references are listed in Appendix B of this thesis.

[ƒ] At the same time, it is recognized that microorganisms attached to particulates will be removed with them.

a buffering capacity that is undesirable if the pH of the water is to be adjusted for reasons such as corrosion control. Industrial consumers may need a clear and colorless water in the manufacture of products such as paper, textiles, foods, and beverages. In the treatment of waste waters, the governing consideration is not only clarification but, commonly in addition, also diminution of the flow of nutrients to the receiving body of water into which the wastes are discharged. Some of these nutrients are finely divided, others in solution.

Flocculation of colored or turbid waters is commonly induced or enhanced through the introduction of coagulating chemicals with or without coagulant aids. The term coagulation then characterizes the entire process of treatment, flocculation being but one step or unit operation in the overall process. In the treatment of waste waters, chemical coagulation, although it improves the efficiency of clarification processes, must compete with biological flocculation. For, biological precipitation as well as biological assimilation by activated-sludge or trickling-filter processes has been generally successful in removing economically those constituents of waste waters that have been considered most detrimental to receiving waters into which the waste waters are emptied. In the past, sedimentation followed by biological flocculation was, indeed, called complete treatment. Today, thought is being given to the addition of a third or further stage of treatment. Called tertiary treatment or water renovation, this stage may well be a chemical or physico-chemical operation for the removal of relatively minute amounts of unwanted organic or inorganic substances. Flocculation may then be of importance, too.

Surface Chemistry of Colloids

Colloids possess a surface charge created either by adsorbed ions or by unsatisfied coordinate relationships in the particle structure. In simple terms, the resulting potential, as a function of distance from the particle, determines the stability of the colloid. However, by itself, the surface chemistry of colloids is not of primary concern in this thesis. In the following chapter, therefore, only those aspects of colloid chemistry which are essential to this investigation will be discussed and then but briefly. Three standard works(2,3,4) on this subject are listed in the references.

Flocculation Mechanisms

Flocculation is said to be either perikinetic or orthokinetic (from peri, meaning near; ortho, meaning proper or correct; and kinetic, meaning of or resulting from motion). These terms are attributed to Wiegner(5) and relate respectively to flocculation caused by Brownian or random motion of the particles within the fluid (perikinetic) and flocculation caused by systematic movements or transport of the particles (orthokinetic) within the fluid. They bear no resemblance to Langelier's later terminology(6) in which the distinction is largely one of surface charge and potential. Since Wiegner's definitions are older and more widely accepted, they are used in this thesis.

The problems of perikinetic flocculation lie largely in the realm of colloid chemistry and hydraulic motions are of small consequence. Orthokinetic flocculation, however, because of its dependence on systematic movement of the particles, admits the possibility of influencing flocculation through motions of the fluid itself and, through it, of the particles. It is this aspect of flocculation that is of immediate concern in this thesis.

Biological Flocculation

The hypothesis on which this research is based is that fluid motion plays an important role in the activated sludge process by controlling floc size, constitution, and activity. The activated sludge process may indeed be described in more general terms as aerobic biological flocculation. Concepts useful in designing chemical flocculation operations should, therefore, be of similar value in the design of the activated sludge process. Moreover, they may resolve otherwise unexplainable conflicts in the literature about the efficacy of different types and rates of aeration.

It was postulated that certain performance parameters of the activated sludge process, particularly those characterizing the floc formed and its effectiveness, could be related to the types of motion generated in the fluid. Among likely parameters are growth rate, constitution, activity, ultimate size, and density. Some shift in the biota of the floc was anticipated.

Essential to this investigation was an apparatus in which well defined, closely controlled, and easily characterizable fluid motions could be induced, the motions simulating as nearly as possible the motions assumed to be of significance in the existing theoretical conceptualization of flocculation and in possible future modifications of flocculation theory.

Shift to Chemical Systems

During the design and construction of the prototype apparatus for biological systems, the authors decided that preliminary investigations of flocculation in chemical systems might provide a useful introduction to basic flocculating phenomena and their measurement. They would avoid the need for maintaining a continuous supply of activated sludge invariant in composition, concentration, and constitution; eliminate the need for oxygenation of the fluid; permit ready preliminary testing of needed apparatus; and expedite, by use of simpler apparatus, possible modification of the test cell. Furthermore, it would be possible to tie observation closer to existing theory. Available information on chemical flocculation, thought to be abundant, would provide useful correlations between the two flocculating systems. Unfortunately, the authors soon found that published data on chemical coagulation are in fact scarce, and that much of the information does not lend itself to analysis in the fashion they desired. Therefore, their initial studies soon suggested that chemical flocculation deserved investigation on its own account. In consequence, they directed their researches to orthokinetic flocculation in chemical systems rather than biological systems.

Idealized Concept of Coagulation

As stated earlier, the term coagulation describes a series of operations that result in the destabilization of a colloid and lead to its removal from the suspending fluid. Ideally, it is possible to distinguish four sequential steps if the primary action of each step is assumed to be unique to it. This assumption will be examined later. The four steps are: (1) dispersion of the coagulant; (2) nucleation; (3) flocculation; and (4) phase separation. As the coagulant is being distributed through the liquid (dispersion), particles are formed by nucleation, either through precipitation, polymerization, or some other mechanism. At the beginning, the particles are small. They populate the initial suspension of flocs and grow or flocculate (flocculation) until they are large enough for efficient separation from the water. By sedimentation or filtration, or both, the flocs eventually are taken from the water (phase separation) carrying with them the suspended or dissolved materials they are intended to remove.

Inclusion of phase separation as a unit operation of coagulation is open to question, because sedimentation and filtration often proceed without coagulation. However, the converse is not true. As a process, coagulation remains incomplete without phase separation.

There is an additional and perhaps more compelling reason for counting phase separation part of coagulation. Within each step, fluid motion is implied either relative to the containing chamber or relative to the particles in the containing liquid or relative to both. The effective fluid motions can be characterized by a mean temporal velocity gradient which, as will be shown in the next chapter, is a basic factor in the theoretical analysis of orthokinetic flocculation. The suggestion is, therefore, that a unifying concept of coagulation, as here portrayed, may be expressed in terms of the optimal values of the mean temporal velocity gradient within the different steps of coagulation, the time during which the water undergoing treatment is subjected to a given gradient, and the relative concentration of flocs and other particles destined for coagulation and phase separation.

Approach Used in This Thesis

Of primary concern in this thesis is the flocculation step. Although perikinetic flocculation does take place immediately following nucleation, the importance of orthokinetic flocculation mounts as the particles grow; it soon becomes dominant. The investigations here reported seek to disclose those avenues of research on the effects of fluid motion on flocculation that might fruitfully be followed. Studies of the variation of floc size with flocculation time and mean velocity gradient within a given coagulation system will be stressed, and the suitability of the idealized concept of coagulation examined. Finally, a theoretical basis for orthokinetic flocculation will be examined, and a mathematical model of flocculation constructed.

That this thesis is exploratory in nature must be emphasized. A number of studies were discontinued although initial results proved promising. This was done, in part, because difficulties encountered, although not insurmountable, could have been resolved only at great expense in time and money. It was thought that other facets of the problem were more interesting and that as many different aspects of flocculation should be studied as possible. A number of areas for future study were disclosed in this way. Some of them, indeed, should of themselves provide good material for other theses.

Chapter 2

LITERATURE REVIEW

Physical Chemistry of Coagulation

Only two aspects of the chemistry of colloids are inherently important to the investigations reported in this thesis: colloid destabilization and the formation of precipitates.

Colloid Destabilization

As mentioned earlier, the charges accumulated on colloidal particles stabilize them. Flocculation is inhibited when the particles have similar charges and repel each other. It is promoted when they have opposite charges and attract each other. Coulombic repulsion decreases rapidly with increasing distance between particles, and van der Waal's attraction increases even more rapidly with decreasing distance. The resultant interactions form a vector field spatially, but not necessarily symmetrically, distributed about the particle.

The energy to move a unit charge from infinity to a specific point on or near the surface of a colloidal particle is a measure of the particle's resistance to flocculation. Unfortunately, its magnitude is not readily found. However, it approximates the energy to move an ion from the bulk of the solution to a specified point at or near the surface of the colloidal particle. This parameter is called the potential of the particle, the name of the potential depending upon the position of the point, or locus of points, to which the ion is transported. Among possible sites of reference, the plane of "shear" has found widest acceptance. It is the locus of points surrounding the particle and separating the water, or solvent, bound to the particle from the water that is free to move with respect to the particle. The potential so referenced is called the zeta potential.

Since the charge on a colloid is determined primarily by ions adsorbed on or included in the structure of the colloid, the decrease of potential with distance from the particle is determined principally by ions in the surrounding solution. These ions screen off the field intensity and reduce it to a negligible quantity within relatively short range. As a result, the resistance of a colloid to flocculation is strongly affected by ion concentration in solution. The effectiveness of the ions, particularly those of opposite charge (counterions), depends to a remarkable extent upon their valence. With increasing valence the concentration of counterions giving equivalent shielding decreases exponentially. This is the well-known Shulze-Hardy rule.

Until recently, chemical studies and interpretations of coagulation have centered on the Shulze-Hardy rule and the "salting out" of colloidal sols. Peterson(7), Bartow(8), Black(9), Theriault(10), Miller(11), and others have contributed to our knowledge of coagulation of natural waters as it is affected by various ions in solution. The references in this chapter open the necessary gateway to the literature for those who would explore these topics more completely.

Evidence that polyvalent metal coagulants do not induce coagulation in the same fashion as other multivalent ions was presented in 1949 by Langelier(12), who showed that clay colloids are coagulated with alum at much lower concentration than expected on the basis of "charge neutralization" by a trivalent ion. He also reported that the "exchange capacity" of the colloidal sol - the susceptivity of the sol to replacement of one type of adsorbed ion by another - is an important factor in determining the required coagulant dosage for coagulation by charge neutralization or by polyvalent metals such as alum. At high exchange capacities the dose for both types of coagulant is found to be the same; whereas at lower exchange capacities the alum dose must be smaller and the salt dose for charge neutralization higher. In explanation, Langelier offered a zone concept of coagulation wherein the ability of the polyvalent metals to provide a binder material for the floc explained the considerably smaller dosage required. Coagulation occuring at this level, Langelier called orthokinetic; high dosage coagulation he called perikinetic.

Langelier's zone concept, elaborated(13) in 1953, found wide acceptance by sanitary engineers. More recently, however, investigators have concluded that this explanation is inadequate if not entirely erroneous. Thus, Stumm and Morgan(14) have shown that the zone effect is produced by improper control of pH and alkalinity and that at the pH of precipitation (nucleation) the average charge of the aluminum species in solution, per atom of aluminum, is at most monopositive, not tripositive as commonly assumed. They have reported also that complexes formed between the polyvalent metal ions and ionizable functional groups, e.g., hydroxyl, carboxylic, and phosphato-groups, contained in the colloids or in the water may account for the usefulness of these ions as coagulants.

Clearly, the mechanisms by which coagulants really act remain to be resolved. A combination of charge neutralization and complex formation should account for most of the action since the complex ions formed by the coagulant may have large valences even though the average charge per metal atom is small.

Formation of Precipitates

According to the concept of coagulation proposed in the introductory chapter of this thesis, essentially all of the chemical reactions are confined to the nucleation phase. During nucleation, the first insoluble precipitates are formed. They comprise, therefore, the initial population of flocs. A knowledge of the characteristics of these particles would improve our understanding of the physical process of flocculation. Unfortunately, needed information is sparse, but the articles reviewed in this chapter give some clues to the formation mechanism.

Stumm and Morgan(14), summarizing the results of others, report that the acid characteristics of hydrated iron and aluminum ions lead to the formation of polyhydroxide complexes which tend to polymerize and form first colloidal hydroxo polymers and eventually hydrous oxide precipitates. Chemical reaction schemes are contained in the paper. The polymerization mechanism is essentially one of successive hydrolysis (olation) and dehydration (oxolation). The extent to which such reactions proceed is highly pH dependent.

In a paper entitled "The World of Fine Particles," Turkevich(15) discusses the formation of colloidal particles in gaseous media as follows:

> "The mechanism of smoke production involves three steps, nuclei formation from vaporized atoms, growth of these nuclei into particles and the coagulation of the particles into filamentous aggregates."
>
> "Pure materials do not seem to grow readily in the gas phase and this may be due to the perfection of the nuclei formed from pure materials. Only when fine particles have imperfections, chemical or physical, is there a driving force for growth."
>
> "Thus, in the preparation of the plates of aluminum oxide monohydrate, the following steps can be distinguished by electron microscope examination. The first product of the interaction of the aluminum ion with the hydroxyl is the formation of small granules of aluminum hydroxide. These granules soon aggregate to form flexible chains. These grow in length, developing lateral forces. If the latter are strongly developed, the fibers line up forming a platelike crystal. If, on the other hand, the lateral forces are not strongly developed, a gel will result with a structure similar to that of a pile of randomly oriented match sticks. .... The detailed mechanism of the formation of fine particles in solution remains to be worked out. .... The formation of large particles is not a random process but follows certain laws which cannot readily be deduced."
>
> ".... If the nucleation takes place rapidly, stops, and then is followed by growth without aggregation, the particles will be of uniform size. If .... the nucleation, growth, and aggregation take place simultaneously, there will be in the resultant particles a large distribution in size and a great variety in the shape."

Baylis(16),at the 1961 Rudolphs Memorial Conference, reported that electron micrographs of alum floc show a filamentous random-coil structure. This is similar to the description of Turkevich of floc formation in which the lateral forces are not strongly developed. A gel type structure is commonly observed in water treatment practice.

In summary, the coagulation of colloids commonly found in natural waters appears to be accomplished partially by neutralization of the charge on the colloidal particle and partially by complex formation between the coagulant and the colloidal sol. There may be some adsorption of dissolved material and entrapment of the colloidal particles, but detailed evidence seems to be lacking. The precipitates formed during nucleation are probably filamentous complex-polymers arranged in a random coil. The kinetic aspects of nucleation for polyvalent metal ion coagulants are yet to be studied successfully.

KINETICS OF FLOCCULATION

Keeping in mind the conceptual subdivision of the coagulation process into discrete steps, operations, or regimes, and the assumption that essentially all chemical reactions are completed during nucleation, let us consider the mechanisms by which nuclei grow into particles sufficiently large for phase separation, e.g., sedimentation or filtration. The pertinent equational relationships can be developed from the large amount of information in the literature on simple colloid systems. In the following section of this chapter, liberal use has been made of Overbeek's presentation of this subject in his "Kinetics of Flocculation."(17)

Perikinetic Flocculation

For a colloid sol in which forces of repulsion between particles may be neglected - when, for example, an excess of electrolyte is present - von Smoluchowski(18,19) suggested in 1916 that, under steady state conditions, the number of particles diffusing radially into a sphere centered on a stationary particle must be constant and equal to the number of particles colliding with the central one. In terms of Fick's first diffusion equation, therefore,

$$I = 4\pi Dr^2 \frac{\partial n}{\partial r}$$

where I is the number of collisions per unit time, D the diffusion constant of the particles, r the distance from the origin, and n the number of particles per unit volume. Solving for the limits $n = 0$ when $r = R$, and $n = N$ when $r = \infty$, where N is the concentration of particles and R the distance between centers of two particles forming a lasting contact, $I = 4\pi DRN$; and if the central particle is also subject to diffusion, $D = D_1 + D_2$ where D_1 and D_2 are the diffusion coefficients of two particles of different size. But since there are N such central particles per unit volume, $I = 4\pi DRN^2$, and the number of collisions between particles of sizes i and j is generally:

$$I_{ij} = 4\pi D_{ij} R_{ij} n_i n_j \qquad (2\text{-}1)$$

where R_{ij} is approximately equal to the sum of the radii of the individual particles and D_{ij} is the sum of their individual diffusion coefficients. If a particle of size i conjoins with one of size j to form one of size k, therefore, the rate of change in particle numbers is

$$\frac{dn_k}{dt} = \frac{1}{2} \sum_{\substack{i=1 \\ j=k-i}}^{k-1} 4\pi D_{ij} R_{ij} n_i n_j - n_k \sum_{i=1}^{\infty} 4\pi D_{ik} R_{ik} n_i \qquad (2\text{-}2)$$

where the first summation gives the time rate of formation of particles of size k, and the second the number of size k that grow into larger ones.

If the radius of interaction R_{ij} is assumed to be exactly the sum of the radii of the interacting particles $r_i + r_j$, and the combined diffusion coefficient D_{ij} equals $D_i + D_j$, the probability of collision $D_{ij}R_{ij}$ may be written

$$D_{ij}R_{ij} = (D_i + D_j)(r_i + r_j) \qquad (2\text{-}3)$$

Since the diffusion coefficient varies inversely with particle size,

$D = \frac{K}{r}$, and equation (2-3) may be rewritten

$$D_{ij}R_{ij} = \left(\frac{K}{r_i} + \frac{K}{r_j}\right)(r_i + r_j) = D_1 r_1 \left(\frac{1}{r_i} + \frac{1}{r_j}\right)(r_i + r_j) ,$$

or

$$D_{ij}R_{ij} = D_1 r_1 \left(2 + \frac{r_i}{r_j} + \frac{r_j}{r_i}\right) \qquad (2\text{-}4)$$

When r_i and r_j are closely equal,

$$D_{ij}R_{ij} \doteq 4\ D_1 r_1 \doteq 2\ D_1 R \qquad (2\text{-}5)$$

where $R \doteq 2\ r_1$.

By substituting equation (2-5) in equation (2-2), von Smoluchowski made use of this simplification to arrive at the following analytic solution for the rate of flocculation:

$$\frac{dn_k}{dt} = 4\pi D_1 R \left[\sum_{\substack{i=1 \\ j=k-i}}^{k-1} n_i n_j - 2n_k \sum_{i=1}^{\infty} n_i \right] \qquad (2\text{-}6)$$

The rate of change of the total number of particles, irrespective of their size, then becomes

$$\frac{d\sum_{k=1}^{\infty} n_k}{dt} = 4\pi D_1 R \left[\sum_{i=1}^{\infty} \sum_{j=1}^{\infty} n_i n_j - 2 \sum_{k=1}^{\infty} \sum_{i=1}^{\infty} n_k n_i \right]$$

$$= -4\pi D_1 R \sum_{i=1}^{\infty} \sum_{j=1}^{\infty} n_i n_j = -4\pi D_1 R \left(\sum_{k=1}^{\infty} n_k\right)^2 \qquad (2\text{-}7)$$

Here the consideration of all possible combinations removes the summation restriction on the index j. The rate of change of the total number of particles is of second order, and integration for the initial conditions $n = N_o$ when $t = t_o$ and $n_{(j+1)} = 0$ when $t = t_o$ for all values of j can be accomplished. Accordingly, if N_t is the total number of particles at time t,

$$N_t = (\sum_{k=1}^{\infty} n_k)$$

or $$\int_{N_o}^{N_t} \frac{dN_t}{(N_t)^2} = -4\pi D_1 R \int_{o}^{t} dt$$

It follows that $\frac{1}{N_o} - \frac{1}{N_t} = -4\pi D_1 Rt$

whence $$\frac{N_t}{N_o} = \frac{1}{1+4\pi D_1 RN_o t} \qquad (2\text{-}8)$$

The time required for the number of particles to be halved ($N_t/N_o = 1/2$) then becomes:

$$T = \frac{1}{4\pi D_1 RN_o} \qquad (2\text{-}9)$$

where T is called the time of flocculation. Use of the half-life concept permits the simplification of equation (2-8) to

$$\sum_{k=1}^{\infty} n_k = N_t = \frac{N_o}{1+\frac{t}{T}}$$

or $$\frac{N_t}{N_o} = \frac{1}{1+\frac{t}{T}} \qquad (2\text{-}10)$$

By means of equations (2-6) and (2-10), the time dependence of the number of particles of size k may now be determined for successive values of k as:

$$\frac{d\left(\frac{n_k}{N_o}\right)}{dt} = \frac{1}{T(N_o)^2}\left[\sum_{i=1}^{k-1} n_i n_{(k-i)} - 2n_k \sum_{i=1}^{\infty} n_i\right]$$

and for k=1,
$$\frac{d\left(\frac{n_1}{N_o}\right)}{dt} = \frac{1}{T(N_o)^2}\left[\sum_{i=1}^{o} n_i n_{(1-i)} - 2n_1 \sum_{i=1}^{\infty} n_i\right]$$

$$= -\frac{2\,n_1}{T(N_o)^2}\sum_{i=1}^{\infty} n_i = -\frac{2\,n_1}{T(N_o)^2}\left(\frac{N_o}{1+\frac{t}{T}}\right)$$

It should be noted that $n_o = 0$ and $\sum_{i=1}^{\infty} n_i = \sum_{k=1}^{\infty} n_k = N_t$.

By integration, therefore,

$$\int_1^{\left(\frac{n_1}{N_o}\right)} \frac{d\left(\frac{n_1}{N_o}\right)}{\left(\frac{n_1}{N_o}\right)} = -2\int_0^t \frac{dt}{T\left(1+\frac{t}{T}\right)} = -2\int_0^t \frac{dt}{(T+t)}$$

and
$$\frac{n_1}{N_o} = \left(\frac{T+t}{T}\right)^{-2} = \frac{1}{\left(1+\frac{t}{T}\right)^2} \qquad (2\text{-}11)$$

For k = 2 and initial conditions $n_2/N_o = 0$ when $t = 0$, furthermore:

$$\frac{d\left(\frac{n_2}{N_o}\right)}{dt} = \frac{1}{TN_o^2}\left[\sum_{i=1}^{1} n_i n_{(2-i)} - 2n_2 \sum_{i=1}^{\infty} n_i\right]$$

$$= \frac{1}{TN_o^2}\left[n_1^2 - 2\,n_2 N_t\right]$$

$$= \frac{1}{TN_o^2}\left[\frac{N_o^2}{\left(1+\frac{t}{T}\right)^4} - 2\,\frac{n_2 N_o}{\left(1+\frac{t}{T}\right)}\right]$$

or
$$\frac{d\left(\frac{n_2}{N_o}\right)}{dt} + \frac{2(n_2/N_o)}{T\left(1+\frac{t}{T}\right)} = \frac{1}{T\left(1+\frac{t}{T}\right)^4}$$

and
$$\frac{n_2}{N_o} = \frac{(\frac{t}{T})}{(1 + \frac{t}{T})^3} \qquad (2\text{-}12)$$

The general solution is:
$$\frac{n_k}{N_o} = \frac{(\frac{t}{T})^{k-1}}{(1 + \frac{t}{T})^{k+1}}. \qquad (2\text{-}13)$$

Figure 2-1 depicts these equations graphically.*

The proportion of particles of size k existing at a given time may be found from equations (2-10) and (2-13) as
$$\frac{n_k}{N_t} = \frac{(\frac{t}{T})^{k-1}}{(1+\frac{t}{T})^k} = \frac{T}{t} (\frac{t}{T + t})^k \qquad (2\text{-}14)$$

and the time of flocculation may be evaluated by utilizing the Einstein equation for the diffusion coefficient $D_1 = K_B(\text{Temp})/(6\pi\mu r_1)$, where K_B = Boltzman constant = 1.38×10^{-16} erg per degree, Temp = temperature in degrees Kelvin, and μ = viscosity of dispersing medium, gram per cm. sec, as $T = 3\mu/[4\ K_B(\text{Temp})N_o]$. For water at 20 C (293 K) as the dispersing medium,
$$T = \frac{3x1.01x10^{-2}}{4x293x1.38x10^{-16}N_o} \div \frac{2x10^{11}}{N_o} \qquad (2\text{-}15)$$

measurements of T varying from one second to one minute being common(17) in most experimental studies of rapid flocculation.

Slow flocculation occurs when the repulsion forces of the colloid have not been completely repressed (as was the case previously). This phenomenon has also been analyzed by von Smoluchowski, who asserted that the equations useful in analyzing rapid flocculation become valid for slow flocculation if the time of flocculation T is corrected by a constant α representing the fraction of collisions leading to a lasting combination. Accordingly,

---

*Throughout this thesis, figures are placed at the end of each chapter.

$$T = \frac{1}{4\pi D_1 R N_o \alpha} \tag{2-16}$$

The formulation of von Smoluchowski for rapid flocculation agrees satisfactorily with experimental studies(17), but his analysis of slow flocculation as a uniform retardation of rapid flocculation is less successful. In some experiments the analysis seems to hold rather well; in others, it fails completely. Moreover, there is, as yet, no theory for relating the coefficient α to the electrical or chemical properties of the sol. Fuchs(20) has made a more complex analysis of slow flocculation, but its application is limited because of difficulties in the numerical evaluation of his equations.

In 1926, Müller (21,22) extended the von Smoluchowski theory to heterodispersed sols by showing that the value of $D_{ij}R_{ij}$ is always greater than 4 D_1r_1 for $r_i \neq r_j$, i.e., that collision of particles equal in size is less frequent than collision of particles unequal in size. Examination of equation (2-4) shows this to be indeed true. The relationship is

$$D_1r_1\left(2 + \frac{r_i}{r_j} + \frac{r_j}{r_i}\right) = D_1r_1 \left\{4 + \left[\sqrt{\frac{r_i}{r_j}} - \sqrt{\frac{r_j}{r_i}}\right]^2\right\} \tag{2-17}$$

However, a tenfold difference in radii only produces a threefold difference in collision frequency (see Figure 2-2).

From equation (2-14), the ratio of the number of particles of size k to the number of unit size is

$$\frac{n_k}{n_1} = \left(\frac{t}{T + t}\right)^{k-1} \tag{2-18}$$

and if k is assumed to represent the volume of a floc formed by the conjunction of a particle of volume i with one of volume j or k = i + j, r_k is proportion to $k^{1/3}$, at least for spherical particles, and for $r_k/r_1 = 10$, k = 1000. Unless t is much larger than T, therefore, the ratio n_k/n_1 must be very small, and the enhanced frequency of collision is not likely to disturb the rate of flocculation appreciably.

For an initially bi-disperse sol in which the two particle sizes differ widely, the Müller effect is pronounced (see Figure 2-3). Sanitary engineers have often put the Müller effect to good use (perhaps unwittingly) by introducing clays and colloidal silicates into water as coagulant aids for color or turbidity removal.

Orthokinetic Flocculation

That agitation improves the rate of flocculation has been known for years. A similar effect has been reported for centrifuging. A theory accounting for this improvement was proposed by von Smoluchowski(19) in 1917. His analysis is examined in the following paragraphs.

Assume that a particle of size j is located in a laminar flow-field with a velocity gradient du/dz, that the particle center is the origin of a Cartesian system of coordinates, and that u is the fluid velocity in direction X. Then for a particle of size i to conjoin with the central particle, it must be brought sufficiently close for van der Waal's forces of attraction to induce collision. The locus of particle i satisfying this requirement is a sphere centered on the origin and of radius R_{ij}, where $R_{ij} = r_i + r_j$ and r_i and r_j are the radii of spheres defining the range of attraction of van der Waal's forces for the individual particles. The number of i-particles contacting the central j-particle is therefore equal to the number of such particles moving into a sphere of radius R_{ij} surrounding the j-particle. If the particles are assumed to follow the streamlines that would exist in the fluid in the absence of particles, their number would equal the product of the rate of fluid flow q into the sphere and the number of i-particles per unit volume of fluid (see Figure 2-3), or

$$dq = \left(z \frac{du}{dz}\right)\left(2 \sqrt{R_{ij}^2 - z^2}\right) dz \qquad (2\text{-}19)$$

It follows that, for n_i i-particles per unit volume, the number J_i of contacts of i-particles with the central j-particle per unit time and volume is

$$J_i = \int_A n_i dq = 2n_i \int_{z=0}^{R_{ij}} \left(z \frac{du}{dz}\right)\left(2 \sqrt{R_{ij}^2 - z^2}\right) dz$$

If du/dz is constant over the range of integration,

$$J = 4\, n_i \frac{du}{dz} \int_0^{R_{ij}} z \sqrt{R_{ij}^2 - z^2}\, dz \qquad (2\text{-}20)$$

$$= \frac{4}{3}\, n_i \frac{du}{dz} R_{ij}^3 \qquad (2\text{-}21)$$

For n_j central particles per unit volume, therefore,

$$J_{ij} = \frac{4}{3} n_i n_j R_{ij}^{\ 3} \frac{du}{dz} \tag{2-22}$$

and, approximating R_{ij} by the sum of the particle radii $(r_i + r_j)$,

$$J_{ij} = \frac{4}{3} n_i n_j (r_i + r_j)^3 \frac{du}{dz} = \frac{1}{6} n_i n_j (d_i + d_j)^3 \frac{du}{dz} \tag{2-23}$$

where $d_i = 2\ r_i$, etc. The rate of change of the number of k-particles may then be written as:

$$\begin{aligned} \frac{dn_k}{dt} &= \frac{1}{2} \sum_{\substack{i=1 \\ j=k-i}}^{k-1} \frac{4}{3}\ n_i n_j (r_i + r_j)^3 \frac{du}{dz} - n_k \sum_{i=1}^{\infty} \frac{4}{3} n_i (r_i + r_k)^3 \frac{du}{dz} \\ &= \frac{2}{3} \frac{du}{dz} \left[\sum_{\substack{i=1 \\ j=k-i}}^{k-1} n_i n_j (r_i + r_j)^3 - 2\ n_k \sum_{i=1}^{\infty} n_i (r_i + r_k)^3 \right] \end{aligned} \tag{2-24}$$

Further analytical treatment does not seem feasible at present.

If the velocity gradient is not constant throughout the volume of the colloidal suspension, the local rates of flocculation must be averaged. As discussed later, Camp(35) has suggested how to do this for the entire volume of fluid.

According to von Smoluchowski, perikinetic and orthokinetic flocculation can be compared in terms of the number of collisions per unit time and volume. From equations (2-1) and (2-22), the ratio of collision rates is

$$\frac{J_{ij}}{I_{ij}} = \frac{\frac{4}{3}\ n_i n_j R_{ij}^{\ 3} \frac{du}{dz}}{4\pi n_i n_j D_{ij} R_{ij}} = \frac{(R_{ij})^2 \frac{du}{dz}}{3\pi D_{ij}} \tag{2-25}$$

Introducing the Einstein equation for the diffusion coefficient and the earlier approximation $D_{ij}R_{ij} = 4\, D_1 r_1 = 2\, K_B(\mathrm{Temp})/(3\pi\mu)$, this ratio becomes

$$\frac{J_{ij}}{I_{ij}} = \frac{\mu (R_{ij})^3 \frac{du}{dz}}{2K_B(\mathrm{Temp})} \qquad (2\text{-}26)$$

and for $du/dz = 1\ \mathrm{sec}^{-1}$ and a water temperature of 20 C,

$$\frac{J_{ij}}{I_{ij}} = \frac{1.01\mathrm{x}10^{-2}(R_{ij})^3}{2\mathrm{x}293\mathrm{x}1.38\mathrm{x}10^{-16}} = 1.25\mathrm{x}10^{11}(R_{ij})^3$$

For $J_{ij} = I_{ij}$, $R_{ij} \doteq 2\mathrm{x}10^{-4}$ cm, i.e., orthokinetic and perikinetic flocculation proceed at equal rates when the radius of interaction is two microns. However, when R_{ij} = 10 microns, the rate of orthokinetic flocculation is more than 100 times the rate of perikinetic flocculation. It follows that perikinetic flocculation is probably rate-controlling during early flocculation, e.g., before the first appearance of visible floc, but orthokinetic flocculation soon becomes dominant in determining the rate of agglomeration.

Tuorila(5) and Müller(23) have extended von Smoluchowski's analysis to include flocculation during sedimentation. Here, differences in the settling velocities of particles are the velocity gradients. By allowing for the curvature of streamlines in the vicinity of a particle, Müller arrives at a differential equation that is hopelessly complex. Simplifying it to obtain a workable solution, his equation becomes similar to von Smoluchowski's. However, Müller reports that sedimentation effects are significant only within a limited range of particle sizes. More specifically, the larger particle must have a radius

$$r \geq \left[\frac{40\ K_B\mathrm{Temp}}{\pi\ g\ \rho}\right]^{1/4} \qquad (2\text{-}27)$$

where r is the particle radius, ρ the particle density, and g the acceleration by gravity, and the smaller particle a radius

$$r \geq \left[\frac{1.2\ K_B\mathrm{Temp}}{\pi\ g\ \rho}\right]^{1/4} \qquad (2\text{-}28)$$

The size of the smaller particle is limited by its susceptibility to Brownian motion; that of the larger by the requirement of an appreciable differential in settling velocity. At a reported(24) minimum specific gravity of 1.002 for iron flocs, and a water temperature of 20 C, for example, the minimal particle radii are 150 μ (large) and 62 μ (small).

Application of Orthokinetic Flocculation Concepts to Water Treatment

Early Investigations

The inherent importance of agitation in chemical coagulation of turbid or colored water was first recognized by Langelier(25). Writing about the design of the Sacramento, California, water treatment plant, he told of bench-scale flocculation of suspensions by mechanical mixing. Although his results were not rigorously quantitative, they did suggest a peripheral paddle speed of 1.5 fps as optimal for floc growth. Stirring for 20 minutes produced an excellent floc; for 15 minutes a good floc. Accordingly, Langelier is generally credited with introducing machine stirring into jar-test experiments (see Black(26)).

In the Sacramento design mixing speeds decreased progressively in four series-operated flocculation tanks. According to Hyde[27], who designed the plant together with Langelier, the mean rotational velocities of the water masses in the tanks were 2.0, 1.5, 1.0, and 0.5 fps and the associated mean temporal velocity gradients, G, can be estimated from the design data as 200, 130, 70,and 25 sec^{-1} respectively. Quoting Hyde, "large, dense, rapidly settling flocs" were produced "from sulfate of alumina syrup", and the following conclusions, with estimated values of G added as a matter of interest, were drawn by him from studies and experiments for 1919-1921:

"1. Mean rotative water velocities ranging from 1.5 to 2.0 fps ($G =$ 130 to 200 sec^{-1}) in the first or primary tank of a series are valuable in causing a rapid mixing of coagulant and water in starting flocculation.

2. Mean rotational velocities much greater than 1.5 fps ($G = 130$ sec^{-1}) if prolonged, have a tendency to reduce, rather than increase, floc sizes (with sulfate of alumina as coagulant).

3. Velocities lower than 0.5 fps ($G = 25$ sec^{-1}) are not highly effective in producing satisfactory floc masses.

4. With a number of tanks in series, a progressive decrease in mean rotational velocity from the first to the last tank produces the best results, judged by the criteria stated above. [The criteria of a good floc are size, specific density, and toughness, all tending to produce a rapid subsidence and a satisfactory degree of clarification, preparatory, in the normal case, to rapid sand filtration.]

5. A theoretical flowing-through period of 40 min at the rated capacity of a typical rapid sand filter plant (125 mil gal per acre per 24 hr) is highly satisfactory with tanks carefully designed to reduce short-circuiting.

6. The subsiding velocity of good floc is about 0.1 fps."

In 1930, Fleming(28) and two years later Wilcomb(29) suggested a sequential coagulation process with mixing as the first step and conditioning as the second. As conceived by them, the function of mixing was the dispersal of the coagulant; that of conditioning, the agglomeration of particles preparatory to sedimentation and filtration. According to Willcomb, the colloidal floc particles formed "almost instantaneously." Hence, nucleation occurred within the mixing phase. About conditioning, he said: "The problem involved is to increase the size of the particles by accretion and this is best brought about by beating them together."

In 1933, Nolte and Kramer(30) reported that paddle velocities of 0.5 to 1.5 fps (measured at two-thirds the distance from the axis to the tip of the blade) were optimal for flocculation of turbid water, and that velocities either lower (0.15 fps) or higher (3 fps) than this were unsatisfactory; that 30 min of flocculation was generally as satisfactory as 60 min at most paddle speeds; and that the longer flocculation time was detrimental at 1.5 fps because of particle breakup. Other findings were that reducing the paddle speed during flocculation did not give better results than maintaining the same paddle speed within the optimal range for the same flocculation time; and that in split treatment, in which the coagulant was added to one-half the water and kept from the other half until it had been agitated enough to form floc, these preformed flocs were not effective in removing turbidity. They also found that inadequate coagulant dosage could not be offset by increased time of flocculation, but that a slow paddle speed for a long flocculation time was nearly as effective as a high paddle speed for a short flocculation time. More specifically, they concluded that a paddle speed of 0.15 fps for 120 min produced much the same results as a paddle speed of 1.0 fps for 15 min. Assuming that the mean temporal velocity gradient (G) is proportional to the three-halves power of the paddle velocity and expressing the time (t) in seconds, the non-dimensional product Gt will be seen to be of the same order of magnitude for the two conditions of operation.

In studying the effects of mechanical agitation by paddles at three different shaft speeds, Leipold(31) varied the size and placement of the paddles and observed the quality of the floc produced when a turbid solution was flocculated with alum for various periods of time. He concluded, in 1934, that required flocculation time was not much affected by paddle location, but greatly so by paddle dimensions relative to the dimensions of the mixing vessel. His general conclusions may be summarized as follows:

1. The controlling parameters in paddle design are paddle area per unit water volume, paddle length per unit vessel diameter, and paddle speed in terms of peripheral velocity;
2. it is possible to compensate for low paddle speeds and/or small paddle areas by increasing the time of flocculation; and
3. high paddle peripheral speeds tend to break up floc.*

---

* Leipold's data can be analyzed by Camp's methods (see later), and this is done following the discussion of Camp's work.

In 1934, Dempster(32), and five years later Dennis(33), noted that flocs did not break up significantly in passing through the orifices of stilling walls in sedimentation basins provided that the velocities were less than 1.5 fps, thus corroborating what has already been said about peripheral paddle velocities.

Contributions by Camp

In 1940, Camp(34) published the first of several important papers on coagulation reporting, with Root and Bhoota, studies on the effect of temperature on rate of floc formation. The principal conclusion was that temperature was not significant so long as coagulation was performed at optimum pH. It was postulated that coagulation proceeds in three stages: (1) formation of molecular precipitates; (2) formation of colloidal floc particles; and (3) growth of colloidal floc particles to a size satisfactory for sedimentation. Relating these stages to the conceptual operations in coagulation presented earlier, the first stage corresponds to nucleation; the second to perikinetic flocculation; and the third to orthokinetic flocculation.

A second paper, published in 1943 by Camp and Stein(35), introduced the concepts of von Smoluchowski and Tuorila. Although there is no reference to von Smoluchowski's work, his paper is listed (in different context,to be sure) in Camp's publication of 1940. The primary contribution of the 1943 paper is the replacement of von Smoluchowski's local velocity gradient (du/dz) by the mean temporal velocity gradient (G), approximately equal to the rate of energy dissipation per unit volume of flocculating suspension. Several equations for estimating G in different types of mixing basins are proposed, the one for paddle flocculators being:

$$G = \left[\frac{C_d A_p V^3}{2 \nu \text{V}}\right]^{1/2} \qquad (2\text{-}29)$$

where G is the mean temporal velocity gradient (normally $\sec^{-1}$), C_d the coefficient of drag of paddles, A_p the area of paddle blades, V the velocity of paddles relative to the water, ν the kinematic viscosity of water, and V the volume of the flocculation tank.

In 1946, Camp dealt with the topic "Sedimentation and the Design of Settling Tanks."(36) The sections on flocculation and flocculent suspensions are of particular interest here, and are quoted at length.

> (Page 921) "The particles of flocculent suspensions are fragile and subject to rupture by shear, the shearing strength being less as the particle size increases. Although velocity gradients in the fluid bring small particles together to form larger ones, it is evident that there is a limiting size of particle which is determined by the mean shearing force and the strength of the floc. Since the mean shearing force is proportional to the mean velocity gradient, there is a limiting size corresponding to each value of the mean velocity gradient G; and the size is greater the smaller the velocity gradient."
>
> (Page 922) "In studying the flocculation and settling of iron floc in battery jars, Darrell A. Root found that, with a total time of mixing and quiescent settling in excess of 75 minutes any increase in mixing time at the expense of settling time up to 60 minutes would improve the settling."
>
> (Page 929) "......the magnitude of the optimum velocity gradient G_o is of great influence on the type of [sedimentation] tank required for economy."
>
> (Page 930) "There is a dearth of experimental data concerning the optimum values of G for the suspensions encountered in practice. .....Reporting on a tunnel section with a flow velocity of 12 ft per min, W. F. Langelier (J.A.W.W.A., 22, p. 1484) stated that settling had been unusually effective in removing turbidity and color from alum-coagulated water. .....The value of G for Langelier's Tunnel....is 0.96 $\sec^{-1}$. Similar computations for

baffled mixing chambers reveal that good floc is produced at values of G as high as 25 $\sec^{-1}$. Hence the value of G_o for alum and iron oxide floc is probably much higher than 1 $\sec^{-1}$. The estimated value of G in the pore constrictions of a rapid sand filter during normal operating conditions is from 200 $\sec^{-1}$ to 400 $\sec^{-1}$. This is too high to promote further coagulation of the fine floc particles within the bed, according to an unpublished paper on microscopic studies by P. C. Stein, ..., but it is obviously not high enough to prevent the floc from sticking to the sand grains. The estimated value of G in the pore constrictions of slow sand filters is from 5 $\sec^{-1}$ to 40 $\sec^{-1}$."

A final paper in this series, entitled "Flocculation and Flocculation Basins"(37) was published in 1955. It summarizes the earlier work and gives additional formulas for estimating G for different flocculation systems, the following equation for multibladed paddle units being an elaboration of equation (2-29):

$$G = \left[\frac{239\ C_d(1-k)^3 S^3 \Sigma\ A r^3}{\mu\ V}\right]^{1/2} \qquad (2\text{-}30)$$

where for G in $\sec^{-1}$, S is the shaft speeds in rps, k the ratio of water speed to shaft speed, A the area of individual paddle blade in ft^2, r the radius to areal centroid of individual paddle in ft, and μ the absolute viscosity of water in lb sec/ft^2.

Most important is the summary of plant operating data for which values of G and Gt were estimated by his equations. Since he used design flows, the values obtained are maximal rather than optimal at 20 $\sec^{-1}$ to 74 $\sec^{-1}$ for G and 2.3×10^4 to 2.1×10^5 for Gt.

In the flocculators at the Cambridge, Massachusetts, water plant, designed and tested by Camp, the mean temporal velocity gradients are:

Final compartment	5 $\sec^{-1}$ (winter) to 7.6 $\sec^{-1}$ (summer)
First compartment	5.6 x final compartment
Second compartment	3.8 x final compartment
Third compartment	1.9 x final compartment

No flocculation times are recorded and observed water speeds suggest that the ratio of water to paddle speed is not constant. Instead it varies from 24 per cent in the high-speed to 32 per cent in the low-speed compartment. Hence, the velocity of the paddles relative to the water rises from 68 to 76 per cent of the paddle speed, while stators diminish the rolling motion of the water.

G values for Leipold's(31) bench studies are shown in Table 2-1. They are based on equation (2-29) and the following assumptions: (1) $C_d = 1.8$; (2) $V = 0.5 \times$ paddle peripheral speed; and (3) Temp = 40 F (average for Leipold's work). Although they may not be fully representative of plant conditions, the range of G values in Table 2-1A is in general agreement with Camp's magnitudes. The Gt values for excellent floc formation fall into the lower portion of his range which, as previously suggested, tends to be maximal. At the same time, there appears to be some dependence on input shaft speed that is not accounted for.

Turning to Table 2-1B, the estimated ratios of Gt for specific floc qualities at constant shaft speeds are seen to be essentially alike for a given quality and hence independent of input shaft speed. In Table 2-1C, the estimated ratios of Gt for specific input shaft speeds at constant floc qualities, too, are essentially alike and hence independent of shaft speed. It follows that input shaft speed is not properly accounted for in the calculations. Most likely is the inaccurate estimation of k, the ratio of the paddle to the water speed, which according to Camp tends to decrease with increasing shaft speeds.

TABLE 2-1

Dependence of Floc Quality on G and Gt Values

Calculated from Data by Leipold(31)

G = mean temporal velocity gradient, sec^{-1}
t = flocculation time, sec

A. Estimated values of Gt and observed floc qualities for specific shaft speeds.

Average of 4 to 7 values per entry

Shaft speed (rpm)	Range of G (sec^{-1})	Average Gt x 10^{-3} for stated floc quality		
		None	Fair	Excellent
38	2.0-11.4	5.9	9.8	14.5
70	5.0-14.3	8.0	13.4	22.2
140	12.8-36.8	18.7	28.9	57.2

B. Estimated ratios of Gt and observed floc qualities for specific shaft speeds.

Shaft speed (rpm)	Ratio of Gt for stated floc quality to Gt for no floc		
	None	Fair	Excellent
38	1	1.66	2.46
70	1	1.67	2.78
140	1	1.55	3.06
Mean Value	1	1.63	2.77

C. Estimated ratios of Gt and observed shaft speeds for specific floc qualities.

Floc quality	Ratio of Gt for stated speed (rpm) to Gt at 38 rpm		
	38	70	140
None	1	1.36	3.17
Fair	1	1.37	2.95
Excellent	1	1.53	3.96
Mean Value	1	1.42	3.36

Accordingly, G should become larger rather than smaller. The absence of stators from Leipold's flocculators may have modified and even reversed this effect.

Recent Studies.

In 1953, Bean(38) advanced a "displacement factor" for the design of agitators. The factor is actually the ratio of the time-rate volume of liquid swept out by the rotating paddles and supports to the time-rate of flow through the tank. The factor is read from calibration curves and does not seem to be widely acceptable. Moreover, the terms comprised in the displacement factor appear in the parameter Gt.

In 1957, Hudson(39) stated that "conventional flocculation aims to produce floc that will settle at only 0.8 in. per minute," whereas a solids contact reactor will produce floc settling at almost twice this rate. He found that values of Gt less than 10^4 are generally unsatisfactory; that values of G in excess of 40 sec^{-1} produce poorly settling floc even when the water is thoroughly flocculated; and that G values of approximately 10 to 15 sec^{-1} seem to obtain most commonly in mechanical flocculating chambers.

In a thesis presented to the University of London in 1955, Ritchie(40) suggested a new approach to the study of flocculation. Using apparatus based on a design by Mason and his co-workers at the Pulp and Paper Research Institute of Canada, he attempted to study flocculation in liquids subjected to well-defined shear gradients. Since his results are generally inconclusive and cannot be summarized with meaning, specific aspects of his work are referred to more appropriately in later chapters of this thesis.

Since 1950, Mason and his associates at the Pulp and Paper Research Institute of Canada have published a succession of papers describing particle motions in flocculation. Motivation for these papers is an interest in pulp-fiber flocculation during the manufacture of paper. At the beginning, gross aspects of pulp-fiber flocculation were studied, but interest soon progressed to observation and prediction of particle motions in sheared suspensions. Much of the work was summarized by Mason and Bartok(41) in 1959. The references cited are a key to their original publications.

The apparatus used by Mason _et al_. to provide a well-defined shear gradient in a liquid comprises a pair of coaxial cylinders enclosing a liquid in the annulus between the cylinders.* The cylinders rotate in opposite directions and form a streamline of zero velocity near the center of the annulus. It is a simple matter to observe particles lying on this streamline microscopically and to study the interactions between these particles and others lying away from the streamline and, consequently, possessing a velocity relative to the observed particle.

Mason's results of immediate importance for this thesis are summarized in the following paragraphs of this chapter. Although other aspects of his work are preparatory to the formulation of a mathematical model of hydrodynamic capture of particles, such a formulation is not yet possible. However, some of Mason's results of this kind will be referred to in later portions of this thesis.

---

*Since a similar apparatus was used in the author's research, the hydrodynamics of the system are described in a subsequent chapter of this thesis.

In general, Mason found that, under his experimental conditions, the collision frequency for spheres agrees within one percent with the value predicted by von Smoluchowski. However, in many cases physical contact is absent during collision. For $0.5 \leq (d_i/d_j) \leq 2.0$, where d_i/d_j is the ratio of the diameters of the interacting spheres, separation of the particles is not observed, and the doublet so formed behaves like a rigid particle. In qualitative agreement with the predictions of Müller embodied in equations (2-27) and (2-28), interacting spheres having a diameter ratio outside of this range remain separated at all times.

The path of one particle around another closely follows the streamlines of laminar flow about a sphere but, unfortunately, there is some deviation from the predicted path in the vicinity of the central particle. This prevents further mathematical analysis at this time.

Since particles subjected to a velocity gradient rotate about their mass centroids, the period of which is inversely proportional to the velocity gradient, a non-spherical particle can be characterized, for purposes of coagulation, by the effective volume swept out during its rotation. This volume is proportional to r^2, where r is the ratio of particle length to particle diameter for rod-like particles. For ellipsoids of revolution, this quotient is equivalent to the axis ratio. The particle population may exhibit a characteristic, preferred orientation in a statistical sense.

Fluid drops (and presumably other non-rigid particles) may circulate internally within their effective volumes. This causes the streamlines to be deflected differently in the vicinity of the particle. The extent to which the streamlines are affected depends upon the ratio of the fluid viscosities inside and outside the drop. When the ratio is infinite, as is true for rigid spheres, the deflection is greatest. With decreasing viscosity ratios, it decreases monotonically.

Studies of the deformation and breakup of liquid drops indicate two primary modes of breakup: drops with internal viscosity greater than the viscosity of the suspending fluid tend to form ellipsoids, continually necking down the center until they break; drops with internal viscosity less than the viscosity of the suspending medium assume a sigmoidal shape, and attrition occurs at the end points by the formation of small droplets.

Available information on aerodynamic capture of particles has been summarized in 1960 under the editorship of Richardson(42). Attention is directed chiefly to the capture of very small particles by a much larger "collector" particle. Because of the complexity of interaction of the streamlines when particles come into close proximity, there is little information on capture of particles with diameters larger than one-tenth the diameter of the collecting particle.

Because of their momentum, particles with densities differing from the density of the suspending medium may stray from the streamline on which they were traveling. For a particle of greater density, the efficiency of a collector particle, expressed as the ratio of the area of fluid swept by the collector to the projected area of the collector, is greater than would be indicated by the streamlines alone. The converse is true for particles less dense. The collector efficiency, E, can be expressed as a function of three non-dimensional parameters (see Figure 2-4), or

$$E = f \left(\frac{U\rho_2 R}{\mu} , \frac{\rho_1}{\rho_2} , \frac{r}{R} \right)$$

where U is the velocity of the particle relative to the collector, ρ_1 the density of the particle, ρ_2 the density of the suspending fluid, μ the viscosity of the fluid, r the radius of the particle, R the radius of the collector, and E equals y_c^2/R^2 , where y_c is the critical initial offset of the particle from the center of the collector.

Hocking (see reference 42) has studied the collision efficiency for small drops (up to 30 microns in radius for the collector drop) in purely viscous flow for values of $\frac{r}{R} < 1.0$. According to him, the collection efficiency increases remarkably with increasing size of the collector drop and, for a given size of collector drop, the efficiency is maximal for values of $0.65 \leq \frac{r}{R} \leq 0.76$. This is in general agreement with Mason's observations. Lack of information on the collection efficiency for drops larger than 30 microns prevents the direct incorporation of Hocking's work in this thesis.

SUMMARY

General conclusions drawn from this review of the literature may be brought together as follows:

1. At the beginning, chemical coagulation forms random coil complex-polymers of the metal ion coagulant to which the color or turbidity is bound. The incipient flocs are colloidal in size and nature.
2. Flocculation proceeds according to von Smoluchowski's perikinetic model when the particles moving about in the fluid are smaller than 4 microns in diameter and follows some modification of his orthokinetic model when the particles are larger.
3. Operating records of water treatment plants and laboratory studies of coagulation indicate that the success of flocculation during chemical coagulation of color or turbidity depends upon the degree and extent of agitation of the suspension.
4. Present concepts of orthokinetic flocculation are applicable, in a limited fashion, to the flocculation of chemically formed floc, but the degree of limitation is known only qualitatively. Its nature has not yet been explored experimentally.
5. A suitable range of mean temporal velocity gradients in sec^{-1} appears to be $2 \leq G \leq 40$, and a suitable time of flocculation t in seconds generally satisfies the condition $5000 \leq Gt \leq 50,000$, where the product Gt is a dimensionless number.
6. The role of flocculation in the coagulation process has not been determined experimentally with any degree of exactness.

In the subsequent chapters of this thesis, some of the unresolved problems identified in this chapter are explored.

Chapter 3 contains numerical solutions of von Smoluchowski's equations for perikinetic and orthokinetic flocculation. Modifications of the equations, proposed either by the authors of this thesis or by others, are considered; and their effects upon the original equations are discussed.

In Chapter 4 are reported the details of construction of the apparatus used in the authors' studies. The hydrodynamic characteristics of the test cell are presented, and some limitations on the operation of the cell are discussed.

The results of floc growth studies using this apparatus are shown in Chapter 5, together with a discussion of the problems and techniques of floc measurement.

The effect of mean velocity gradient and time of flocculation on the rate of coagulation of color and turbidity is discussed in Chapter 6. The purpose of this chapter is twofold: to clarify the role of flocculation in a coagulation process; and to substantiate the conceptual operations of coagulation previously developed.

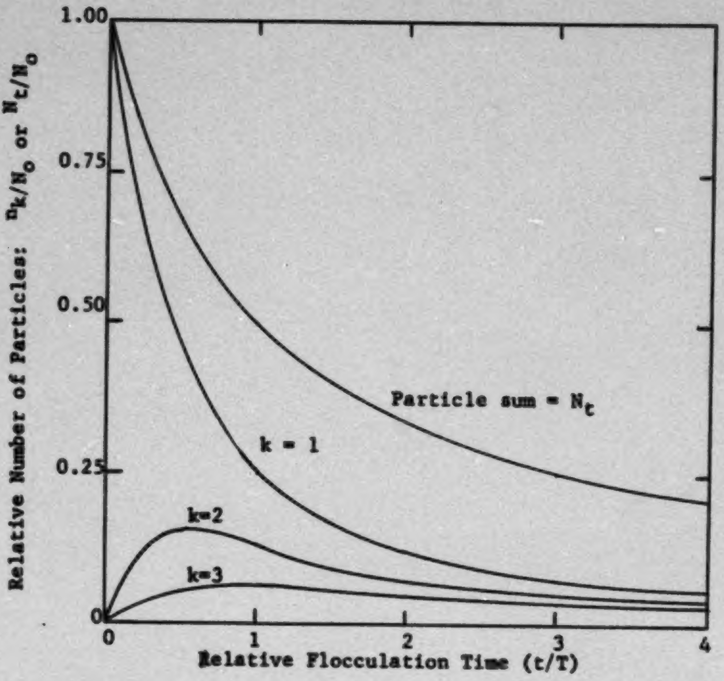

FIGURE 2-1: CHANGE IN NUMBER OF PARTICLES OF STATED SIZE DURING PERIKINETIC FLOCCULATION (After Overbeek)

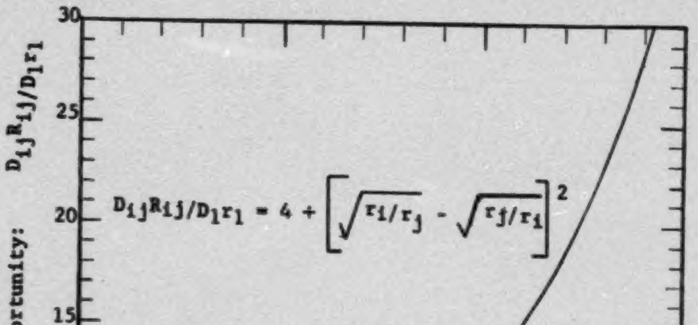

FIGURE 2-2: EFFECT OF HETERODISPERSION ON CONTACT OPPORTUNITY IN PERIKINETIC FLOCCULATION

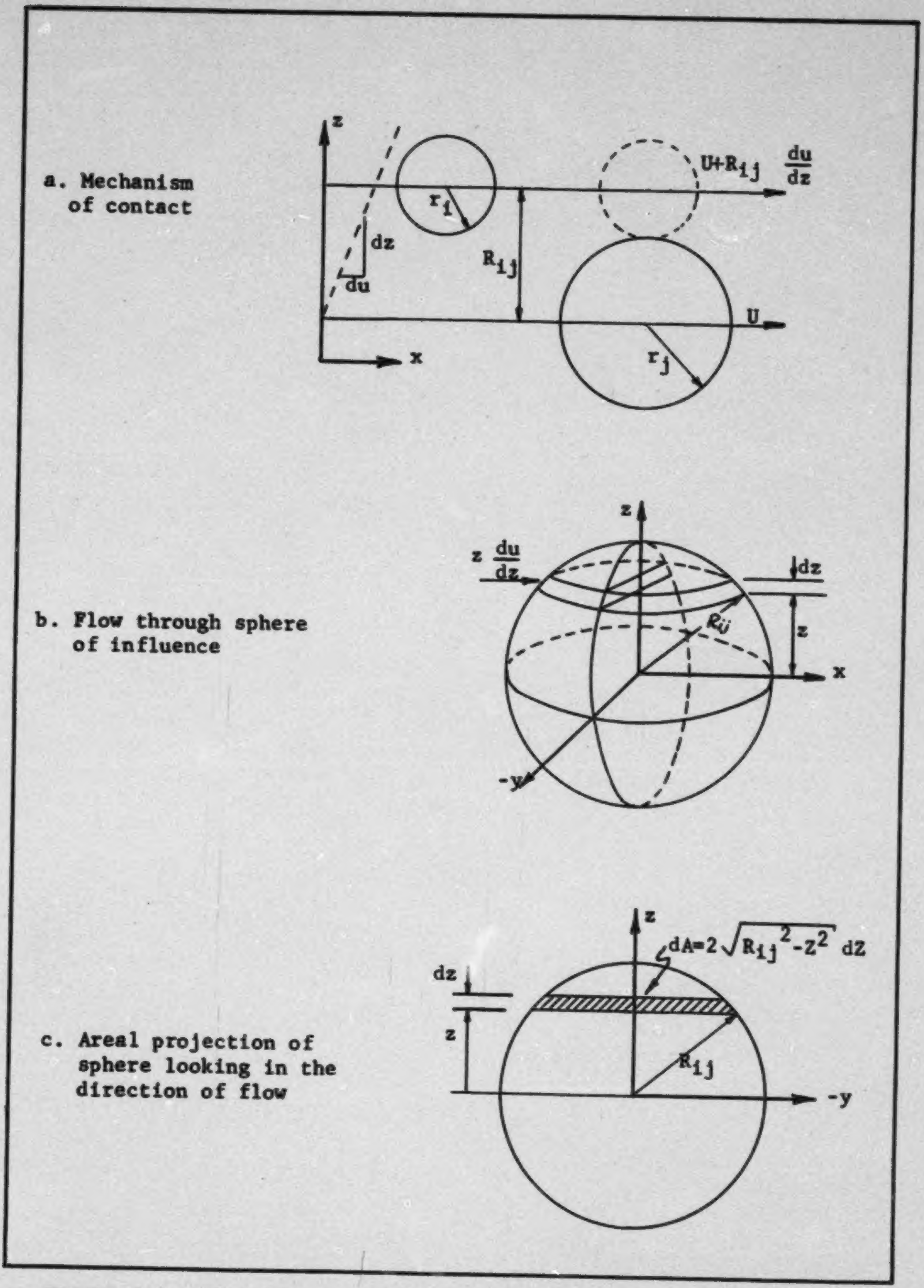
z
U+R_ij du/dz
r_i
dz
du
R_ij
U
x
r_j
z
z du/dz
dz
R_ij
z
x
-y
z
dA=2√(R_ij²-Z²) dZ
dz
z
R_ij
-y

a. Mechanism of contact

b. Flow through sphere of influence

c. Areal projection of sphere looking in the direction of flow

FIGURE 2-3: DEFINITION SKETCHES FOR ORTHOKINETIC FLOCCULATION

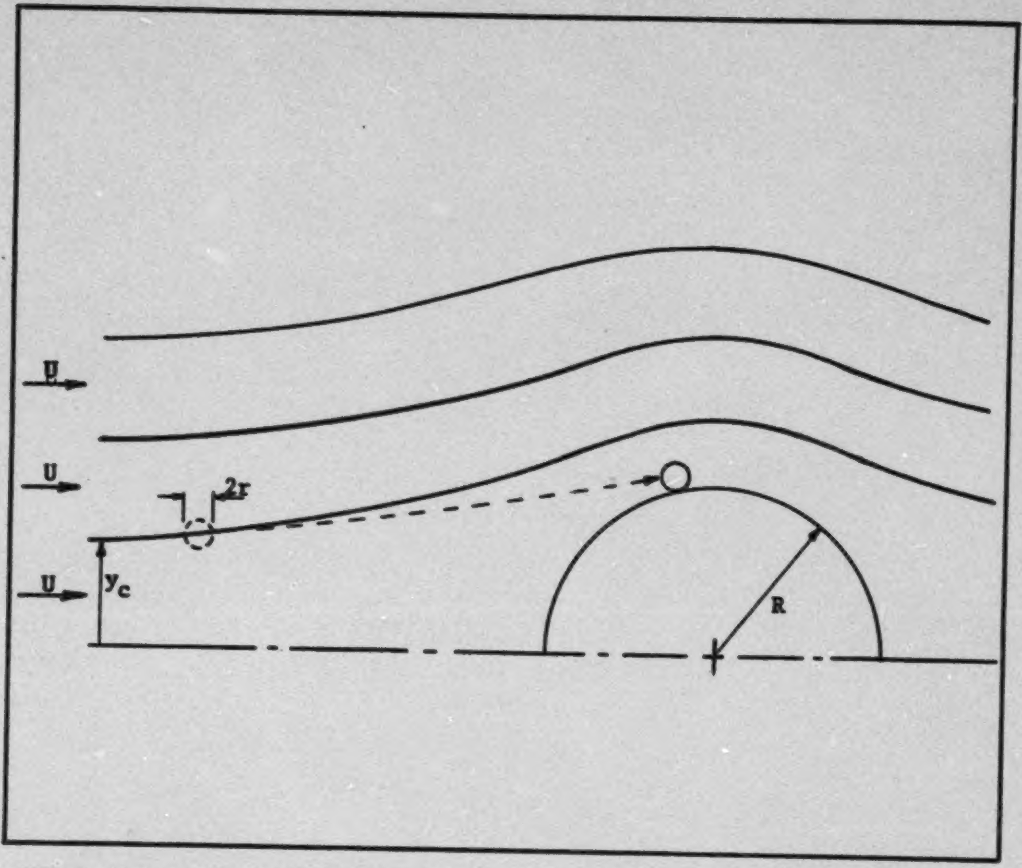

FIGURE 2-4: MOMENTUM INDUCED DEPARTURE OF PARTICLE FROM STREAMLINE

The dashed line represents the path taken by a particle of density greater than that of the suspending fluid.

Chapter 3

PARTICLE SIZE STUDIES: MATHEMATICAL MODELS

Information presented earlier in this thesis supports the hypothesis that floc growth during chemical coagulation is strongly a matter of orthokinetic flocculation. In a quantitative sense, however, little is known about the mechanism of floc growth. The equations derived by von Smoluchowski and others nearly forty years ago are not being applied, and there has been no attempt so far to express the rate of change of floc size during flocculation in numerical terms.

To fill this gap in information and provide a basis for interpreting the experimental studies reported later in this thesis, pertinent numerical computations were made with von Smoluchowski's equations.

General Computation Techniques

All calculations were performed on an I.B.M. digital computer (Model 7090) with FORTRAN II mnemonic coding. Although the equations for both perikinetic and orthokinetic flocculation were programmed, only a few perikinetic computations were made. The main effort was placed on modifications of von Smoluchowski's orthokinetic flocculation model.

The aim of the studies was threefold: examination of the role of equational parameters; evaluation of promising modifications of the equation; and prediction of particle growth patterns for comparison with observed results.

For computational purposes, orthokinetic flocculation is best expressed in terms of equation (2-23):

$$J_{ij} = \frac{1}{6}\frac{du}{dz} n_i n_j \; (d_i + d_j)^3 \qquad (2\text{-}23)$$

It will be remembered that J_{ij} is the number of contacts per unit time and volume between the n_i particles of diameter d_i and the n_j particles of diameter d_j in a laminar flow field with a constant velocity gradient du/dz. By assuming that the volume of the smallest particle is unity and that all particles are spherical and of integral volume, the relationship between volume and diameter was fixed by assigning a unit diameter and unit projected area to a particle of unit volume. Accordingly, there corresponds to the index i or j for particle volume a diameter and projected area equally the one-third and two-thirds power of the index respectively. It is assumed, furthermore, that when a particle of volume i comes into contact with a particle of volume j, a new particle k with volume i + j = k is formed.

Arising from equation (2-23) is the differential equation (2-24) expressed in diameters rather than radii:

$$\frac{dn_k}{dt} = \frac{1}{12}\frac{du}{dz}\left[\sum_{\substack{i=1\\ j=k-i}}^{k-1} n_i n_j \; (d_i+d_j)^3 - 2n_k \sum_{i=1}^{\infty} n_i \; (d_i+d_k)^3\right] \qquad (2\text{-}24)$$

For integration of this equation in terms of diameter instead of radius, discrete time intervals (iterations), for which the particle size-distribution is held fixed, were considered. The indices i and j were set to unity, and the number of contacts was computed for the appropriate values of n_i, n_j, d_i, and d_j. Since each contact between an i- and a j-particle decreases the number of i- and j-particles by one unit and increases the number of k-particles by one unit, running totals of the increments and decrements were kept separate from the fixed particle size distribution. The index j was then increased sequentially over the range 1 to (limit), followed by a unit increment in i and a second series of increments in j, until both indices had covered the range 1 to (limit). The running total of the changes in particle size distribution was then used to correct the fixed distribution before stepping up the iteration number by one and repeating the process.

Ideally, the limit placed on the range of values for the subscripts i and j should be infinity, but computer memory space is finite and computation time expensive. Accordingly, a limit of 40 was not exceeded. The number of iterations was restricted for similar reasons.

Implicit in the chosen range of subscripts is the existence of particle volumes up to twice the limit of the indices. If any size beyond the index limit were stable, the rate of formation of particles approaching it in volume would be significantly biased. A particle exceeding the index limit in volume would not be considered to undergo further contacts and, therefore, would cease to grow. To avoid this type of bias, the maximum volume was set at the index limit. In the simplest case, contacts that would lead to the formation of particles beyond the index limit were dropped from consideration and the particles were kept at their original size.

Expressed in FORTRAN mnemonics, the final equation for computation was:

```
CTS = 0.5*XKK*PC*PCC*( (DIA(M) + DIA(N))**3)        (3-1)
```

where CTS is J_{ij}, PC and PCC are n_i and n_j respectively, DIA(M) and DIA(N) are d_i and d_j respectively, the single asterisk calls for multiplication and the double asterisk for exponentiation, and XKK is a parameter reflecting (1) du/dz, or mean temporal velocity gradient G, (2) a factor relating iteration number to time, (3) a factor relating actual particle volume to unit volume, (4) a factor relating the cubes of the unitized and geometric diameters $(6/\pi)$, and (5) the numerical factor (1/6) found in the original equation.

The multiplier (0.5) serves two functions. When $i \neq j$, it offsets the duplication of index combinations associated with sequential advancement of index magnitudes; when $i = j$, it helps to place the number of particles n_j in substantial accord with the equation for combinations of n objects taken 2 at a time $n!/[(n-2)!2!] = (0.5)n(n-1)$. Substitution of (n_j-1) for n_j resulted in full accord. To minimize errors caused by rounding, fractional numbers of particles were not replaced by integers.

The remainder of the program dealt primarily with input and output of data and, in addition, with modifications of von Smoluchowski's equation. The following output information of the computer was provided in tabular form:

1. Up to maximum particle size, a table of particle sizes and initial numbers, sizes being reported as volumes, diameters, and projected areas, and their logarithms.
2. At pre-selected iteration numbers, a table of mean sizes and standard deviations in size, total numbers of particles, and standard deviations in numbers, and size distribution. For truncation, a repetition of this information.

3. At the end, a table of selected input data and program identifications with a summary of mean sizes and total numbers for the preselected iteration numbers.

Appendix C to this thesis contains a simplified flow chart of the program together with a list of input variables and their meaning, a copy of the actual program, and a sample of output data.

Perikinetic Flocculation

Studies of perikinetic flocculation were confined to a comparison of von Smoluchowski's approximation $D_{ij}R_{ij} = 4\ D_1r_1$ with Müller's more precise formulation $D_{ij}R_{ij} = D_1r_1\ [\ 4 + (\sqrt{ri/r_j} - \sqrt{r_j/r_i}\ )^2\ ]$ for a monodisperse colloidal suspension. A comparison of bi-disperse systems is included in the preceding chapter of this thesis.

Figure 3-1A shows the calculated number of particles for increasing flocculation times. The ordinate is expressed as a ratio of the calculated to the initial number of particles, the abscissa as the ratio of the time t, or number of iterations, to the half-time T, determined graphically as the number of iterations needed to halve the initial number of particles, N_o. Co-linear curves were obtained for the von Smoluchowski and Müller equations, the flocculation half-time being slightly shorter by Müller's equation.

Time rate of floc growth in terms of mean particle diameter is depicted in Figure 3-2 with coincidence of the curves for the suggested time scale ratio.

The analytic solution for the time rate of change in total number of particles obtained by von Smoluchowski's approximate value for $D_{ij}R_{ij}$ was second order with respect to the number present. As shown in Figure 3-3, this kinetic expression is linearized by plotting N_o/N against normalized time. The solid line follows the analytic solution; the plotted points are calculated values. The agreement is generally good, but, at large time ratios, the calculated number ratios veer away from linearity. Some disagreement was expected with the calculation techniques used. Interestingly enough, the points obtained with the approximate value of $D_{ij}R_{ij}$ (as is true for the analytic solution) diverge more than the points based on the exact value. Obviously, an analytic solution including the Müller expression for $D_{ij}R_{ij}$ should diverge from linearity in the opposite direction.

Particle size distributions for various flocculation times based on Muller's expression are shown in Figure 3-4. The distributions are essentially J-shaped and cannot be linearized in arithmetic or logarithmic probability plots, although such plots are helpful. A maximum particle volume of 40 units for the computation may be inferred from the curves.

Orthokinetic Flocculation of Monodisperse Systems

Breakup

That particle growth had to be kept at or below some maximum volume was prescribed by available computer capacity. As reported in the second chapter of this thesis, however, this limitation does not produce an unreal situation, since particle size is in fact shear-controlled within a given flow field. Reported in this section are possible forms of floc breakup and the effect of floc breakup on floc growth pattern.

Four simple ways of breakup during flocculation were considered. In all of them any floc larger than a set maximum size becomes unstable and breaks up. In the first instance, breakup reproduces the constituent particles unchanged in size and other properties. In the next three instances, the unstable, oversized particle breaks up to form two, three, or four particles of integral and approximately equal volume. The first method of breakup is equivalent to nonformation of flocs larger than the maximum. It is also a special case of the second in which breakup produces a prescribed subdivision into two equally sized, and essentially secondary, flocs.

How particles decrease in total number because of conjunction and breakup during flocculation under otherwise identical conditions is shown in Figure 3-5 for each of the four ways of breakup. Assumed conditions are a maximum particle volume of 20 and an intensity of contact represented by a value of C = 0.02 as explained in the next section of this chapter. Although they start along the same course, the curves are seen to diverge and approach different limiting numbers that increase in size as the number of possible secondary particles becomes larger. The flocculation half-times T were identical with a value of 17.7.

How floc particles increase in size is shown in Figure 3-6 for the volume size measures. Plots of particle diameter, area, and logarithms of all three size measures resembled Figure 3-6 closely. The first breakup growth pattern is seen to cut across the rest, and there is no unique optimum time of flocculation because all of the size parameters increase monotonically during flocculation.

What the size distributions of the particles become after selected time intervals of flocculation is shown in Figures 3-7 and 3-8 for the first and third ways of breakup. In the first, flocs near maximum volume become dominant as flocculation progresses, in the second dominance shifts to sizes 14 and 15, in the third to sizes 8 and 9, and in the fourth to sizes 5, 6, and 7. Particle size distributions for the second and fourth breakups are not illustrated here, but the fourth is shown in Chapter 5.

Input Variables

Three parameters of the computer equation for orthokinetic flocculation function as input variables: XKK, N_o, and MAXVOL. The last of these has no basis in theory since it is a compromise variable designating the limiting particle volume. If the value of XKK is kept constant throughout a given computational study, it may be combined with N_o to form a new constant C reflecting both initial particle concentration and mean temporal velocity gradient, or

$$C = (XKK)(N_o) = A\ G\ N_o \qquad (3\text{-}2)$$

where A contains all of the factors previously included in XKK except G.

If the total number of particles is assumed to decrease in time according to the second-order relationship,

$$\frac{dN}{dt} = -\ K\ N^2 \qquad (3\text{-}3)$$

as in von Smoluchowski's formulation of perikinetic flocculation, integration between the limits $N = N_o$ when $t = 0$ and $N = N$ when $t = t$, states that

$$\frac{N_o}{N} = 1 + N_oKt \qquad (3\text{-}4)$$

By setting $N_o/N = 2$, the half-time of flocculation T is then found to be

$$T = \frac{1}{N_oK} \qquad (3\text{-}5)$$

If, finally, XKK is assumed to be proportional to K, or XKK = BK, it follows that

$$(XKK)(N_o)(T) = B = CT \qquad (3\text{-}6)$$

and

$$GT = \frac{B}{N_oA} \qquad (3\text{-}7)$$

Three conclusions can now be drawn: (1) independent variation of the parameters XKK and N_o affects the rate of flocculation in proportion to their product C; (2) the value of the non-dimensional product GT is inversely proportional to the initial concentration of particles; and (3) the parameter GT does not have a unique value characteristic of optimal flocculation but varies inversely with the coagulant dosage. We assume that the half-time of flocculation T is a suitable index of the optimal period of flocculation and that the initial number of particles is proportional to the coagulant dosage. There is the further conclusion that suitable adjustment of the mean temporal velocity gradient will compensate for too little or too much coagulant provided that the chemical dose is large enough to satisfy the chemical requirements of the system and that shear-controlled sizing is disregarded.

That the parameter B in equation (3-6) is substantially constant is shown by the computer results summarized in Table 3-1. Here each reported run is unique in some respect.

TABLE 3-1

CONSTANCY OF THE PARAMETER B = (XKK)(N_o)(T) AS DETERMINED FROM COMPUTER RESULTS

	RUN	MAXVOL	BREAKUP	(XKK)(N_o)=C	T	B
	11	40	3	0.02	8.7	0.17
	12	20	3	0.04	4.0	0.16
	13	20	3	0.01	17.7	0.18
(a)	14	8	3	0.01	18.6	0.19
	15	20	3	0.02	8.7	0.17
(a)	19	8	1	0.01	18.2	0.18
	21	20	1	0.01	17.7	0.18
(b)	25	20	1	0.01	17.7	0.18
	27	20	2	0.004	44.9	0.18
(c)	28	20	1	0.01	18.8	0.19
	29	20	2	0.01	17.7	0.18
	30	20	4	0.01	17.7	0.18

(a) A low value of MAXVOL may be expected to increase the flocculation half-time T.

(b) Only selected contacts permitted: $\frac{1}{2} \leq \frac{d_i}{d_j} \leq 2.0$

(c) Only selected contacts permitted: $\frac{2}{3} \leq \frac{d_i}{d_j} \geq 1.5$

How parameters XKK, N_o, and MAXVOL influence the progress of flocculation is shown in Figures 3-9 and 3-10 for the third way of breakup. At a given value of MAXVOL, the chosen scale ratios are seen to suppress possible effects of changing the remaining variables with exception of the half-time of flocculation. At other values of MAXVOL, the steady-state number of particles rises and falls as would be expected, but the floc growth pattern remains substantially unaltered.

Linearization of the composite curve (MAXVOL = 20) in Figure 3-9 on the assumption that the decrease in particles by flocculation is first or second order was not successful; neither was the introduction of a limiting value for floc size. It will be remembered that perikinetic flocculation, by contrast, was found to be kinetically of second order and that introduction of a limit into the perikinetic studies reported earlier in this chapter became noticeable only at large flocculation times.

The major difference between the orthokinetic and perikinetic flocculation equations discussed in this chapter is the factor $(d_i + d_j)^3$ within the summations. For a given pair of indices this factor is a constant and one might speculate that it could be replaced in the orthokinetic equation by some function of the mean particle diameter at a given time. However, an examination of available experimental results does not warrant further investigation of this possibility at this time.

Selective Contacts

Müller, in 1928, and Mason, in 1955, suggested that streamline curvature and particle momentum may keep particles of a given size from combining with a full range of particles of other sizes. Size restriction for contact may be written $1/\text{RANGE} \leq d_i/d_j \leq \text{RANGE}$. If, for example, the value of RANGE is made 2, then $1/2 \leq d_i/d_j \leq 2$, and only particles with diameter ratios satisfying this inequality may conjoin or flocculate. How this restriction affects particle numbers, mean diameters, and volume distributions is demonstrated in Figures 3-11, 3-12, and 3-13 respectively.

The decrease in the total number of particles during flocculation (Figure 3-11) is seen not to differ appreciably from that for the four ways of breakup (Figure 3-5). The pattern of floc growth (Figure 3-12), on the other hand, shows a considerably slower increase in mean floc diameter when the range of selective contacts is narrowed. Retardation of growth is accentuated beyond the half-time of flocculation. As shown in Figure 3-13, a particle size distribution for a RANGE value of 1.5 retains many of the earmarks of the first way of breakup (Figure 3-7).

Initially Polydisperse Systems

That initially polydisperse systems have higher initial floc growth rates is shown by Figure 3-14 for five different initially pentanomial particle-size distributions when its values are compared with those recorded for monodisperse systems. See, for example, Figure 3-6. The characteristics of the five initial frequency distributions are detailed in Table 3-2.

TABLE 3-2

Initial Particle Size Distributions for Orthokinetic Flocculation of Polydisperse Sols

Run No.	Type of Distribution	Particle Volume	Number of Particles	Distribution Parameters
31	Rectangular	1	200	
		2	200	Arith. mean volume = 3.00
		3	200	Arith. std. deviation = 1.414
		4	200	
		5	200	
32	Arithmetically normal approximation	1	66	
		2	242	Arith. mean volume = 2.997
		3	383	Arith. std. deviation = 1.060
		4	242	
		5	66	
33	Logarithmically normal (geometric) approximation	1	325	
		2	565	Geometric mean volume = 1.676
		3	98	Geom. std. deviation = 1.462
		4	11	
		5	1	
35	Distribution calculated from von Smoluchowski perikinetic flocculation equations: $t/_T = 1.0$	1	513.00	Arith. mean volume = 1.839
		2	265.50	Arith. std. deviation = 1.108
		3	128.25	Geom. mean volume = 1.587
		4	64.12	Geom. std. deviation = 1.685
		5	32.06	
36	Distribution calculated from von Smoluchowski perikinetic flocculation equations: $t/_T = 4.0$	1	297.60	Arith. mean volume = 2.563
		2	238.08	Arith. std. deviation = 1.370
		3	190.46	Geom. mean volume = 2.182
		4	152.37	Geom. std. deviation = 1.795
		5	121.90	

Computer simulations showed that the rectangular and arithmetically normal distributions gave similar values for the half-time of flocculation (T = 6.5 and 6.2 respectively), and that floc growth was essentially identical for a time scale ratio of $^{t}/_{T}$. For the geometrically normal distribution, flocculation half-time and floc growth approximated the values obtaining for a perikinetic distribution based on $^{t}/_{T} = 1.0$, the flocculation half-times being 10.0 and 10.3 respectively. For perikinetic flocculation based on $^{t}/_{T} = 4.0$, the flocculation half-time became 7.5, and floc growth was found to be midway between the curves for arithmetically normal and geometrically normal initial distributions. Moreover, Figure 3-14 shows that the rate of floc growth is essentially the same for the five different distributions. Accordingly, it may be concluded that polydispersion of the initial sol affects both the flocculation half-time and the initial mean particle size, and that rate of flocculation is essentially insensitive to the type of size distribution of the initial sol.

Summary and Conclusions

The examination of von Smoluchowski's equations by computational methods, which is reported in this chapter, permits a number of important conclusions to be drawn.

As calculated, perikinetic flocculation conforms well to the analytic equation developed by von Smoluchowski, and Müller's expression for $D_{ij}R_{ij}$ does not yield significantly different results for a monodisperse initial sol.

Solution of von Smoluchowski's equation for orthokinetic flocculation suggests that floc growth takes an orderly course. Mean floc size becomes asymptotic to the imposed limiting floc size, and breakup does not substantially alter the pattern of floc growth. Instead it shifts the steady-state size in conformance with the way of breakup. Mean-size measures, whether of volume, area, or diameter and whether arithmetic or geometric, respond in similar ways to changes in the number of particles of each possible size.

Decrease in total number of particles during flocculation cannot be framed either as first-order or second-order kinetic expressions. However, the near-constancy of the product $B = (XKK)(N_o)(T)$ is strongly suggestive of second-order decay. The implication is that the initial number of particles to be flocculated, and hence the initial coagulant dose and concentration of color or turbidity to be removed, may determine what value of Gt is optimal for flocculation*. The mathematical model does not identify a discrete optimum Gt value. Instead, there is an asymptotic approach to an optimum as suggested by the curves included in this chapter. Stationary-state conditions are reached in time, and there is wide latitude in suitable choices. Selection of a design value for Gt must be based on the kind of treatment that is to follow flocculation.

Restraint of the conjunction of particles to a limited range of size ratios retards floc growth, but without noticeable change in form.

Flocculation is more rapid in a polydisperse than in a monodisperse sol, but overall floc growth is not altered substantially.

---

* The reader will recall that XKK is proportional to G (see page 3-4 or equation 3-2). The flocculation half-time T may be a suitable normalizing unit for the optimal flocculation time t.

The computed floc growth patterns discussed in this chapter are compared later in this thesis (Chapter 5) with patterns obtained experimentally.

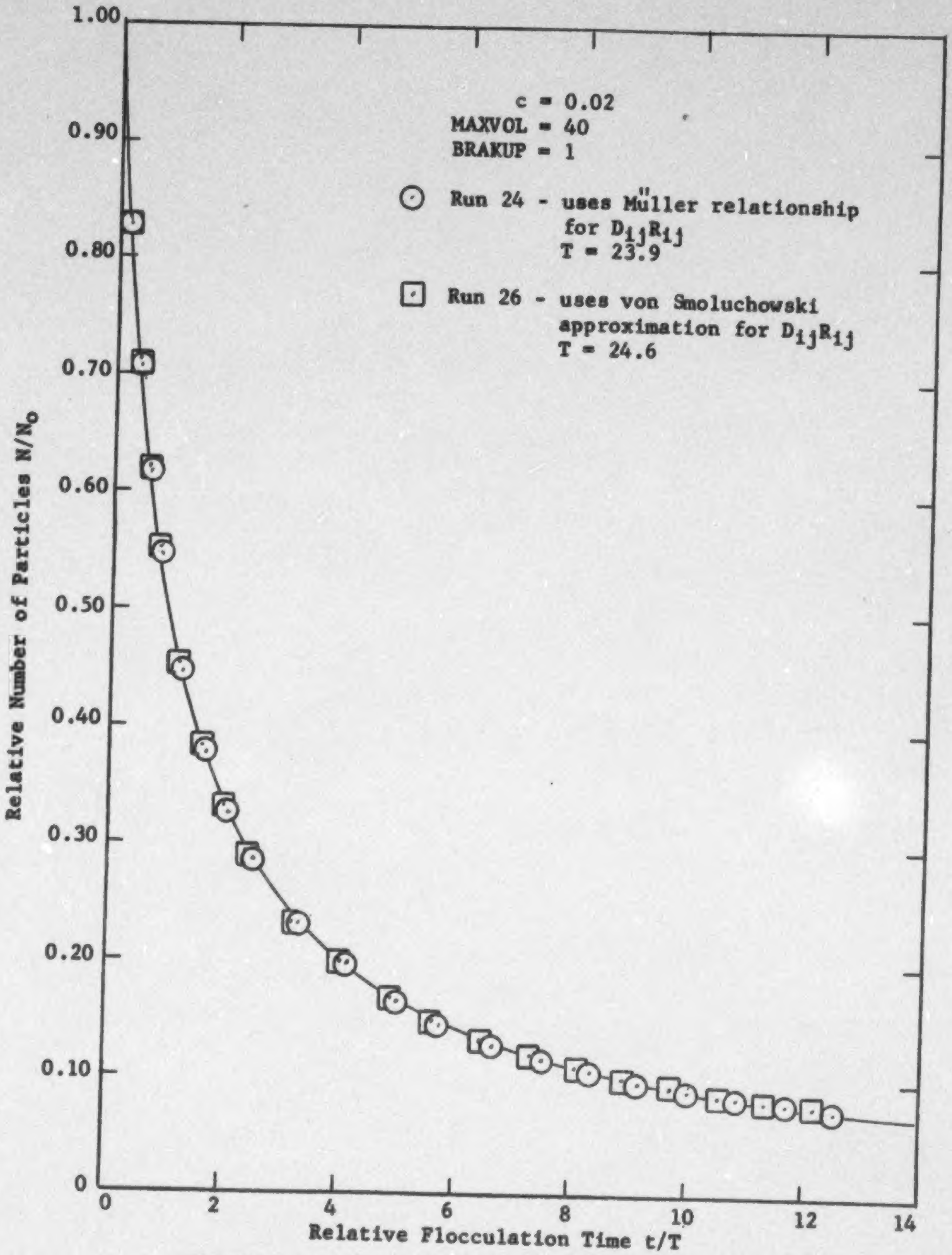

FIGURE 3-1: PERIKINETIC FLOCCULATION: DECREASE IN TOTAL NUMBER OF PARTICLES

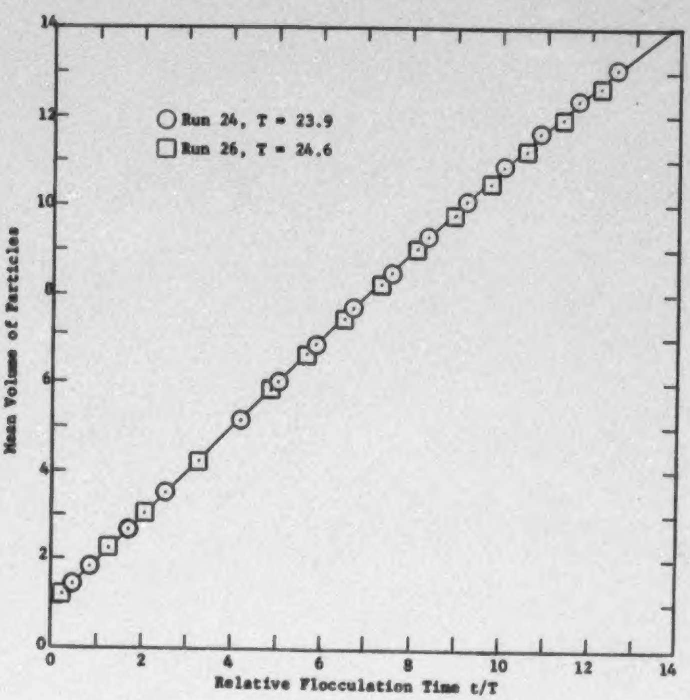

FIGURE 3-2: PERIKINETIC FLOCCULATION: INCREASE IN MEAN SIZE

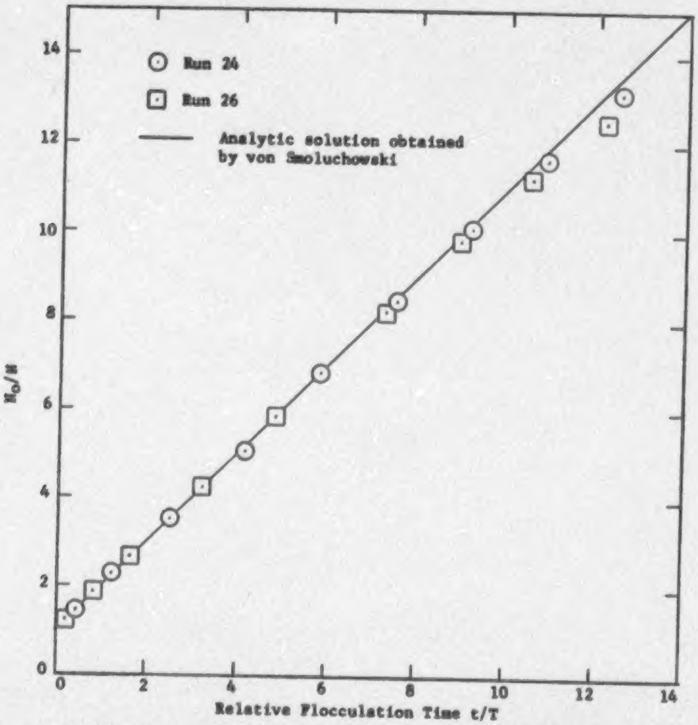

FIGURE 3-3: PERIKINETIC FLOCCULATION: LINEARIZING PLOT FOR SECOND-ORDER DECREASE IN TOTAL NUMBER OF PARTICLES

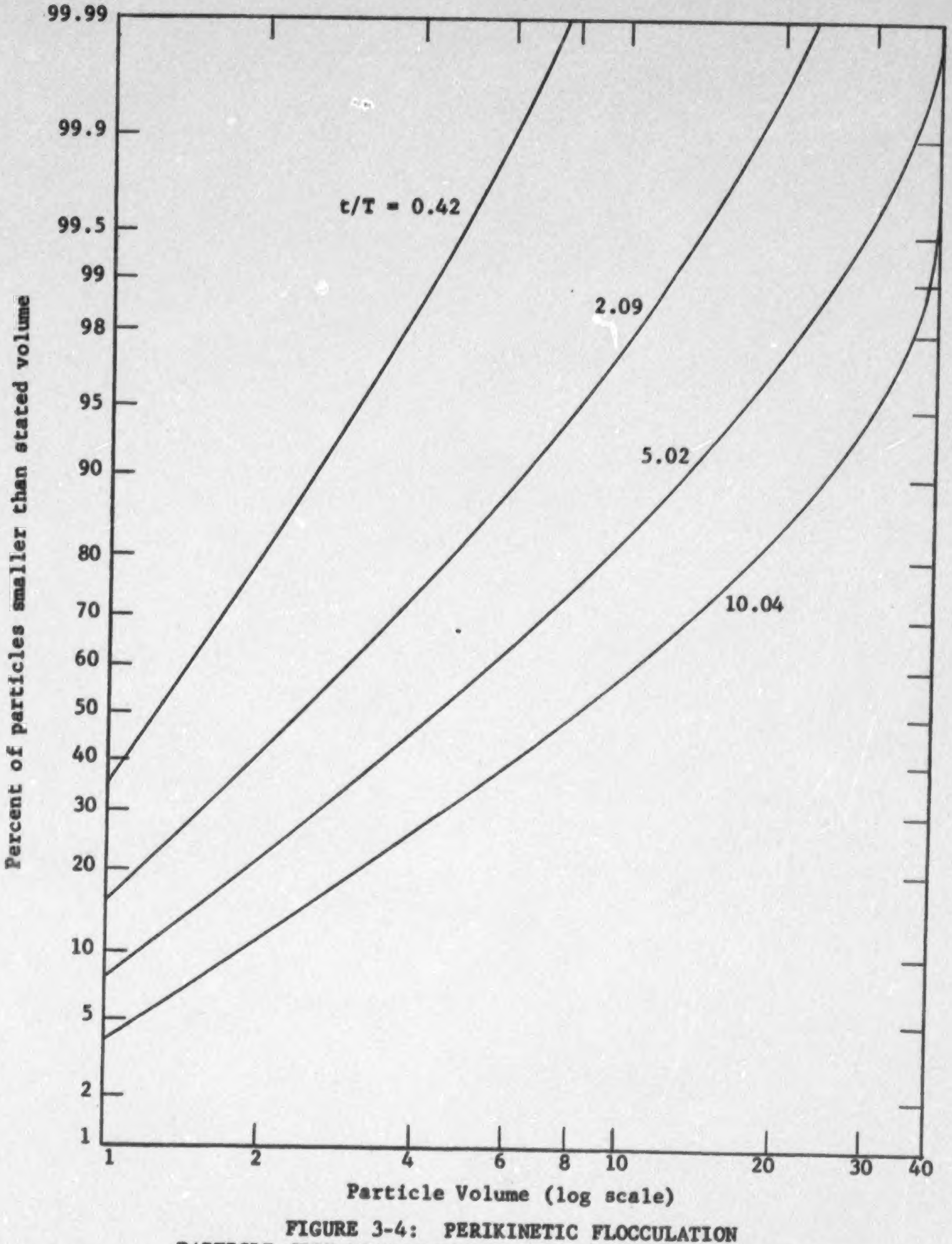

FIGURE 3-4: PERIKINETIC FLOCCULATION
PARTICLE SIZE DISTRIBUTIONS FOR SELECTED VALUES OF TIME
(Taken from Run 24)

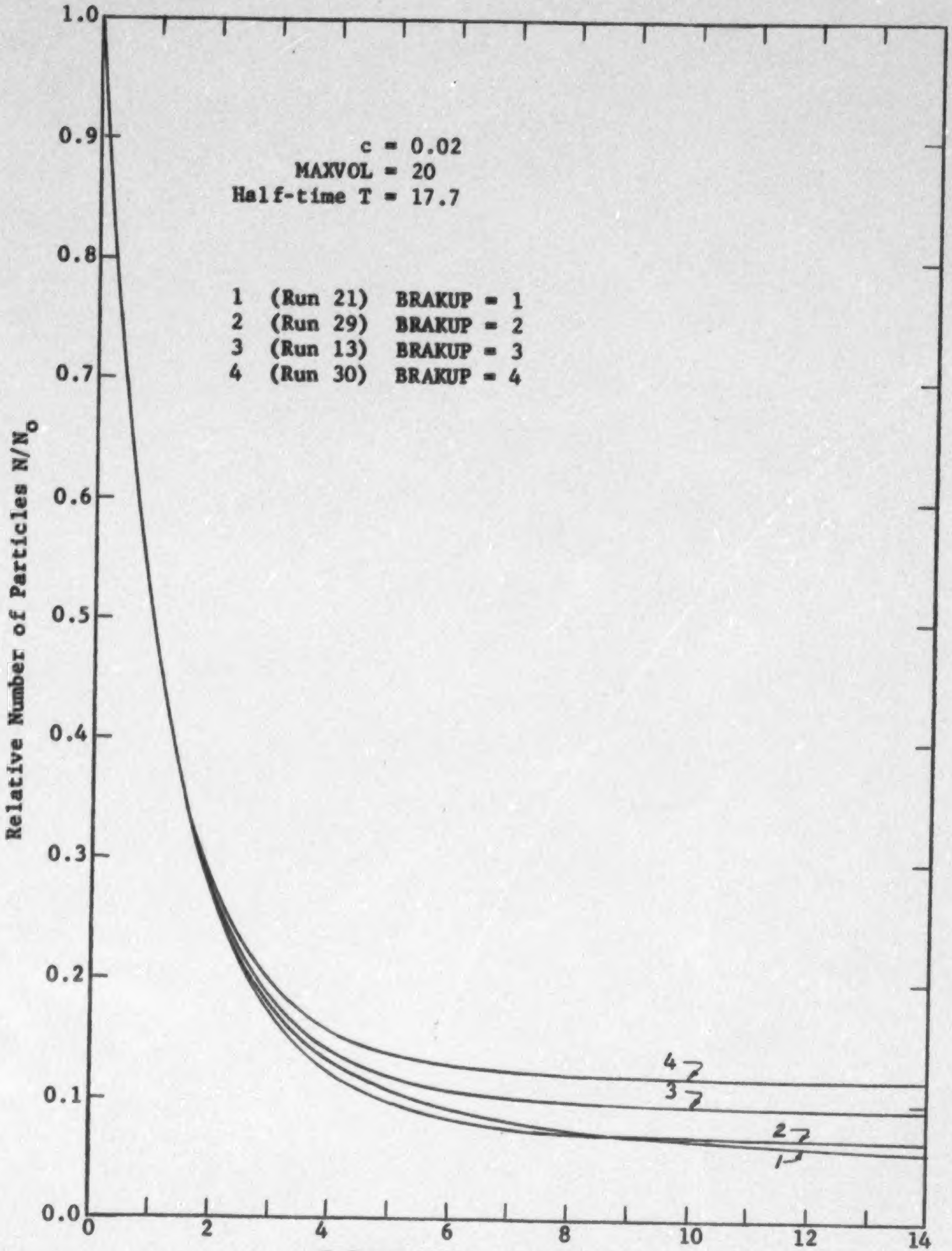

FIGURE 3-5: ORTHOKINETIC FLOCCULATION: EFFECT OF CONJUNCTION AND BREAKUP ON TOTAL NUMBER OF PARTICLES

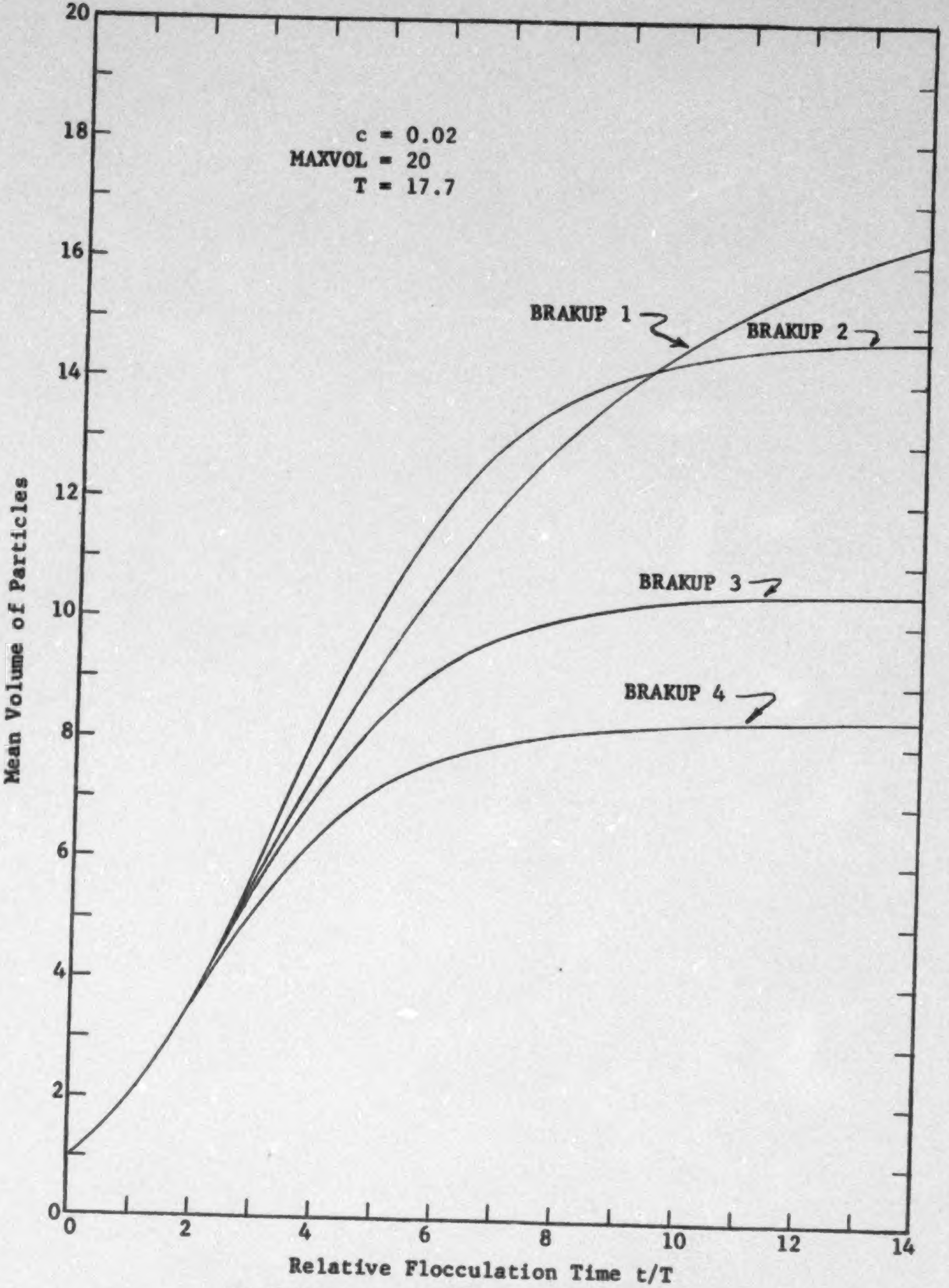

FIGURE 3-6: ORTHOKINETIC FLOCCULATION:
EFFECT OF CONJUNCTION AND BREAKUP ON FLOC GROWTH

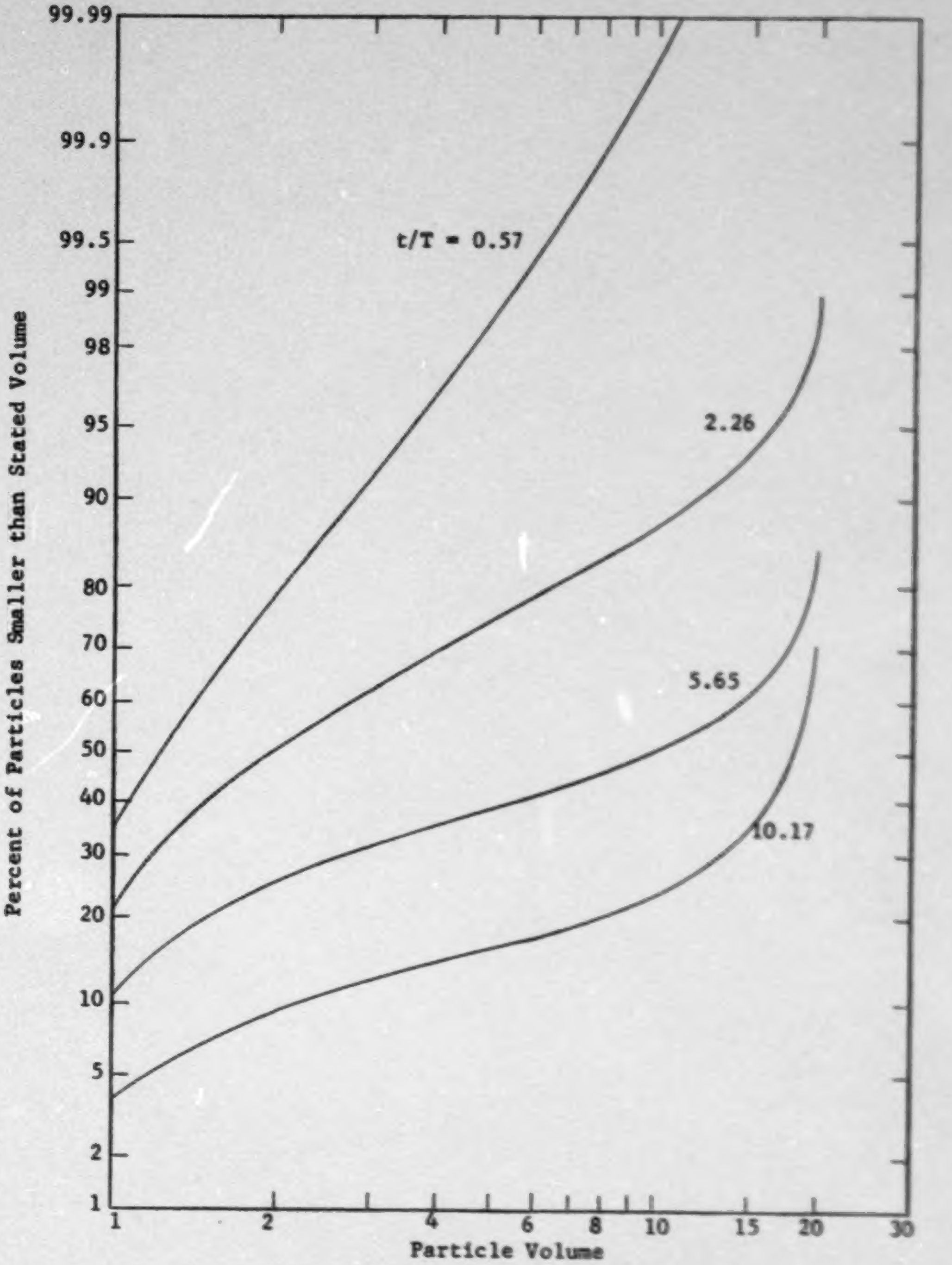

FIGURE 3-7 ORTHOKINETIC FLOCCULATION:
PARTICLE SIZE DISTRIBUTIONS OBTAINED WITH BREAKUP 1
(From Run 21)

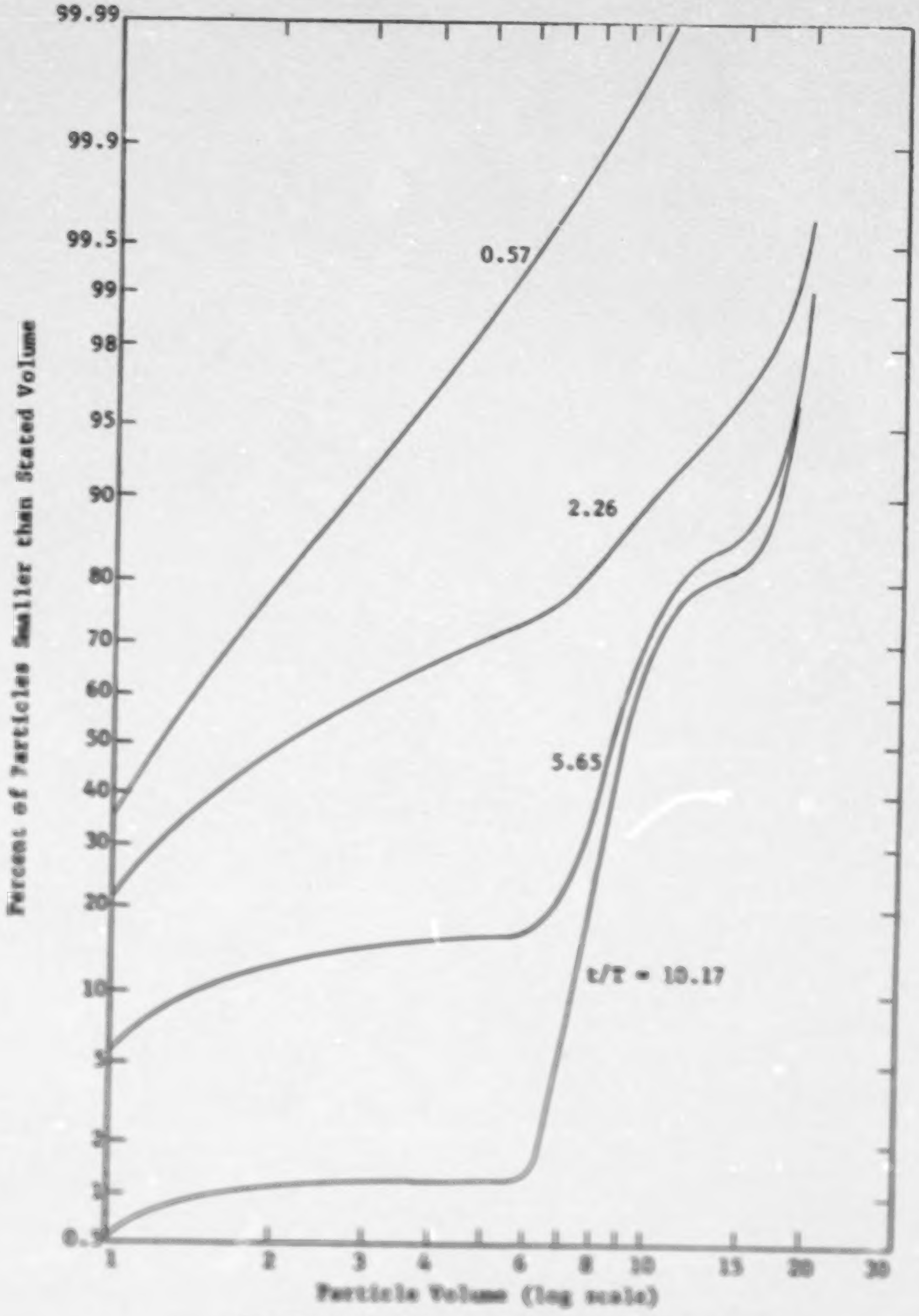

FIGURE 3-8: ORTHOKINETIC FLOCCULATION:
PARTICLE SIZE DISTRIBUTIONS OBTAINED WITH BREAKUP 3
(From Run 13)

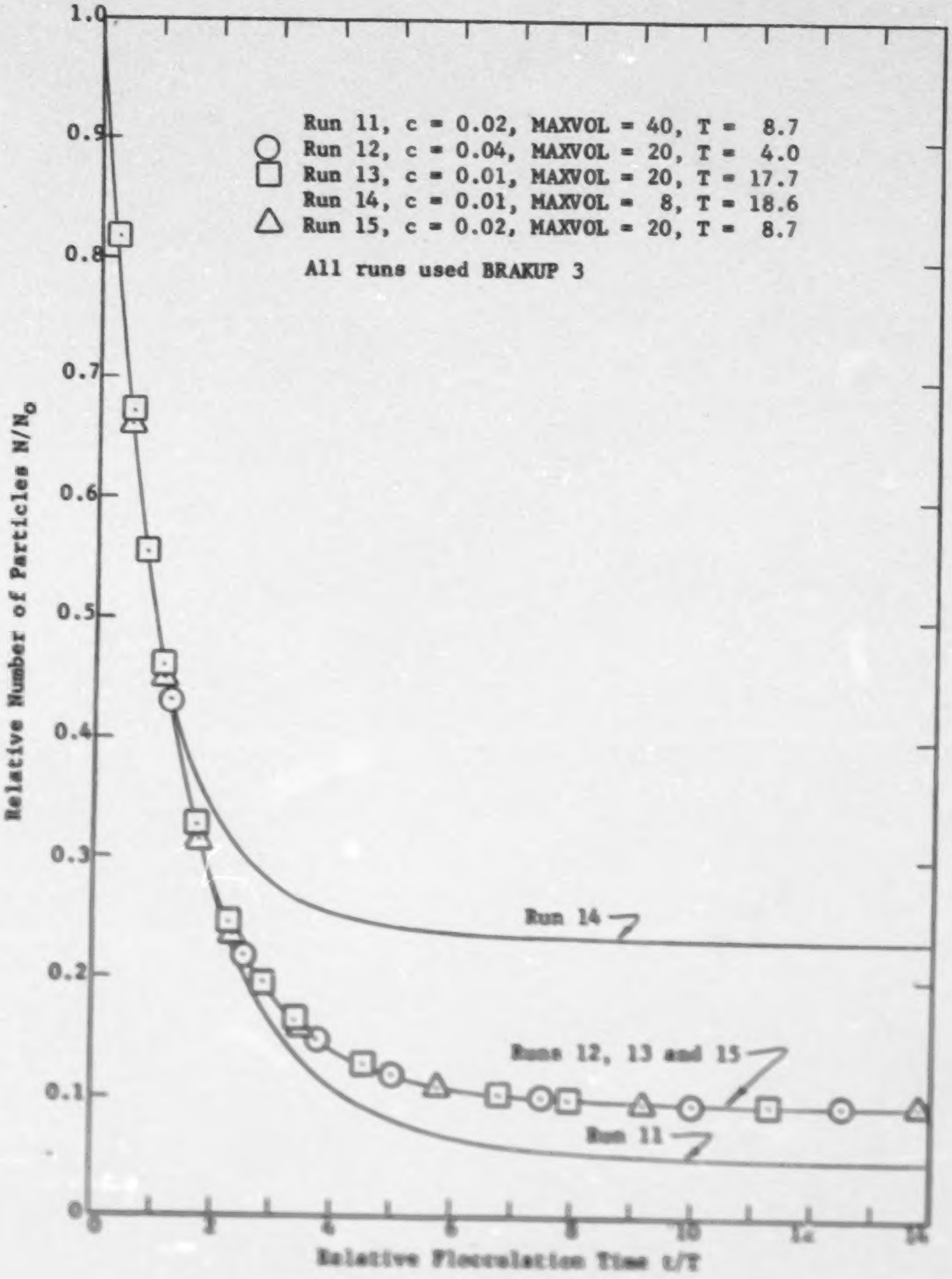

FIGURE 3-9: ORTHOKINETIC FLOCCULATION:
EFFECT OF INPUT VARIABLES ON TOTAL NUMBER OF PARTICLES

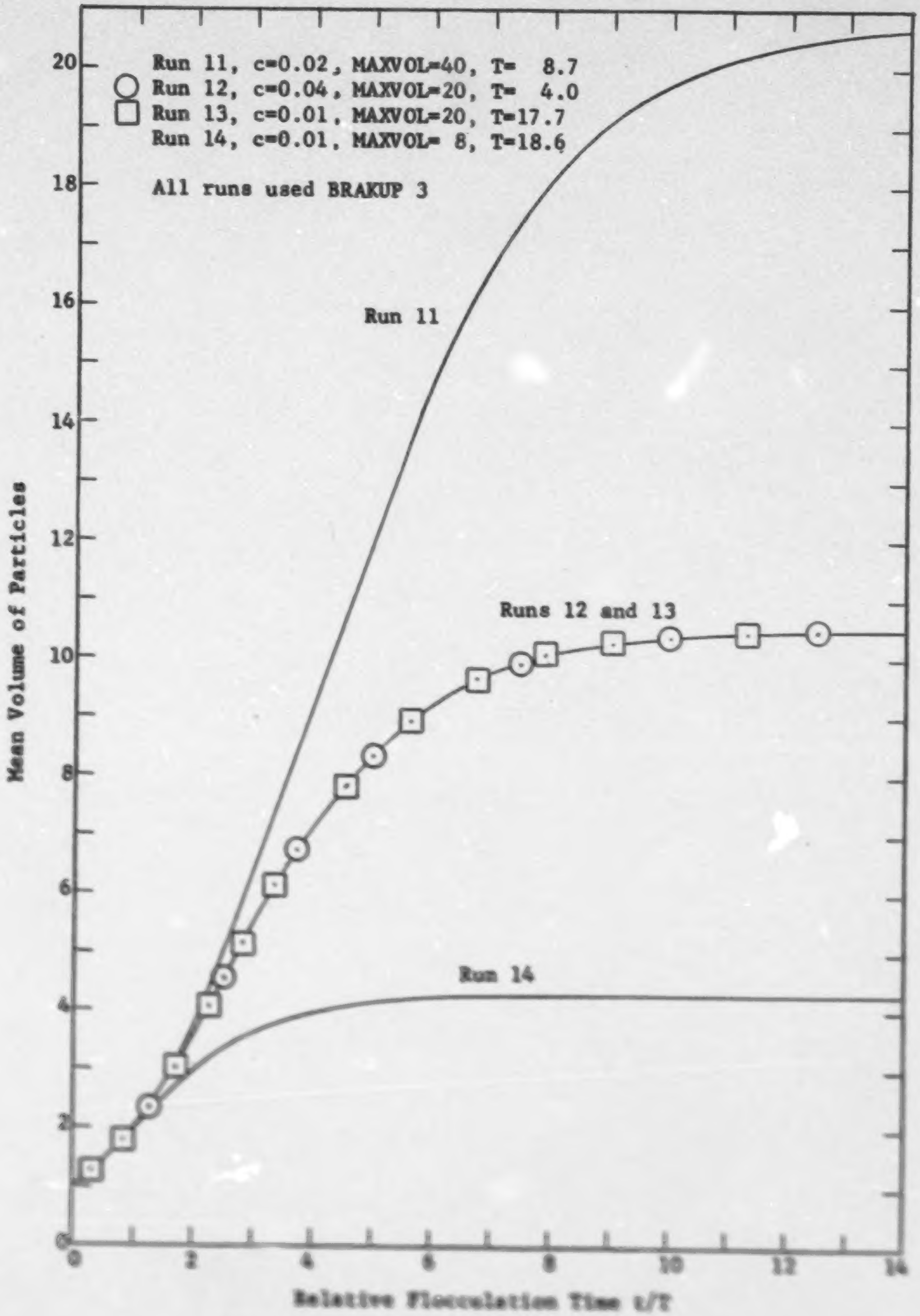

FIGURE 3-10: ORTHOKINETIC FLOCCULATION:
EFFECT OF INPUT VARIABLES ON FLOC GROWTH

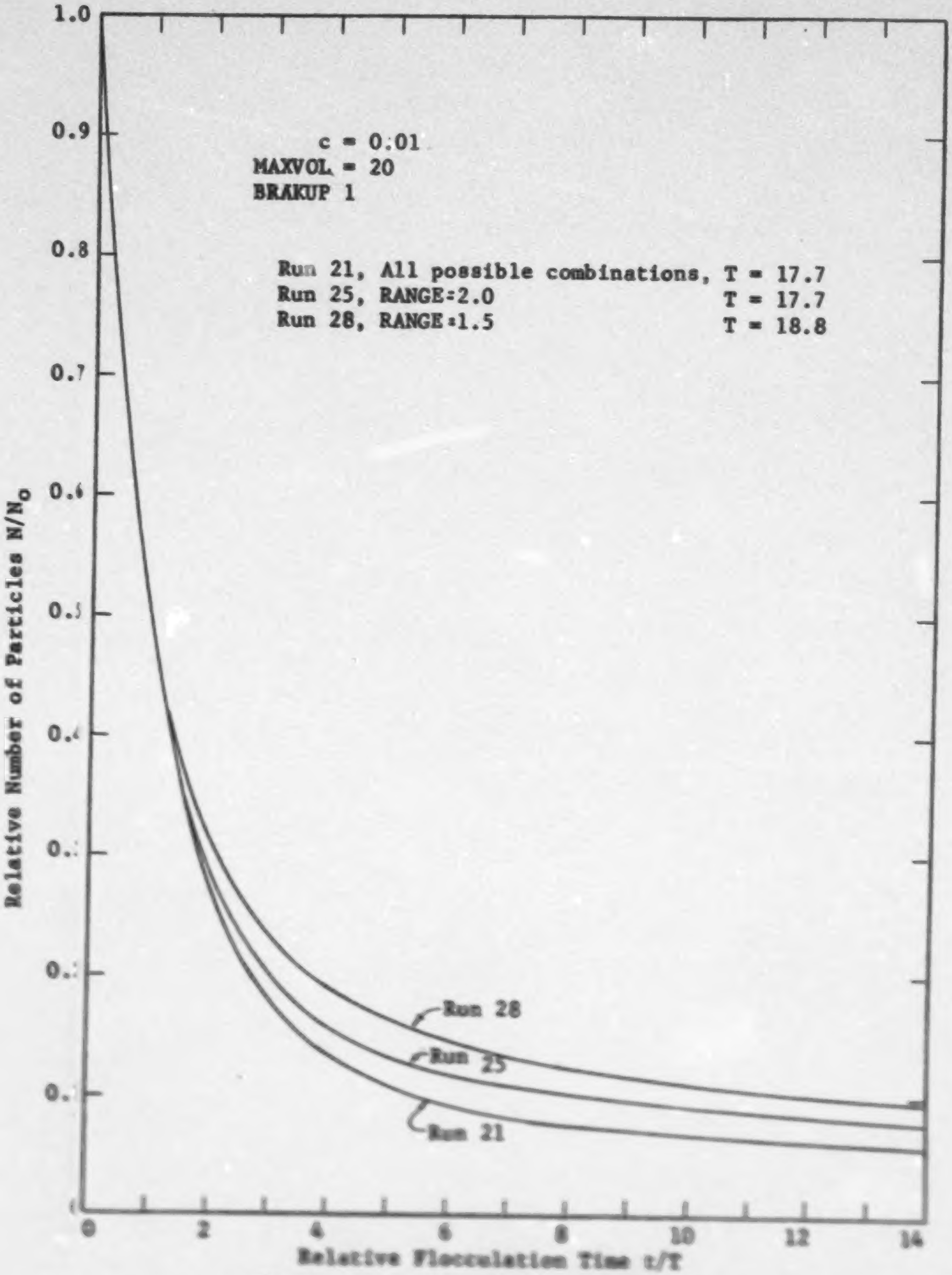

FIGURE 3-11: ORTHOKINETIC FLOCCULATION:
EFFECT OF SELECTIVE COMBINATIONS ON TOTAL NUMBER OF PARTICLES
$(1/\text{RANGE}) \leq (a_i/a_j) \leq (\text{RANGE})$

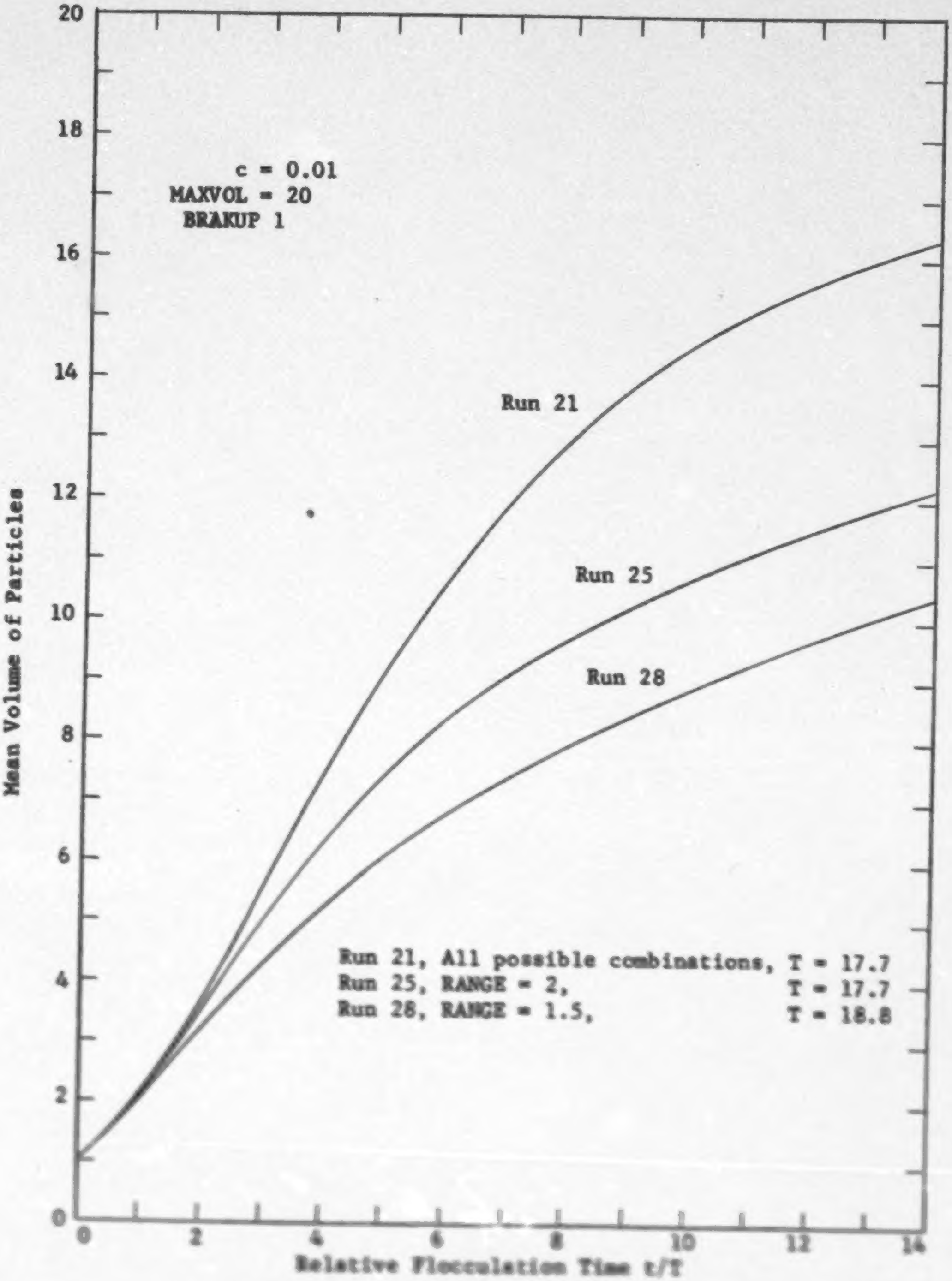

FIGURE 3-12: ORTHOKINETIC FLOCCULATION
EFFECT OF LIMITED CONTACT OPPORTUNITY ON FLOC GROWTH
$(1/\text{RANGE}) \leq (d_i/d_j) \leq (\text{RANGE})$

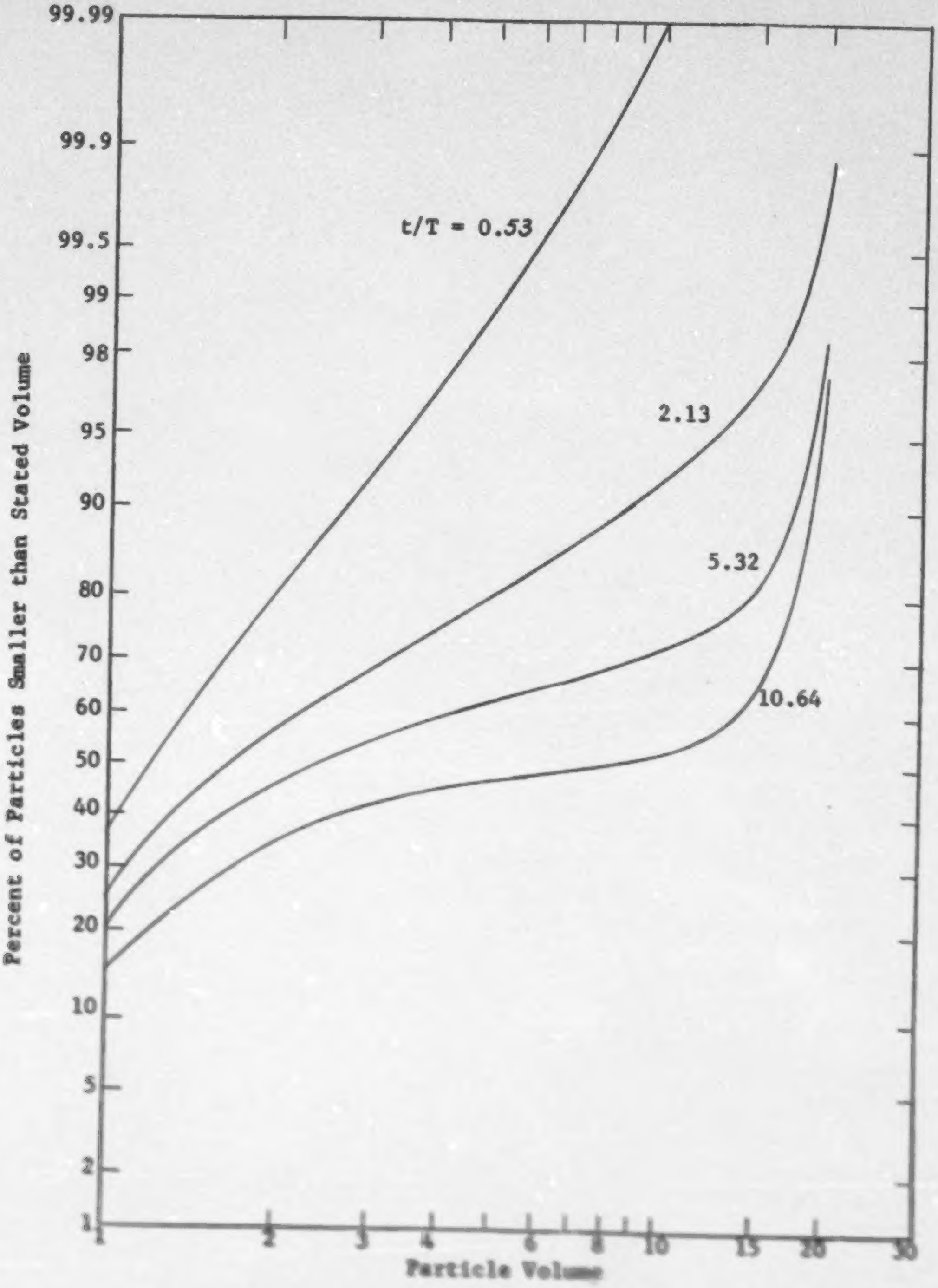

FIGURE 3-13: ORTHOKINETIC FLOCCULATION:
PARTICLE SIZE DISTRIBUTIONS OBTAINED WITH LIMITED CONTACT OPPORTUNITY
From Run 28 (Range = 1.3)

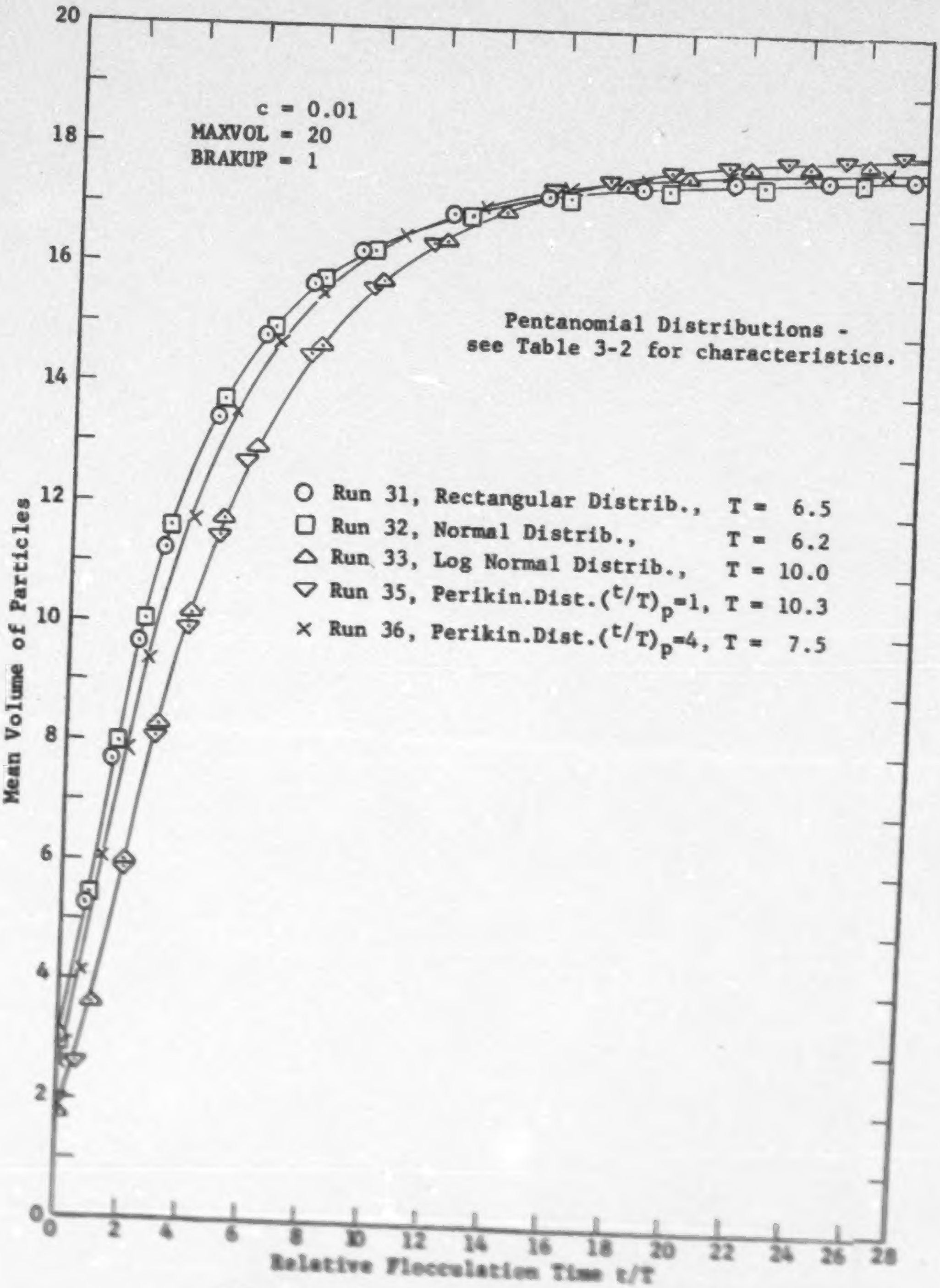

FIGURE 3-14: ORTHOKINETIC FLOCCULATION: EFFECT OF POLYDISPERSION ON FLOC GROWTH

Chapter 4

DESIGN AND CONSTRUCTION OF SHEAR GRADIENT APPARATUS

The enhancement of flocculation by velocity gradients within a suspension of dispersed particles has been postulated and analyzed mathematically in earlier chapters of this thesis. What remains to be presented is the experimental verification of the phenomenon, particularly in the chemical coagulation of water. To this purpose, parameters such as rate of floc growth and rate of color removal will be correlated with the velocity gradients to which floc is exposed, and the mathematical models for orthokinetic flocculation will be examined in the light of experimental evidence.

In practice, paddle agitators are commonly used to enhance flocculation. Unfortunately, they permit only gross estimates of the local velocity gradients that the paddles produce. Accordingly, an apparatus was needed in which known and controlled velocity gradients could be induced.

A possible system would provide Poiseuille flow through a tube. Although this would be suitable for studies over very short exposures, it would become hopelessly cumbersome for the longer flocculation periods used in most water treatment facilities; more especially so, because a vertical tube would be necessary to keep particles from settling onto the tube wall.

More practical is a system used for the study of macro-molecules and polymers and consisting of coaxial cylinders with the test fluid in the enclosed annulus. A device of this kind was employed in flocculation studies first by Mason(41) and later by Ritchie.(40) Its advantages are good definition of the velocity gradient, minimization of sedimentation, and simplification of observation of the flocculation process when the outer cylinder is transparent. The present chapter is devoted to a consideration of the design and construction of suitable devices of this kind.

Hydrodynamics of Flow between Rotating Cylinders

Motion is induced in a viscous fluid contained within the annulus between two coaxial cylinders when one cylinder is rotated relative to the other. If the radius of the outer cylinder is large in comparison with the width of the annulus, the induced flow is like that between parallel boundaries when one boundary is moved past the other, the intensity of drag on either boundary being proportional to the velocity gradient established within the fluid, and the constant of proportionality, therefore, being defined as the dynamic viscosity of the fluid. Fluid motion in annuli was first investigated by Couette(43) in 1890, the ratio of the width of the annulus to the radius of the outer cylinder being 0.017. Since then, many fluid dynamicists have concerned themselves with what has come to be known as "Couette" flow.

Equation of Motion

If the annulus is made wide in proportion to the radius of the outer cylinder, the analogy to flow between parallel plates no longer holds, but the velocity distribution in the fluid can be determined by integration of the Navier-Stokes equations.(44) Calling r the radius to any point in the annulus and letting v equal the tangential and Ω the angular velocity where $v = r\Omega$, "steady, uniform" flow in the direction of rotation transforms the pertinent Navier-Stokes equation to

$$\frac{d^2v}{dr^2} + \frac{1}{r}\frac{dv}{dr} - \frac{v}{r^2} = \frac{d^2v}{dr^2} + \frac{d}{dr}\left(\frac{v}{r}\right) = 0 \qquad (4\text{-}1)$$

or $\left(\frac{dv}{dr} + \frac{v}{r}\right)/dr = 0$, and $\frac{dv}{dr} + \frac{v}{r} = \text{constant}$.

By integration

$$v = Ar + \frac{B}{r} \qquad (4\text{-}2)$$

where A and B are both constants.

Introducing the boundary conditions $v = R_1\Omega_1$ for $r = R_1$, the radius of the inner cylinder, and $v = R_2\Omega_2$ for $r = R_2$, the radius of the outer cylinder, the simultaneous equations become

$$A = \Omega_1 - \frac{B}{R_1^2} = \Omega_2 - \frac{B}{R_2^2} \qquad (4\text{-}3)$$

and the values of A and B are determined as:

$$B = \frac{(\Omega_1 - \Omega_2)R_1^2 R_2^2}{R_2^2 - R_1^2} \qquad (4\text{-}4)$$

and

$$A = \frac{\Omega_2 R_2^2 - \Omega_1 R_1^2}{R_2^2 - R_1^2} \qquad (4\text{-}5)$$

Accordingly, the velocity distribution function is:

$$v = \frac{\Omega_2 R_2^2 - \Omega_1 R_1^2}{R_2^2 - R_1^2} \cdot r + \frac{(\Omega_1 - \Omega_2)\, R_1^2 R_2^2}{R_2^2 - R_1^2} \cdot \frac{1}{r} \qquad (4\text{-}6)$$

This equation is in agreement with the expressions developed by several authors$^{(45,46,52)}$. Its right-hand components are measures, in succession, of rigid-body rotation that is purely rotational and non-dissipative, and vortex motion that is irrotational and dissipative.

Hence, the local shear gradient that induces flocculation is the difference between the rate of change in velocity and the relative solid-body velocity, or

$$\frac{dv}{dr} - \frac{v}{r} = \frac{-2(\Omega_1 - \Omega_2) R_1^2 R_2^2}{R_2^2 - R_1^2} \cdot \frac{1}{r^2} \qquad (4\text{-}7)$$

The mean velocity gradient is then found as*

---

* The mean temporal velocity gradient G may also be determined from the rate of energy dissipation:

$$P = \text{Torque x Angular Velocity} = \tau A r(\Omega_1 - \Omega_2)$$

$$= 2\pi\tau r^2 L(\Omega_1 - \Omega_2)$$

where P is the power or rate of energy dissipation, A is the area of cylinder $2\pi rL$, L being the cylinder length, τ is the intensity of shear stress, and $(\Omega_1 - \Omega_2)$ is the relative angular velocity.

If μ is the dynamic viscosity of the fluid, and the minus sign of the shear gradient is disregarded,

$$\tau = \frac{2\mu(\Omega_1 - \Omega_2) R_1^2 R_2^2}{R_2^2 - R_1^2} \cdot \frac{1}{r^2}$$

and

$$P = \frac{4\pi \mu L(\Omega_1 - \Omega_2)^2 R_1^2 R_2^2}{(R_2^2 - R_1^2)}$$

According to Camp(35),

$$G = \left(\frac{P}{\mu \mathcal{V}}\right)^{1/2}$$

where $\frac{P}{\mathcal{V}}$ is the power dissipation per unit volume, and it follows that

$$G = \frac{2(\Omega_1 - \Omega_2) R_1 R_2}{(R_2^2 - R_1^2)}$$

$$G = \frac{1}{R_2 - R_1} \int_{R_1}^{R_2} \left(\frac{dv}{dr} - \frac{v}{r}\right) dr \qquad (4\text{-}8)$$

$$= - \frac{2(\Omega_1 - \Omega_2)\, R_1^{\,2} R_2^{\,2}}{(R_2 - R_1)(R_2^{\,2} - R_1^{\,2})} \int_{R_1}^{R_2} \frac{dr}{r^2} \qquad (4\text{-}9)$$

$$= - \frac{2(\Omega_1 - \Omega_2)\, R_1 R_2}{R_2^{\,2} - R_1^{\,2}} \qquad (4\text{-}10)$$

Experimental Confirmation

The pertinent equations have been verified experimentally by several investigators(47,48,49,50); most thoroughly perhaps by Taylor in his series of papers on the velocity distribution, torque, heat-transfer properties, and flow stability in annuli ranging in width from 0.02 to 0.38 R_2.

In general, Taylor confirmed the validity of the velocity distribution function, small defects being logically attributed to secondary currents produced by end effects in the experimental apparatus.[*] Later in this section, Taylor's work on velocity distribution is referred to again.

In reference to flow stability, Taylor observed that the rotational speed at which turbulence[†] sets in is smaller when the inner cylinder is rotated and the outer cylinder is held stationary than when the opposite is done. Responsible for this difference was the formation of a cellular vortex disturbance, symmetric about the axis of rotation and periodic along it. With the outer cylinder rotating and the inner cylinder held stationary, flow is always insensitive to disturbance of of this type and, when a critical Reynolds number is exceeded, subject to normal isotropic turbulence alone.

---

[*] See, for example, Figure 3, Part II, page 571 of reference 49.

[†] For rotation of the inner cylinder turbulence begins as cellular vortex-formation.

When both cylinders are rotated, the identification of stability becomes quite complex. Rayleigh(51) proposed the following criterion of stability for an inviscid fluid:

$$\partial(r^2 \Omega)/\partial r > 0 \qquad (4\text{-}11)$$

In analogy to equations (4-3) and (4-6), this becomes:

$$\Omega = \frac{v}{r} = A + \frac{B}{r^2} = \frac{\Omega_2 R_2^2 - \Omega_1 R_1^2}{R_2^2 - R_1^2} + \frac{(\Omega_1 - \Omega_2)\, R_1^2 R_2^2}{R_2^2 - R_1^2} \cdot \frac{1}{r^2}$$

whence

$$r^2\Omega = \frac{\Omega_2 R_2^2 - \Omega_1 R_1^2}{R_2^2 - R_1^2} \cdot r^2 + \frac{(\Omega_1 - \Omega_2)\, R_1^2 R_2^2}{R_2^2 - R_1^2}$$

and

$$\frac{\partial(r^2\Omega)}{\partial r} = \frac{\Omega_2 R_2^2 - \Omega_1 R_1^2}{R_2^2 - R_1^2}\,(2r) \qquad (4\text{-}12)$$

Accordingly, for

$$\frac{\partial(r^2\Omega)}{\partial r} > 0,\ \frac{\Omega_2 R_2^2 - \Omega_1 R_1^2}{(R_2^2 - R_1^2)} > 0\ , \qquad (4\text{-}13)$$

or

$$\Omega_2 R_2^2 > \Omega_1 R_1^2 \quad \text{and} \quad \frac{\Omega_2}{\Omega_1} > \left(\frac{R_1}{R_2}\right)^2 \qquad (4\text{-}14)$$

assuming that $\Omega_1 > 0$, a limitation that does not detract from the generality of the expression, and that the cylinders do not rotate in opposite directions.

Taylor(47) demonstrated that, for a viscous fluid, the Rayleigh criterion may be violated without penalty, particularly when Ω_2 approaches zero. As Ω_2 becomes large, however, no violation can be allowed. The violability of Rayleigh's criterion is called the critical Taylor number (T_c), and there are mathematical formulations for its prediction, such as the 1958 formulation by Chandrasekhar(52) for which he defined the Taylor number, T, as:

$$T = -\left(\frac{2}{\nu}\right)^2 ABR_2^{\,2} = \frac{-(\Omega_2 R_2^{\,2} - \Omega_1 R_1^{\,2})(\Omega_1 - \Omega_2) R_1^{\,2} R_2^{\,4}}{\left(R_2^{\,2} - R_1^{\,2}\right)^2} \qquad (4\text{-}15)$$

where ν is the kinematic viscosity of the fluid and A and B are as in equations (4-4) and (4-5). Chandrasekhar considered a symmetric perturbation of the velocity distribution equation by a periodic disturbance in the direction of the rotational axis and proposed a solution for the critical Taylor number based upon a "characteristic-value" problem involving Bessel functions. Necessary computations are tedious and time-consuming, but Chandrasekhar has tabulated a set of solutions for the case $R_1/R_2 = 0.5$, the correctness of which has been demonstrated experimentally by Donnelley(53,54).

Stability of Flow in Ritchie Apparatus

The primary apparatus constructed by Ritchie(40) in his study of flocculation consisted of two coaxial cylinders which turned in the same direction. The inner cylinder turned faster than the outer, the ratio of the rotational speeds being set by gears at one of three values. Since the motor speed could be varied to provide seven fixed values, 21 different relative rotational speeds could be obtained.

The flow stability of the apparatus can be calculated from the design and operating factors reported by Ritchie* as $R_1 = 3.18$ cm, $R_2 = 6.91$ cm, $R_1/R_2 = 0.46$, $(R_1/R_2)^2 = 0.21$, and $N_2/N_1 = 0.38$, 0.18 or 0.09.

Since the Rayleigh criterion for stability (equation 4-16) requires that Ω_2/Ω_1 be greater than R_1^2/R_2^2 or Ω_2/Ω_1 be greater than 0.21, and since N_2/N_1, which equals Ω_2/Ω_1, is greater than 0.21 in only one instance ($N_2/N_1 = 0.38$), Ritchie's apparatus satisfied the Rayleigh criterion in only one of its three ratios of rotational speeds, although the ratio of 0.18 could be marginal and should be examined further by calculating the critical Taylor number. Rearranging equation (4-15),

$$T = \left(\frac{2}{\nu}\right)^2 \Omega_1^2 R_1^4 \left[1 - \frac{\Omega_2 R_2^2}{\Omega_1 R_1^2}\right]\left[1 - \frac{\Omega_2}{\Omega_1}\right] \Big/ \left[1 - \left(\frac{R_1}{R_2}\right)^2\right]^2 \qquad (4\text{-}16)$$

and since $\Omega_1 = 2\pi N_1/60$, substitution of the given ratios of Ω and R and of $\nu = 1 \times 10^{-2}$ cm^2/sec at about 20 C establishes the numerical relationship

$$T = 7.2 \times 10^4 N_1^2 \left(1 - 4.7 \frac{\Omega_2}{\Omega_1}\right)\left(1 - \frac{\Omega_2}{\Omega_1}\right) \qquad (4\text{-}17)$$

Hence for $\Omega_2/\Omega_1 = 0.18$,

$$T = 9.1 \times 10^3 N_1^2 \qquad (4\text{-}18)$$

and since the smallest value of N_1 used by Ritchie was 20.8 rpm, $T = 3.9 \times 10^6$. To compare this value with values of the critical Taylor number T_c tabulated by Chandrasekhar[(52)] for $R_1/R_2 = 0.50$ as a function of the non-dimensional parameter

---

*See p. 104 of Reference 40.

$$K = \left[1 - \frac{\Omega_2 R_2^2}{\Omega_1 R_1^2}\right] \Big/ \left[1 - \frac{\Omega_2}{\Omega_1}\right] \qquad (4\text{-}19)$$

where $T_c = 1.6 \times 10^4$, 1.7×10^4, 1.8×10^4, and 2.0×10^4 for $K = 0.1$, 0.2, 0.3, and 0.4 respectively, we can estimate that for $\Omega_2/\Omega_1 = 0.18$ and $R_1/R_2 = 0.50$, or $K = 0.35$, $T_c < 2.0 \times 10^4$ while for $\Omega_2/\Omega_1 = 0.10$ and $R_1/R_2 = 0.46$, or $K = 0.20$, $T_c = 1.7 \times 10^4$. Therefore, we must conclude that the critical Taylor number is so much less than the smallest obtainable value of T, namely 3.9×10^6, that flow is unstable.

This conclusion about Ritchie's apparatus would be stronger if it were based on the actual rather than the estimated value of the critical Taylor number. However, necessary calculations did not seem to be warranted. For the speed range $\Omega_2/\Omega_1 = 0.09$, flow must have been unstable. Much of Ritchie's work was done with the apparatus enclosed in a light-proof box, and this may have kept him from noticing the instability of his flows.

Design of Test Cells

First Apparatus

The following criteria were considered important for the design of a test cell: (1) generation of mean shear gradients suited to biological, chemical, and physical flocculation; (2) purely laminar internal flow; and (3) if desired, continuous inflow and outflow. To satisfy these criteria and keep the drive mechanism simple, it was decided to rotate only the outer cylinder. At the same time vortex-type disturbance is avoided, and speed of rotation can be increased without penalty until the onset of isotropic turbulence, a limit well defined by Taylor.

The decision made, the velocity distribution function (equation 4-6) can be simplified because Ω_1 becomes zero. Accordingly,

$$v = \frac{\Omega_2 R_2^2}{R_2^2 - R_1^2} \quad r - \frac{R_1^2}{r} \tag{4-20}$$

$$\frac{dv}{dr} - \frac{v}{r} = \frac{2\Omega_2 \; R_1^2 \; R_2^2}{R_2^2 \; - \; R_1^2} \cdot \frac{1}{r^2} \tag{4-21}$$

and

$$G = \frac{2\Omega_2 \; R_1 \; R_2}{R_2^2 - R_1^2} \tag{4-22}$$

For rotation of the outer cylinder only, Taylor* has determined critical speeds generated at different relative widths of annulus. By fitting a straight line to that part of his plot which corresponds to a relative width of annulus greater than 0.05, the following equation was obtained for the limiting rotational speed:

$$\log \left[\frac{\Omega_2 \; R_2(R_2 - R_1)}{\nu}\right] = 5.75 + 1.88 \log \left[\frac{R_2 - R_1}{R_2}\right] \tag{4-23}$$

Solving for Ω_2 in terms of R_1 and R_2:

$$\log \Omega_2 = 5.75 + 0.88 \log (R_2 - R_1) - 2.88 \log R_2 + \log \nu$$

or $$\Omega_2 = 5.62 \times 10^5 \, \nu \, (R_2 - R_1)^{0.88} / R_2^{2.88} \tag{4-24}$$

---

* Reference 49, page 561

Substituting this value of Ω_2 in equation (4-22), the maximum attainable G value becomes

$$G_{max} = \frac{1.12 \times 10^6 \nu R_1}{(R_2+R_1)(R_2-R_1)^{0.12} R_2^{1.88}} \tag{4-25}$$

Assuming that $\nu = 1 \times 10^{-2}$ cm^2/sec (at approximately 20 C):

$$G_{max} = \frac{1.12 \times 10^4 R_1}{(R_2+R_1)(R_2-R_1)^{0.12} R_2^{1.88}} \tag{4-26}$$

Figure 4-1 is based on this equation. It shows in a family of curves as a function of R_2 the variation in maximum velocity gradients attainable for specified values of annular width. Superimposed are lines of equal rotational speed of the outer cylinder in revolutions per minute.

As can be seen, the maximum allowable width of annulus is 4.57 cm for G values of 100 sec^{-1} or more. A width of at least 2 cm was considered necessary for free growth of particles and the inner cylinder had to be large enough to allow for entrance and exit ports for continuous flow and for aerating the fluid contained in the annulus.

Accordingly, the diameters of the inner and outer cylinders were fixed at 2 and 4 in. (R_1 = 2.54 cm and R_2 = 5.08 cm), leaving an annulus 2.54 cm wide. A length of 24 in. (61 cm) was chosen in order to keep end effects from distorting the velocity distribution. The completed apparatus is shown schematically in Figure 4-2 and photographically in Figure 4-3.

In accordance with equation (4-20), the velocity distribution effected can be generalized in terms of the rotational speed of the outer cylinder N as:

$$\frac{v}{N} = \frac{2\pi}{60} \frac{R_2^{\ 2}}{(R_2^{\ 2} - R_1^{\ 2})} \left[r - \frac{R_1^{\ 2}}{r} \right] \qquad (4\text{-}27)$$

where N is revolutions per minute. For $R_2 = 5.08$ cm and $R_1 = 2.54$ cm, the curve relationship becomes

$$\frac{v}{N} = 0.139\ r - \frac{0.90}{r} \qquad (4\text{-}28)$$

See Figure 4-4.

In accordance with equation (4-22), the mean velocity gradient assumes the following function of rotational speed:

$$G = \frac{2\pi N}{60} \left[\frac{2R_1\ R_2}{R_2^{\ 2} - R_1^{\ 2}} \right] \qquad (4\text{-}29)$$

or, for the author's apparatus,

$$G = 0.14\ N \qquad (4\text{-}30)$$

The variation in local velocity gradient across the annulus may be expressed in terms of the mean velocity gradient or, as shown in Figure 4-5,

$$\left(\frac{dv}{dr} - \frac{v}{r}\right)/G = \frac{R_1 R_2}{r^2} = \frac{12.9}{r^2} \qquad (4\text{-}31)$$

Centripetal acceleration and, hence, centrifugal force vary with position in the annulus and with the rotational speed of the outer cylinder. The functional dependence of these parameters is expressed by equation (4-28). The result, expressed in terms of gravitational acceleration, is:

$$\frac{a_n}{g\ N^2} \times 10^6 = 19.68r - \frac{255}{r} + \frac{826}{r^3} \qquad (4\text{-}32)$$

where a_n is the centripetal acceleration, g is the gravitational acceleration and N is rpm. As shown in Figure 4-6, the mean centripetal acceleration averaged for width of annulus is about one-quarter that of gravity when N equals 100 rpm; for volume of annulus, it is not much more. Maximum centripetal acceleration occurs at the outer cylinder wall and is slightly less than six-tenths that of gravity. It is concluded that the maximum allowable rotational speed is determined by inception of centrifugal sedimentation rather than turbulent flow, a finding that was kept in mind in the design of a second shear apparatus.

The drive mechanism for the authors' initial apparatus is a shunt-wound direct-current motor to which groups of step-down pulleys are attached. These cut down the speed of the cylinder from 1200 rpm, the maximum speed of the motor, to approximately 50 rpm. The speed of the motor itself is controlled by a continuously variable resistor in series with the shunt. The lowest obtainable speed of rotation of the cylinder thereby drops to about 10 rpm. The actual rotational speed of the cylinder is monitored by a direct-reading tachometer.

The first test cell, as shown in Figures 4-2 and 4-3, is bounded by a 2 in. (5.08 cm) O.D. stainless steel inner cylinder and a 4 in. (10.16 cm) I.D. Lucite outer cylinder. Lucite end plates are bolted to a Lucite flange glued to the outer cylinder, with O-rings set into the end plates as gaskets. Air bubbles are removed through a small vent in one flange. The length of the annular cell is 24 in. (61.0 cm) and the enclosed volume 3.70 liters. The outer cylinder rides on the inner cylinder through machined oilite bearings in the end plates. A leather washer between the bearings and the cell prevents leakage. Also attached to one end plate is a large fiber gear which drives the outer cylinder and tachometer.

On one side of the cylinder are two 0.5 in. diameter ports each 0.62 in. (edge to edge) from either end of the cell. Stainless steel pipes within the inner cylinder lead from the ports to the outside. The experimental sample is introduced, circulated, and removed through them. They are attached to the inner cylinder with silver solder.

Operational Deficiencies

The completed shear-gradient apparatus was used in all the floc growth studies reported in this thesis. That this model possessed certain deficiencies became evident during experimentation. The most important ones were excessively long time for filling the annulus and floc sedimentation by centrifugation even at relatively low shear gradients, G.

It took five minutes to fill the annulus through the piping in the inner cylinder. This interposed an appreciable time lag between rapid-mix or coagulant dispersion and flocculation. In later studies on coagulation of colored water, the fact that this was a critical weakness of the apparatus was indeed verified.

When G values were pushed up to 10.5 sec^{-1} (75 rpm), many flocs could be observed to move at the exact speed of the outer cylinder because they had been thrown into contact with this cylinder by centrifugal force. This did not occur to any noticeable extent at lower rotational speeds.

Modified Test Cell

The defects of the first shear-gradient device were avoided in a second one which is shown in Figure 4-7. Filling time was cut down by reducing the volume of the annulus and changing the filling arrangements. Cell volume was decreased by cutting down both its width and its length. Filling was speeded up by pouring the sample into the upended cylinder after unscrewing the top, or free, end plate. The filled unit was tilted back into a horizontal position to avoid the sedimentation that takes place when the rotational axis is vertical. The supporting foundation and drive mechanism were modified to permit the shift in axis orientation, and the end plates of the annulus were slightly tapered to allow air bubbles to escape through a release cock in the center of the screw cap while the cylinder was still vertical.

The dashed lines in Figure 4-7 at the drive end of the annulus outline a flange that was attached to the inner cylinder at a later stage of development of the cell. Its purpose will be explained further on. At the same time that the flange was added, a thin teflon disk was placed between the end walls of the inner and outer cylinder to fill the small volume originally provided for clearance and to provide a bearing surface.

It was more difficult to avoid centrifugal action at wanted shear gradients. There had to be a compromise between the desired G value and the minimum acceptable width of annulus. The maximum allowable centripetal acceleration within the annulus of the modified apparatus was set at 0.3 g. This is reached at a rotational speed of about 72 rpm in the original test cell. A maximum rather than a mean centripetal acceleration was chosen for design purposes because the maximum is readily identified as

$$(a_n)_{max} = \left(\frac{2\pi N}{60}\right)^2 R_2 \tag{4-33}$$

Combination with equation (4-29) and elimination of N yields the design parameter

$$\frac{(a_n)_{max}}{G^2} = \frac{(R_2^2 - R_1^2)^2}{4R_1^2 R_2} \tag{4-34}$$

The numerator of this parameter was fixed at 294 cm sec^{-2} and the values of R_1 corresponding to given values of R_2 were found, by trial and error, for shear gradients G of 20 sec^{-1}, 50 sec^{-1}, and 100 sec^{-1}. The results obtained are recorded in Figure 4-8 in which the maximum permissible width of annulus is plotted as a function of the radius of the outer cylinder. The curve which demarks the limit of laminar flow was obtained by simultaneous elimination of the rotational speed from equations (4-24) and (4-33). The relationship for this curve is

$$R_2 - R_1 = 0.00136\, R_2^{2.705} \tag{4-35}$$

Because the number of innovations in the design of a second apparatus was large, a pilot model was constructed. The outer cylinder radius of 5.08 cm of the first apparatus was retained, but the inner cylinder radius was increased from 2.54 cm to 3.81 cm. This left an annulus 1.27 cm wide. The calculated limiting value of G was 25.4 sec^{-1}. Replacement of the chosen inner cylinder by a larger or smaller one had been made simple and the limitation on G did not seem unduly severe.

According to equation (4-29), the mean velocity gradient of the new cell was

$$G = 0.36\ N \tag{4-36}$$

and the local shear gradients were calculated from equation (4-31) to range from 1.33 G at the inner cylinder to 0.76 G at the outer one.

For flocculation runs, the coagulating solutions were combined in a beaker, placed on a paddle stirrer* for rapid mixing, and poured into the annulus through the open end of the cell in its vertical position; the cap was screwed on carefully to avoid bubble entrapment, a small volume of liquid being allowed to escape through the open vent cock; and the cell shifted to its horizontal position before starting the drive unit.

The apparatus was driven by a 1/50 -HP synchronous motor with worm-gear speed reducer having an output shaft speed of 287.5 rpm. A cone nappe with 0.8 taper and 2 in. maximum diameter was attached to the motor output-shaft. A rubber-edged pulley on the main drive shaft of the apparatus was driven by contact with the cone nappe, the drive motor being so aligned that the cone element through the contact point of the pulley was parallel to the axis of the main drive-shaft.

The pulley, attached to the drive shaft with a set screw, could be shifted in position along the cone element to vary the speed of the drive shaft. A 2 1/2 in. gear on the drive shaft meshed with a 5 in. gear of the test cell when the cell axis was made horizontal and the cell speed could be varied from 0 to 165 rpm.

---

* A paddle stirrer of the type commonly employed for jar tests was used here. The apparatus is described more completely in Chapter 6.

Trials of the new apparatus showed that secondary currents set up in the annulus, apparently by the rotation of the end walls of the cell, distributed the floc unevenly within the annulus. The secondary currents travelled along the outer cylinder wall towards the middle of the cell where they changed direction to return to the end walls along the inner cylinder wall. Flocs were divided thereby into three distinct size groups. Midway along the axis of rotation of the annulus, there was an accumulation of large flocs; in the neighborhood of the end walls, an accumulation of flocs of medium size; and in between, an accumulation of the smallest flocs only. Creation of such a secondary flow pattern had been expected, but dye tests of the first cell had shown but small rates of flow and the formation of but a single vortex across the entire length of the annulus rather than two counter vortices each covering half the length. Moreover, there was no selective separation of floc into particles of different sizes. Secondary currents took control because the second device was relatively short and narrow and the mass of water relatively small.

In order to reverse one secondary vortex and reinforce the other to establish a single vortex, a stationary flange was introduced into the inner cylinder at its closed end. The flange reached across the annulus and, unlike the opposite wall of the annulus, it did not rotate. The result was good. In general, flocs were distributed evenly through the cell, although particles did appear to grow more rapidly at the free end of the annulus during the first two or three minutes of flocculation because of a high shear gradient within the space between the screw cap and the end of the stationary inner cylinder.

The modified apparatus was not used for floc growth studies. Instead, a small number of color-removal experiments were conducted with it. They are reported in Chapter 6 of this thesis.

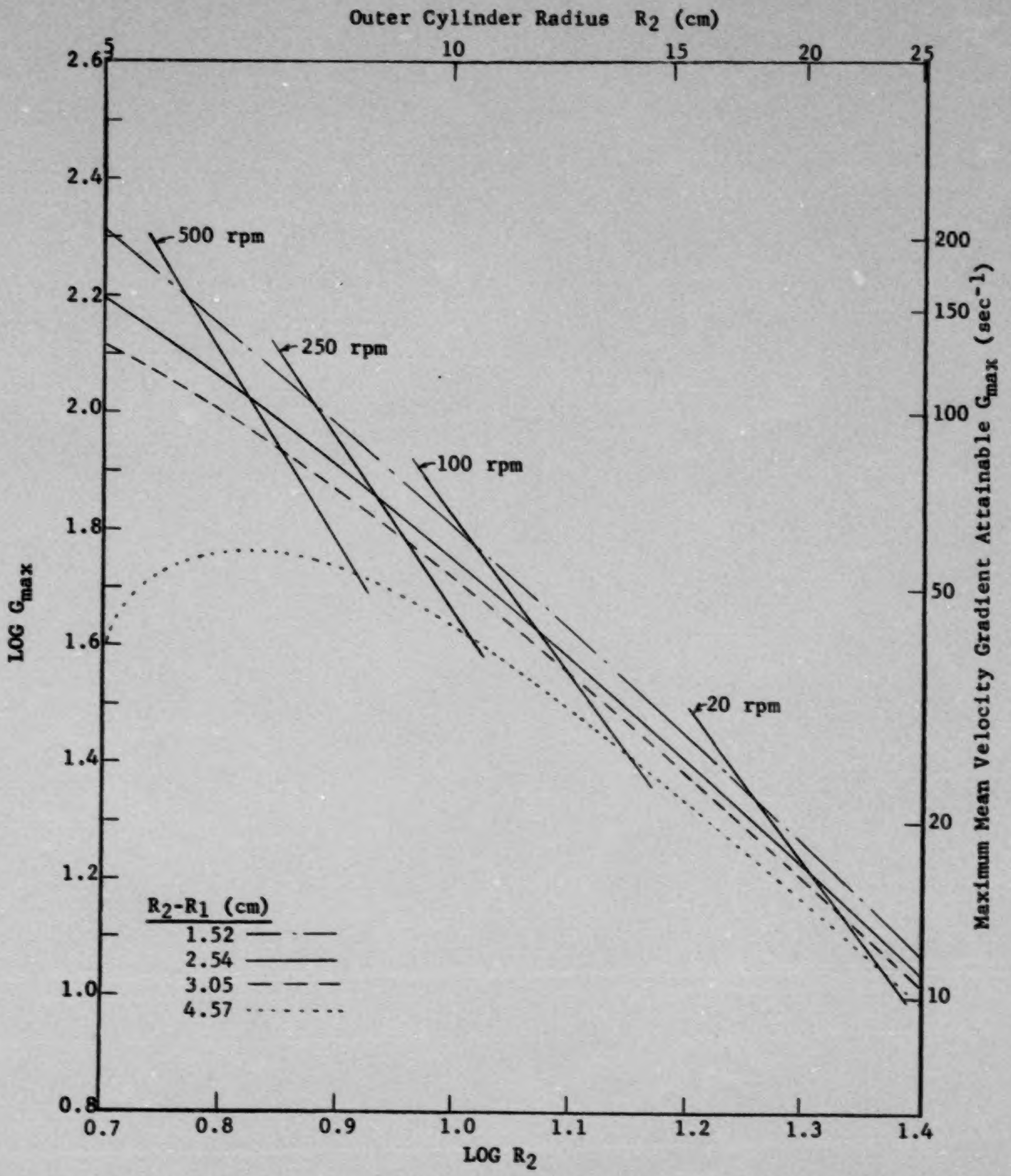

FIGURE 4-1: SHEAR APPARATUS DESIGN CHART

Logarithmic plot of the maximum mean velocity gradient attainable as a function of the radius of the outer cylinder for specified widths of the annulus. Also shown are the corresponding maximum rotational speeds in rpm.

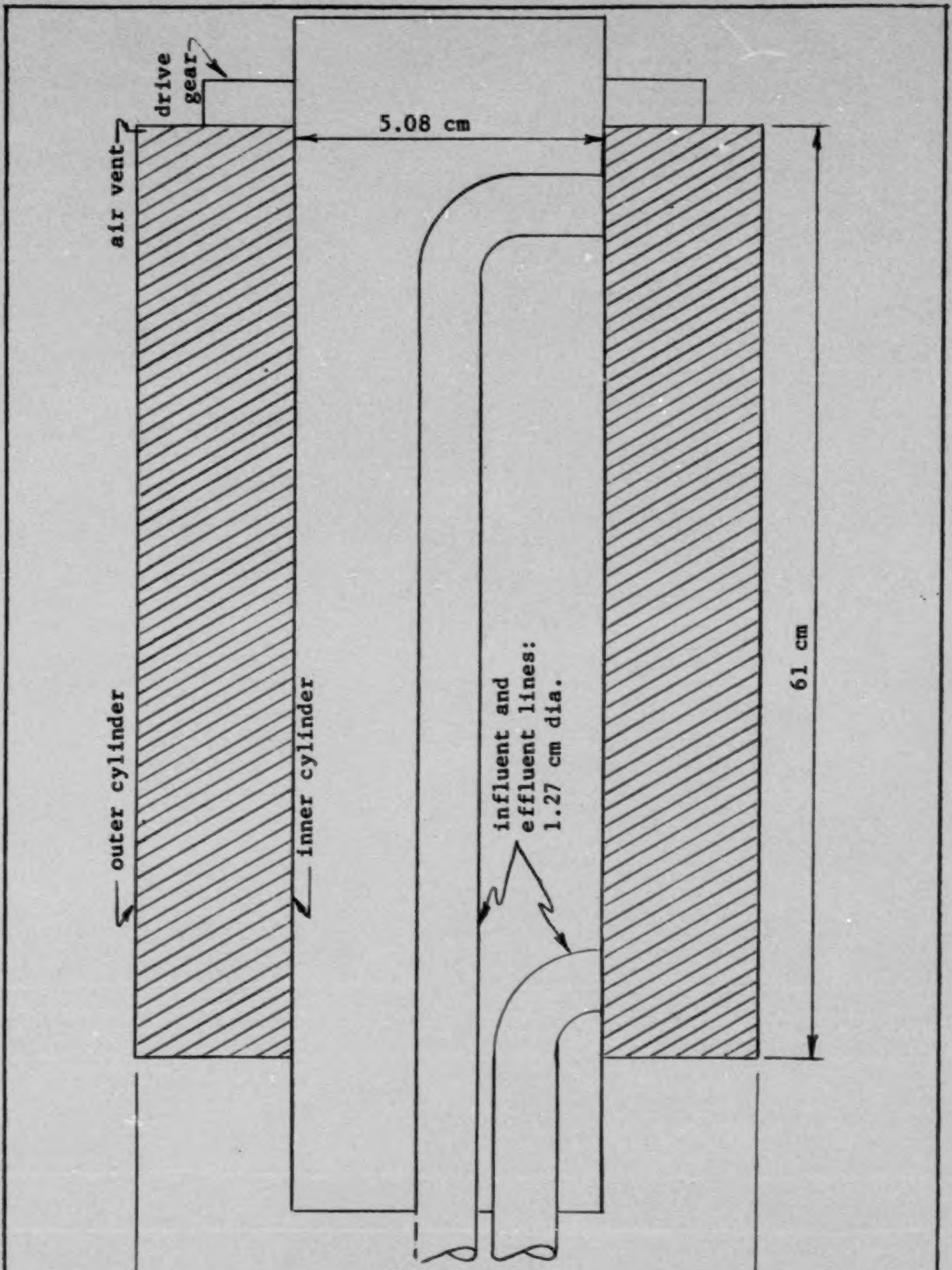
drive gear
air vent
5.08 cm
outer cylinder
inner cylinder
influent and effluent lines: 1.27 cm dia.
61 cm
10.16 cm

FIGURE 4-2. SCHEMATIC DIAGRAM OF FIRST SHEAR APPARATUS. Shaded area designates flocculation chamber. Drawing is not to scale.

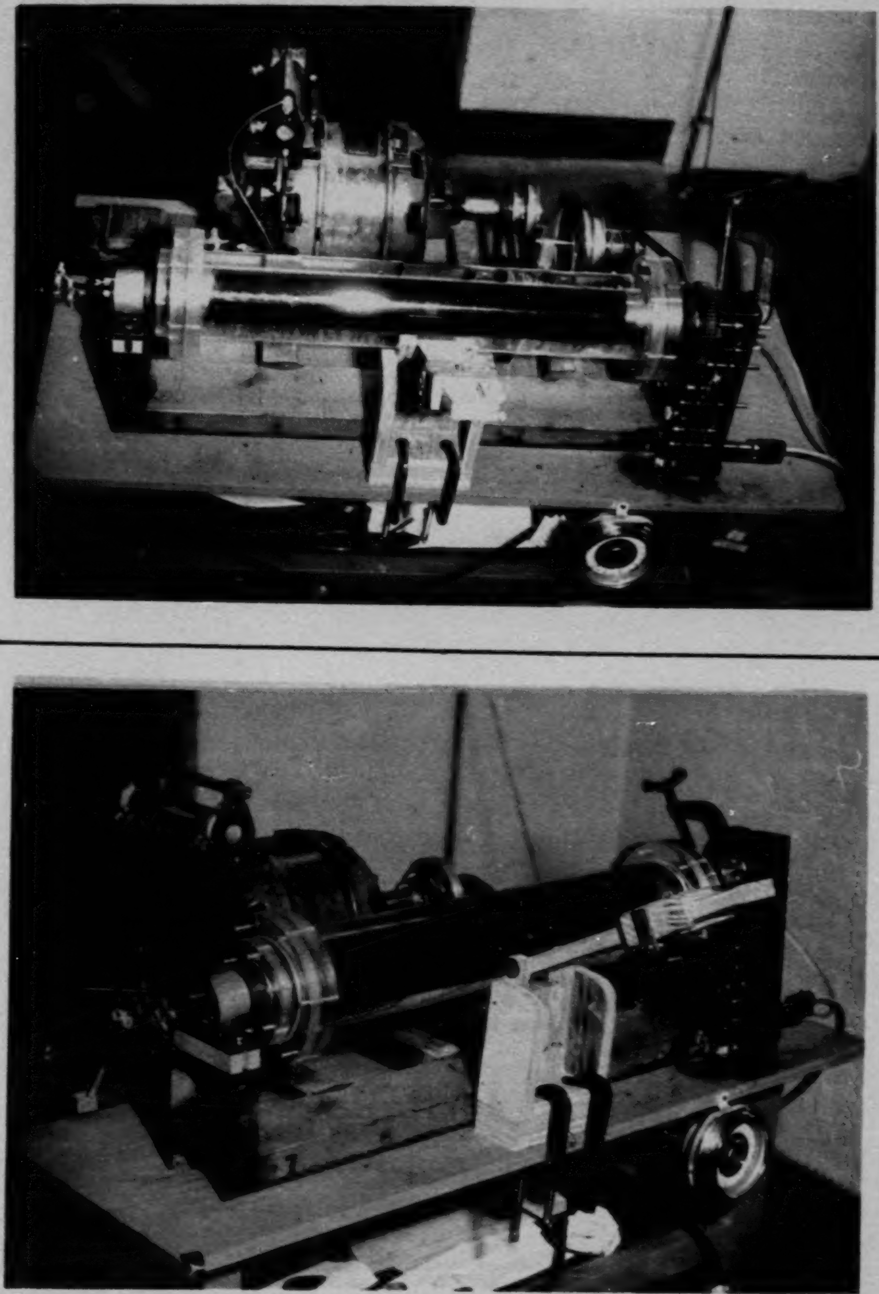

FIGURE 4-3. TWO VIEWS OF FIRST SHEAR APPARATUS.
Wooden bracket serves as camera mount.

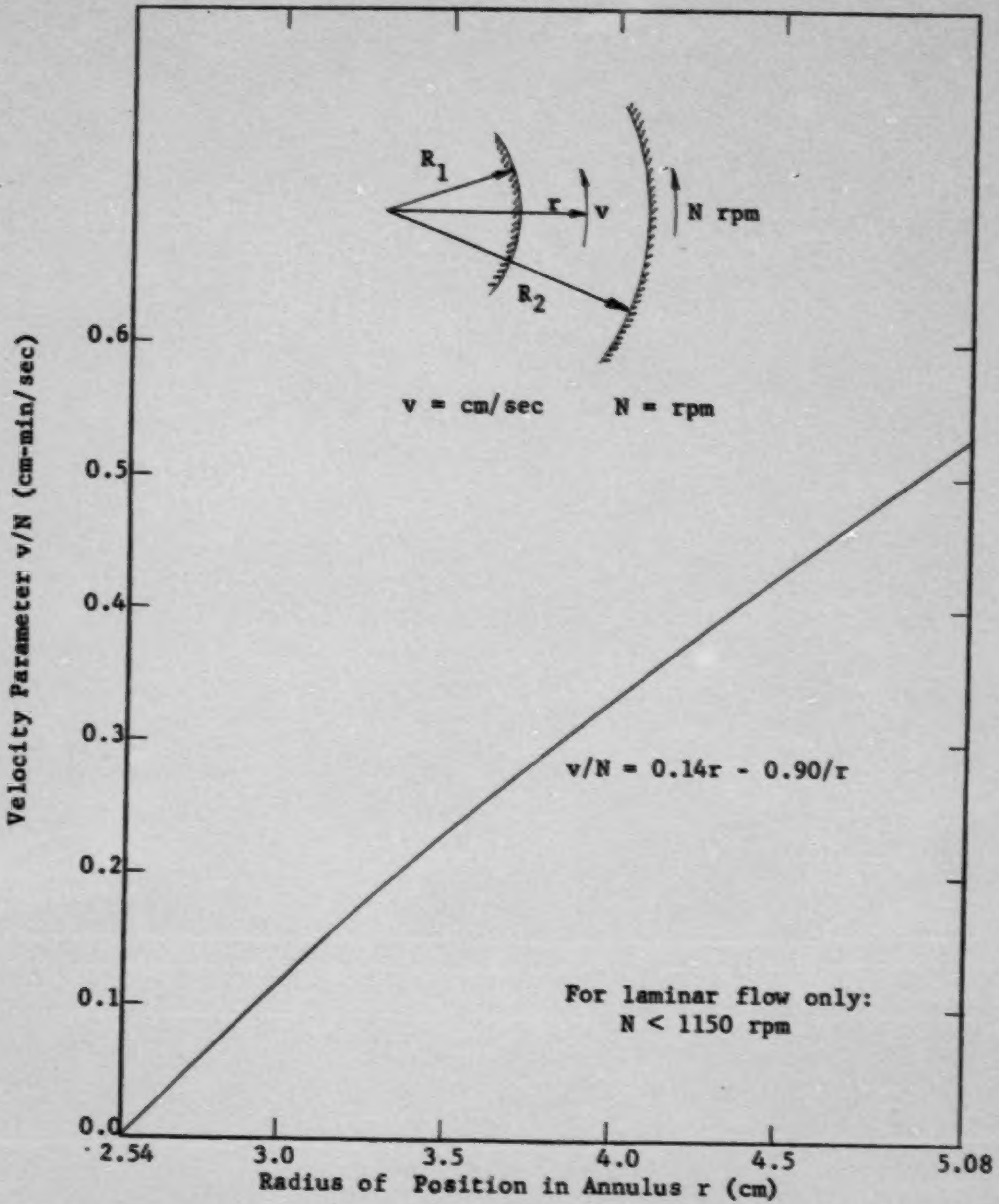

FIGURE 4-4. VELOCITY PARAMETER AS A FUNCTION OF POSITION IN ANNULUS FOR FIRST SHEAR APPARATUS.

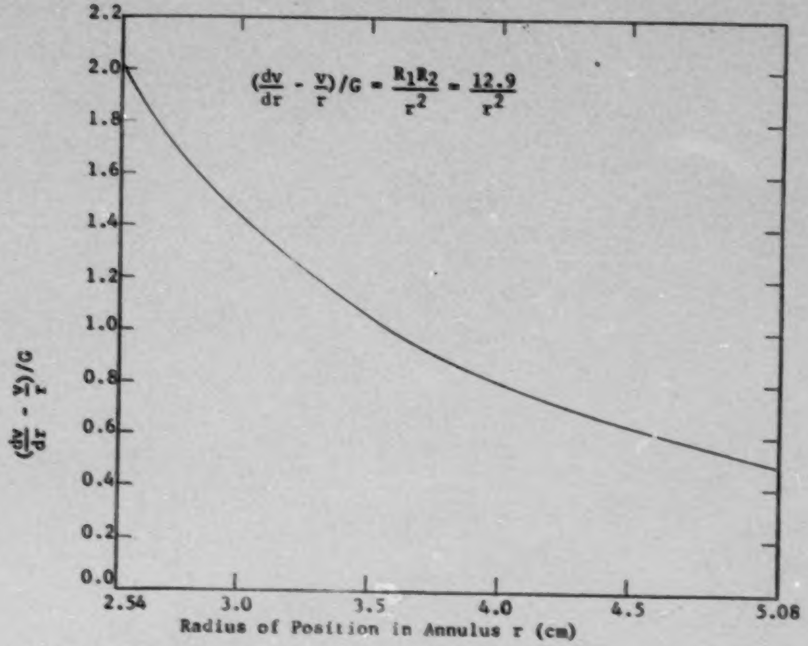

FIGURE 4-5. VARIATION IN SHEAR GRADIENT ACROSS ANNULUS OF FIRST SHEAR APPARATUS

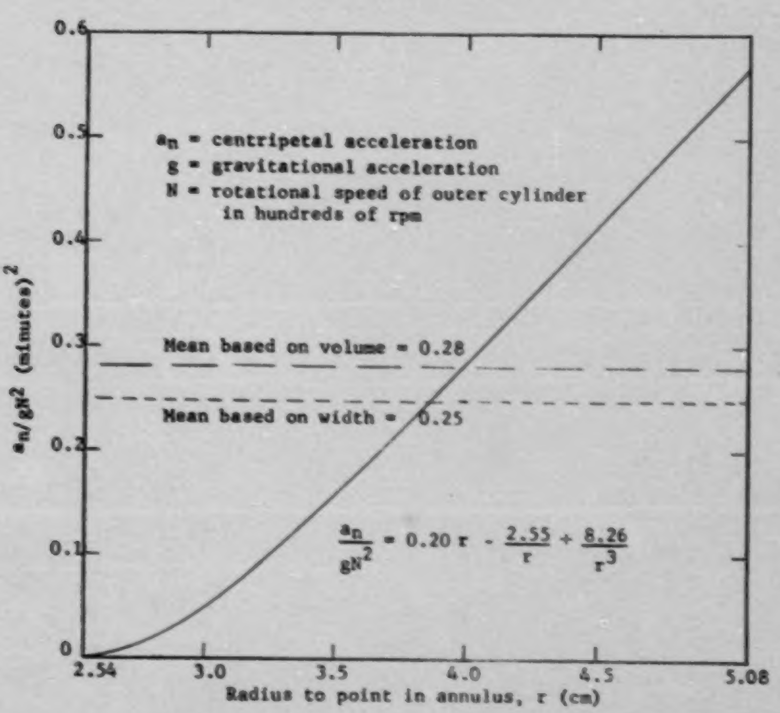

FIGURE 4-6. VARIATION IN CENTRIPETAL ACCELERATION PARAMETER WITHIN ANNULUS OF FIRST SHEAR APPARATUS.

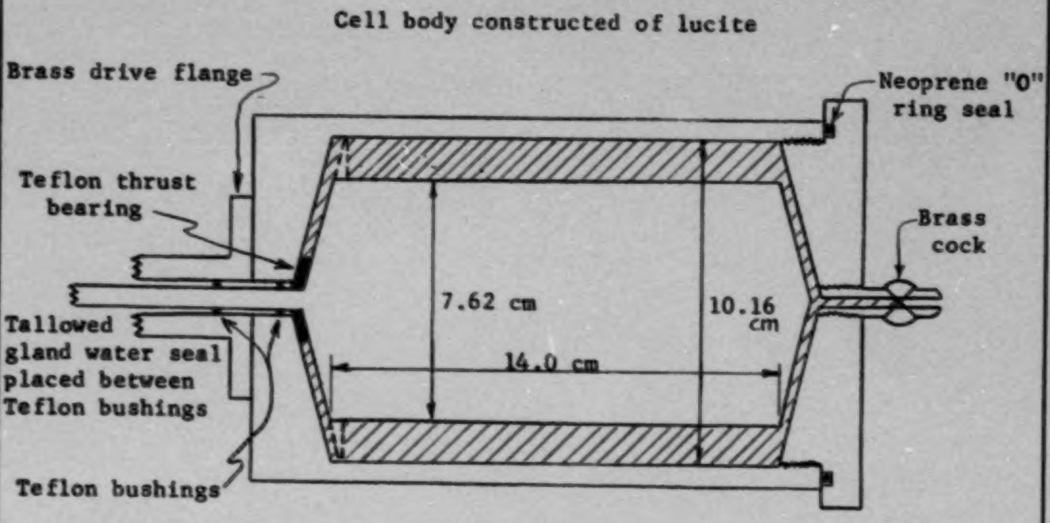
Cell body constructed of lucite
Brass drive flange
Neoprene "O" ring seal
Teflon thrust bearing
Brass cock
7.62 cm
10.16 cm
14.0 cm
Tallowed gland water seal placed between Teflon bushings
Teflon bushings

(a) Sectional View

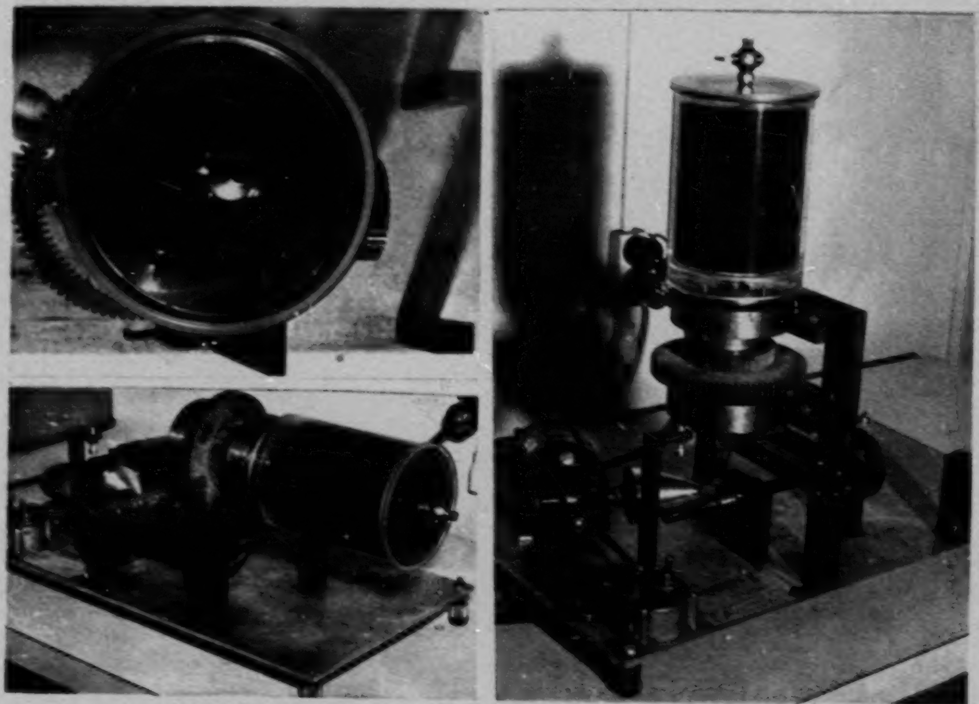

(b) Three Exterior Views

FIGURE 4-7. SECOND SHEAR APPARATUS

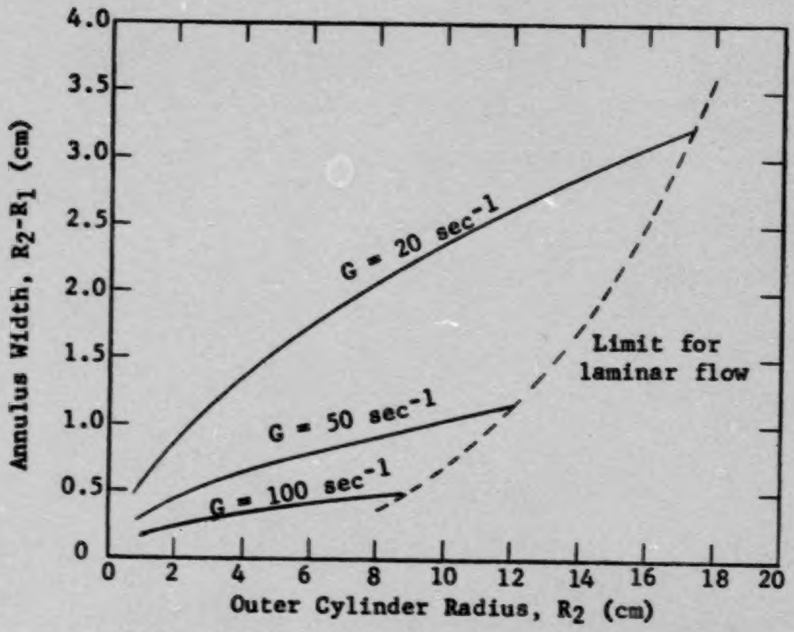

FIGURE 4-8. MODIFIED SHEAR APPARATUS DESIGN CHART. Maximum centripetal acceleration equal to 0.3 times acceleration of gravity.

Chapter 5

FLOC GROWTH STUDIES

The conception of coagulation as a four-stage process in which each stage is a separate operation implies that a unique purpose is served by each operation. As stated before, the primary role of flocculation is the promotion of floc growth for ease of "phase separation" or removal from the liquid. For the common processes of water treatment, two floc characteristics are especially important measures of ease of phase separation: floc size, shape being implied, and floc density. A third characteristic, not easily defined operationally, is floc toughness or resistance to breakup. Toughness is more important when floc is separated from the suspending water in the pore space of high-rate filters than when floc drops from suspension in the relative quiescence of a sedimentation basin. There is also the matter of floc breakup during passage of the suspending fluid from flocculation units to phase-separation units.

Of the three floc characteristics, size is measured most readily, yet not simply or fully. Moreover, any workable evaluation of density or of toughness must inherently be referred back to floc size.[*] Determination of both size and density by observing rates of sedimentation generally neglects the flocculation that takes place during sedimentation and so places the results in doubt.

Measurement of Floc Size

Flocs must be measured in place and, insofar as possible, instantaneously. They cannot be examined individually under the microscope, because they are normally too fragile to be withdrawn from suspension. Moreover, if the suspending fluid is not stirred continuously during size measurement, the floc will break up in the decelerating fluid.

---

[*] Accordingly, the term growth refers in this thesis primarily to increases and decreases in size.

Floc size can be measured directly or indirectly. Direct measurements are made on the floc itself or on a suitably recorded image of the floc. Illustrative of indirect measurement is the calculation of particle size from observations of the light-scattering or viscous properties of floc suspensions.

On first thought, light-scattering* measurements seemed promising for the studies. Measurements can be continuous, and data can be recorded without disturbing the flocculating suspension. However, on further thought, this technique was rejected for the following reasons: (1) light-scattering is not readily related to particle size when the particles are irregular in shape - particularly so, when they are large - and particles of known size must be used, in any case, to calibrate the required optical instruments; (2) particle size distributions are not readily identified by light-scattering techniques; (3) necessary equipment is delicate and expensive, and its assemblage and testing are time-consuming. Indeed, no one, as yet, appears to have been successful in applying light-scattering techniques to particle-size measurement during flocculation of large particles.

The method of choice, in the studies here reported, was the evaluation of particle size from photographs of the floc taken in situ. A study of this kind, it was reasoned, would at least provide the preliminary information on which more sophisticated techniques of measurement could eventually be based.

---

* The term light-scattering is meant to include other forms of light measurement techniques such as transmittance and reflectance.

To be successful, two photographic requirements had to be placed in balance. Exposure time had to be short enough to minimize floc motion, and the photograph had to be sharp enough to capture small particles. Unfortunately, floc can, in fact, be magnified only at the expense of increasing the apparent distance traveled by particles during exposure.

Short exposure can be obtained by electronic flash lighting. However, if flash units are to be reasonably priced, flashes can be no shorter than $2x10^{-4}$ sec. How far a floc particle can travel in this time can be estimated from Figure 4-4 in the preceding chapter of this thesis. If the particle is close to the outer cylinder of the annulus and the apparatus is operated at a rotational speed of 100 rpm, particle velocity is about 500 mm/sec. In $2x10^{-4}$ sec, therefore, travel is 10^{-1} mm. At higher rotational speeds the distances are proportionately larger. Restriction of floc movement ruled out high-magnification photomicrography. A reflex camera with extension tubes was used instead. Direct linear magnification up to 4 times the actual size could be achieved, and the film itself could be further magnified.

Strictly speaking, the size of a particle is its volume. For some regular shapes, volume is a function of a single dimension of length; for others, of two or more dimensions of length, generally referred to as diameters. For the settling of particles, the cross-sectional area at right angles to flow is an important dimensional attribute.

Alternative Size Measures

For these investigations, area and diameter were both obtainable and informative measurements, whereas volume was an informative but essentially unobtainable measurement in a practical sense. Common parameters of area for irregular particles are the equivalent circle and the equivalent rectangle. The equivalent rectangle is a measure of shape as well as size. Its length and width approximate those of the floc image, and their product approximates the projected area of the floc.

Preliminary measurements of the equivalent rectangle indicated much observational bias. To avoid this, major and minor diameters were measured to form a product-estimate of area. The major diameter was defined as the longest dimension of the particle, the minor diameter as its widest dimension at right angles to the major axis. Although the resulting area is obviously biased on the large side, identification of the diameters is no longer a matter of personal judgment. This cannot be said about the dimensions of the equivalent rectangle. Use of a single linear dimension was considered, but none of the measures commonly used seemed preferable to the areal parameter just described.

Experimental Procedure

All floc growth studies were performed in the first shear gradient device described in Chapter 4. The camera was mounted near but not at the midpoint of the cylinder directed at right angles to the axis of rotation and downward at an angle of about 30 degrees from the horizontal.

It was an EXA model II reflex camera equipped with a f/3.5 Myer Primotar lens. Extension tubes were fitted to the lens for close-up photography, and the film image was consequently nearly true to size. Three different combinations of tubes gave linear magnifications of 0.75X, 1.28X, and 1.35X.

An Ultrablitz Rocket electronic flash unit with 2×10^{-4} sec flash "stopped" floc motion and provided enough light for photography. The flash tube was held 20 in. above the camera, and its light entered the annulus at right angles to the axis of the camera and the axis of rotation of the cylinder. The beam was sufficiently intense for photographing the floc at a normal level of room lighting and a camera lens aperture of f/16. At the same time, the floc itself could be observed continually and unusual floc conditions noted. The film was Panatomic X, a fine-grained, medium-contrast Eastman Kodak product. Negatives were developed in accordance with the manufacturer's instructions. Some photographs with high-contrast "microfile" film looked promising enough for floc-size studies but showed so little detail of floc structure that overlapping floc images could not be differentiated.

Photographic magnification was identified with the help of three control lines etched at 5 mm intervals on the surface of the inner cylinder of the shear gradient apparatus. At the start of each test - after the annulus had been filled, but before rotation was begun - the camera was focused sharply on these lines and a photograph taken. The camera was then moved back 1/2 in. This shifted the focus to a point well within the annulus without altering the camera lens-to-film distance. Accordingly, magnification remained unchanged, and linear magnification could be computed from the apparent distance between the scribed lines.

The longer dimension of the film negative was kept parallel to the axis of rotation, and the extent of annulus volume reproduced photographically was determined from pictures of additional grids on the inner and outer boundary surfaces of the annulus. Corresponding to a camera magnification of 0.75X was a pictured fluid volume of 38.6 ml, or approximately 1% of the total contents of the annulus. For other magnifications, the volume varied approximately inversely as the square of the magnification.

Interposition of the outer cylinder wall and the intervening layer of water distorted the floc image by refraction. The amount of distortion was determined from photographs of rigid beads attached to a rod fixed at different positions in the annulus. With the camera half an inch back from the focal point on the inner cylinder, the recorded dimensions of the beads parallel to the direction of the rotational axis of the cell were too large or too small by 8% when they were held close to the outer and inner cylinder walls respectively. The discrepancy changed essentially linearly across the thickness of the annulus, and no error was detected when the beads were placed in sharp focus. The photographic dimensions of the beads in the direction of rotation of the cell were consistently too large. The departure was 12% at the outer cylinder, 8% at the point of focus, and 4% at the inner cylinder. Nevertheless, floc measurements were not corrected accordingly because the orientation of flocs was almost infinitely variable in any case.

Some personal judgment entered into recognition of floc boundaries on the film. Some boundaries were not clearly delineated; there was overlapping of flocs; and individual images were not distinctly separated. Presumably, these are compensating errors.

Flocculation runs were ordered as follows. The required amount of coagulant was added to a bicarbonate solution in a 4 liter aspirator bottle and the mixture agitated by inverting the bottle in quick succession about 40 times. The bottle was then placed on a shelf above the shear apparatus and connected by tubing to the ports of its inner cylinder. The flocculation mixture flowed into the test cell by gravity, the rate being controlled by regulating the rate of air escape. This took about 5 min., after which the air vent was closed and rotation of the outer cylinder begun. This was recorded as zero time. Ferric sulfate was the coagulant.

Experiments Conducted

The floc growth tests fell into three categories. In the first, the mean velocity gradient was made the primary variable. Floc growth was recorded photographically while a constant mean velocity gradient was maintained. Observations at G values of 3.2 sec^{-1}, 6.8 sec^{-1}, and 9.3 sec^{-1} composed the set. The same amounts of $Fe_2(SO_4)_3$ and $NaHCO_3$ were used in each experiment, the flocculating mixture being initially $1.6x10^{-4}$ molar in $Fe_2(SO_4)_3$ and 10^{-2} molar in $NaHCO_3$. The resulting pH was 6.8. Figures 5-1 and 5-2 are typical pictures of floc in two of the experiments. Tests conducted at G values greater than 9.3 sec^{-1} proved unsatisfactory because of excessive centrifugal separation of the floc from the liquid.

In the second group of experiments, the reproducibility of the data and the effect of increasing the coagulant dose were tested. The G value was 3.2 sec^{-1}, and the bicarbonate solution was again 10^{-2} molar. However, the coagulant dose was increased fourfold so that the flocculating mixture was initially 6.4×10^{-4} molar in ferric sulfate. The resulting pH was 6.3, a value well within the optimal range for the coagulant as determined by jar tests. Each experiment was repeated twice. A typical sequence of floc pictures from one of the three studies is shown in Figure 5-3.

In the third group of tests, floc growth was observed during coagulation of artificially colored water, 38 mg/l of instant coffee being added to a 10^{-2} molar bicarbonate solution. A coagulant dose of 7.5×10^{-4} mol of ferric sulfate per liter of flocculating mixture was found to be optimal in jar tests. The advantages of instant coffee as a water-coloring agent for coagulation studies are discussed in Chapter 6 of this thesis. Three sets of tests were run, all at constant mean velocity gradients of 3.2 sec^{-1}. The sequence of floc growth pictures shown in Figure 5-4 comes from one of the three experiments comprising the final group.

Analysis of Floc Pictures

The floc images on the films were magnified for measurement. This was done in two ways. In the first, negatives were magnified about 15X by strip-film projection onto a screen; only flocs deemed sharply in focus were measured; about 20 to 40 such particles were found in each frame; and all the films comprising the floc growth studies were examined. The measurements obtained are analyzed in Figures 5-5, 5-6, 5-14, and 5-15.

In the second method of measurement, enlargements were made from the film negatives on 11x14 in. high-contrast Kodabromide paper with a magnification of about 9.5 x. Films for the first category of runs were re-examined in this way. To increase the size of sample comprising each observed point, all of the flocs appearing on the prints were measured no matter whether they were sharply in focus or not. The errors in measurement caused by distortion of the image were accordingly greater. However, many small particles that could not be readily distinguished as in focus were captured. These flocs were generally not visible with the first method of magnification, probably because of poor contrast in the projected negative. The improved contrast of the prints also showed more details of floc structure and so simplified the measurement of overlapping floc images. Moreover, the advantage of the larger size of sample partially offset the disadvantage of lower precision of measurement.

All of the larger flocs in each print were measured individually, the cut-off point being flocs somewhat smaller than $5x10^{-1}$ mm^2. In addition, flocs as small as $7.5x10^{-3}$ to 2.3×10^{-2} mm^2 were measured in representative sections of the prints and their areal contribution added to the overall sample in proportion to the particle count for the print as a whole.

Measurements were examined in three ways. Changes in mean floc size during flocculation were determined for particle size distributions truncated at two or more discrete levels: all flocs larger than $2.3x10^{-2}$ mm^2; all flocs larger than $5x10^{-1}$ mm^2; and, in one case, all flocs larger than 1.0 mm^2. The lowest truncation insured the comparability of data taken from films at different magnifications. The upper levels detailed the behavior of the larger flocs. These analyses are shown in Figures 5-7 and 5-8.

Floc size distribution was also determined in two ways, both of them including all particles larger than 2.3×10^{-2} mm^2 in size. In one, the summation curves recorded the proportional number of particles larger than the various stated sizes; in the other, they recorded the proportional area of floc. Since both types of distribution were much the same, only the distribution by number is shown in Figures 5-9 and 5-10.

Discussion of Results

Flocculation at different G values: The first group of experiments in which G was held constant for each run exhibits well developed time-size maxima or modes in floc growth patterns at different G values (see Figure 5-5). Replotting the observations, as in Figure 5-6, against the non-dimensional product Gt, the modes are seen to fall within the range $7000 < Gt < 11,000$, or near the lower boundary of the range of flocculation presently considered effective. Beyond the mode, mean floc size remains nearly constant during further flocculation.

Re-evaluation of the film records for these data by the second technique of floc measurement produced the results shown in Figure 5-7. Mean floc sizes were calculated from observed size distributions truncated at two or more levels by disregarding, for each mean size, flocs smaller than some terminal magnitude. The smallest size of truncation was $2.3\text{x}10^{-2}$ mm^2, namely, the smallest floc size measured consistently in all three flocculation tests. A second size of truncation was $5\text{x}10^{-1}$ mm^2. At the smaller sizes, measurements were restricted to a few representative sections of each photograph, the results being translated to the larger volumetric sample by a total floc count. In one run, G = 3.2 sec^{-1}, a third truncation size of 1.0 mm^2 was chosen to illustrate the response of large flocs.

Examination of the three floc growth curves in Figure 5-7 at G = 3.2 sec^{-1} shows that the observed mode of the size-time relationship depends on the degree of truncation. As smaller flocs are added to the count, the mode is suppressed more and more until there is none left. Similar conclusions can be drawn for flocculation at G = 6.8 sec^{-1} and 9.3 sec^{-1}, except that modes are not eliminated when the count reaches down to flocs as small as $2.3\text{x}10^{-2}$ mm^2. The floc growth curves of Figure 5-7 agree reasonably well in shape with the curves of Figure 5-5, although the modes or size-shear maxima are more pronounced in Figure 5-5. The curves in Figure 5-7 for G = 3.2 sec^{-1} and truncations at $2.3\text{x}10^{-2}$ mm^2 and $5\text{x}10^{-1}$ mm^2 straddle the curve for the same G value in Figure 5-5. The curve for G = 6.8 sec^{-1} in Figure 5-5 is much the same as that in Figure 5-7 for truncation at $5\text{x}10^{-1}$ mm^2 at the same G value. This is true also for the growth pattern observed at G = 9.3 sec^{-1}, except that the mode appears more quickly in Figure 5-7 than in Figure 5-5. However, there is some doubt about the validity of the curves for flocculation at G = 9.3 sec^{-1} shown in Figure 5-7 because numerous large flocs in the pertinent pictures were out of focus. In this run, the operating speed of the shear gradient apparatus was near the critical point for appreciable centrifugal sedimentation. Undoubtedly, the large flocs had reached the outer cylinder wall where they gained structural support before shearing of the liquid could rupture them. Therefore, the supported flocs could grow much larger than unsupported flocs remaining within the liquid itself. For this reason, the supported flocs were not included in the analysis of the data, thereby virtually excluding flocs of large size from the sample.

Interestingly enough, the rate of floc growth during the first few minutes of flocculation was not proved to be increased by stepping up the G value. If anything, the converse seemed to hold true. Since good photographs could not be taken during the first two or three minutes while flocs were very small, the true effect remains in doubt. For the same times of flocculation, moreover, mean floc size is always less at high G values than at low ones. This is shown more explicitly in Figure 5-8 in which the observed mean floc size at the mode is plotted as a function of 1/G for size-distribution truncations of 5×10^{-1} mm^2 and 2.3×10^{-2} mm^2. Since no mode was observed for $G = 3.2$ sec^{-1} and truncation at 2.3×10^{-2} mm^2, the extreme values of the essentially linear "steady-state" portion of the relationship were used to establish a modal range. According to Figure 5-8, the modal size appears to be nearly proportional to 1/G, the value of the proportionality constant being dependent on the degree of truncation imposed on the floc size distribution. Although the lines drawn do not pass through the origin, they seemingly tend to do so as smaller and smaller flocs are made part of the measurements. Although no firm conclusions can yet be drawn, there is support for the hypothesis that the shear-controlled size limit imposed on flocs is inversely proportional to G.

Floc size distributions at different flocculation times were determined experimentally at G values of 3.2 sec^{-1} and 6.8 sec^{-1}. Flocs smaller than 2.3×10^{-2} mm^2 were omitted from these distributions. As shown in Figures 5-9 and 5-10, through summation curves or distribution graphs by numbers of particles, the curves drawn through the observed values are more or less "S" shaped. With the abscissa and ordinate scales chosen for these figures, frequency distributions which are normalized by a logarithmic transformation plot as straight lines. Departure of the curves from straight lines can be explained in terms of imposed upper and lower limits on floc size. Presumably, the upper limit is imposed by shear; the lower limit, by inability to measure particles of smaller size. Systematic variations about the curves drawn are believed to represent more than experimental error, but the accuracy of the underlying information does not warrant more careful evaluation of the curves. This will be discussed again later.

Comparison with computer results: On first inspection, it would appear that the floc growth curves synthesized by computation do not agree with the experimental curves. However, when truncation is introduced into the computer runs or when truncation is suppressed in the experimental results, similarities appear as illustrated in Run 30, which has already been presented in Figures 3-5 and 3-6 without truncation. Here a breakup into four equisized particles, a maximum particle volume of 20, and a C of 2×10^{-2} were postulated; and, for truncation, all particles smaller in volume than 6 units were excluded from the computation of the mean size. Figure 5-11 shows the mean-size curves generated for both the untruncated and the truncated samples. A maximum size is seen to occur in the truncated sample at a relative flocculation time (t/T) of 2. Additional calculations demonstrated that this level of truncation gives the most pronounced maximum, other levels giving smaller or only relative maxima at about the same flocculation time.

Unfortunately, the computer results cannot be fitted to the experimental curves with scale factors derived from theory. Experimental correlation must be resorted to, and available data are not good enough for this.

Additional evidence of similarity between the model of orthokinetic flocculation and experimental results is presented in distribution graphs by numbers of particles obtained with the model. These are shown, for the untruncated sample, in Figure 5-12 and, for the truncated sample, in Figure 5-13.

Although an overall sigmoidal shape is evident in all curves, the curves for longer flocculation times are humped at certain particle sizes, indicating that a buildup of particle numbers has taken place in these size groups.

The distributions for the truncated samples in Figure 5-13 are shaped like the experimental distributions in respect to time and size. There is positional similarity as well as similarity of curvature. As in Figure 5-10, the short-time-flocculation curve lies farthest to the left and the curve for time of maximum floc size farthest to the right. Departure of the curves from sigmoidal shape is systematic in model distributions as well as experimental distributions. Once again, this similarity supports the argument for the validity of the mathematical model. Consolidation of flocs, wherein a decrease in size is accompanied by an increase in density, may also account for the observed changes in particle size distribution with increasing flocculation time. Consolidation, however, would not be expected to result in accumulation of particles in specific size groupings. Further studies of floc size distributions - especially the accumulation of particles of specific sizes - may tell how flocs break up under the stress of imposed velocity gradients.

The mean ratios of the major and minor diameters of the flocs for samples selected randomly from the measurements of several films ranged from 1.6 to 2.3 with no tendency to change systematically during the course of flocculation. The fact that the mid-point of this range is approximately 2 lends further, although not strong, support to the computer model, since breakup of agglomerated floc particles into four equal parts would leave the ratio unchanged.

Effect of coagulant dose: By increasing the coagulant dose fourfold while keeping the pH near optimum, the results for three repetitive runs shown in Figure 5-14 were obtained. Although the observed points are widely scattered, the lines connecting the arithmetic mean values of the plot remain true to the preceding observations. However, floc growth is seen to be more rapid, and the mean size is observed to decrease uniformly after passing through the mode which was reached after about 7 or 8 minutes of flocculation, or at a Gt value of about 1500. At one-fourth this coagulant dose, the observed optimal Gt value was 7400, or nearly five times as much. Since the theoretical half-time of flocculation has been shown to be inversely proportional to the initial concentration of particles (Chapter 3), and all particles must have been formed from the coagulant itself, the observed quickening of the rate of floc growth is understandable.

At the beginning, the mean floc size produced by quadrupling the coagulant dose was also seen to rise. However, after a lapse of about 60 minutes, the mean size was more nearly that observed at the lower coagulant dosage, too.

Coagulation of color: Floc growth during coagulation of a solution of instant coffee is traced in Figure 5-15 for three repetitive runs. Once again, also, the pattern of behavior runs true to type, and mean floc size is like that with a comparable dose of coagulant in the absence of color. However, the time to reach maximum floc size is lengthened. The presence of wetting and dispersing agents in soluble coffee powder may explain this time shift, but this is only a suggestion. Studies of the rate of color uptake reported in the following chapter give it no support.

That the observed mean floc size is larger at higher coagulant dosages is perhaps explained by a shift in the truncation level with the measurement technique employed. If the observed increase in mean floc size were real, dependence of shear-controlled sizing on the concentration of coagulant used would be implied. A possible explanation of the shift is that the smaller flocs lie in the shadow of the more numerous large-floc images within each frame of the film.

Conclusions

The studies reported in this chapter suggest that within the limits of experimentation, floc growth during coagulation with chemicals follows much the same pattern at the different shear gradients employed (G = 3.2 to 9.3 sec^{-1}). Within the range of coagulant doses studied, a mode or maximum in the mean floc size developed within 40 minutes from the start of flocculation when only the larger flocs were taken into account. This pattern of behavior can be fitted in principle by a modified form of the von Smoluchowski equation for orthokinetic flocculation. The modification postulated in this thesis is the action of a breakup mechanism upon agglomerations larger than some critical size resulting in the creation of a number of approximately equal-sized particulate components; in one pertinent case four. The growth pattern is then simulated not only by increases in mean floc size during flocculation but also by distributional changes in particle sizing.

In order to generate a mode or maximum size in the growth pattern predicted by the model selected, the smallest particles had to be excluded* from mean-size computations. Truncation of this nature is not unlike that imposed on the experimentally measured floc sizes by the fact that very small flocs were not visible in the photographs.

The dependence of the rate of floc growth on the initial number of particles in suspension and, hence, on the coagulant dose, is demonstrated semi-quantitatively by the shift in time of occurrence of the mode with varying dosage. The agreement of experimental data with theoretical prediction is well within tolerances compatible with the accuracy of the information.

Shear-controlled sizing of flocs is shown to be a function of the mean velocity gradient, G, its probably form being an inverse proportionality between maximum floc size and velocity gradient. As yet, this functional relationship has not been incorporated in the model.

---

* Computations performed after this thesis was written suggest that truncation is not needed for the generation of a mode or maximum if the breakup mechanism and input variables for the model are properly adjusted.

Although the proposed mathematical model is not perfect, it does suggest that this first approach is promising. However, much remains to be done.

The rate of floc growth was retarded by the addition of instant coffee to the suspending fluid. If the added powder had only increased the particulate concentration of the water, this would have been contradictory to what has been said about the effect of suspended-particle concentration. However, the powder also contains constituents, such as wetting agents, some of which may retard floc growth. Since the observed floc-size maximum was not changed by the addition of coffee, we may assume that the toughness of the floc was also not affected. Whether floc growth would take place in naturally colored waters in the same way was not demonstrated. However, studies reported in the next chapter of this thesis did show that the rate of color uptake by floc was much the same for water colored by instant coffee and by natural color.

Computations based on the mathematical model proposed in this thesis suggest that there cannot be an optimal magnitude of the non-dimensional parameter Gt that is applicable to all chemical flocculation systems. In the mathematical model, the value of the product GT, where T is the half-time of flocculation rather than the flocculation period, was shown, for instance, to be proportional to the initial concentration of particles present in the system. In chemical coagulation of water, the initial number of particles would depend, in part, on the dosage of coagulant used. Laboratory observations of chemical floc growth in the absence of coloring substances did indeed indicate that the time of occurrence of the mode or maximum mean size varied approximately in proportion to the dosage of coagulant used. Hence, a suitable design parameter for flocculators should include, beside the product Gt, the initial number of particles present. This number could be estimated from considerations of raw water quality and required coagulant dose. However, the observed retardation of floc growth when instant coffee was introduced as coloring agent adds to the complication of a three-parameter relationship alone.

Although the production of large flocs may not be the best gauge of flocculator performance, the occurrence in time of a maximum mean size when only the largest flocs are considered does suggest the possibility of optimizing the design of coagulation* processes on an economic basis. Conceivably the observed decrease in mean floc size that follows attainment of the maximum size could be the result of either floc breakup or floc consolidation.

If the decrease in floc size is not offset by a corresponding increase in floc density - that is, if the floc simply breaks up - flocculation should be terminated when the maximum mean size has been reached. Subsequent sedimentation could then be held to a minimum without foregoing the removal of a sizeable proportion of the floc mass; and a small increase in filter capacity or reduction in length of filter run should then be sufficient to insure removal of the remaining small-sized flocs without lowering the quantity of the plant effluent.

If, on the other hand, the decrease in floc size is the result of floc consolidation rather than floc breakup, it stands to reason that flocculation should be continued until the balance between increasing density and decreasing size no longer improves the settling velocity of the flocs significantly, or until an optimal economic balance between flocculator and settling basin capacities is struck.

---

* Recall that, as defined in this thesis, coagulation includes phase-separation operations.

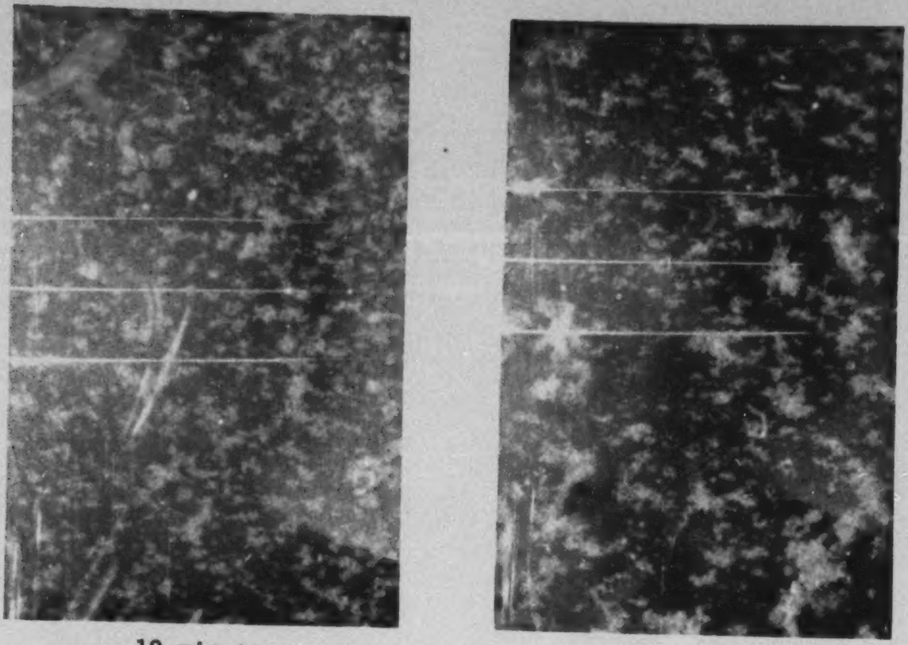

10 minutes

20 minutes

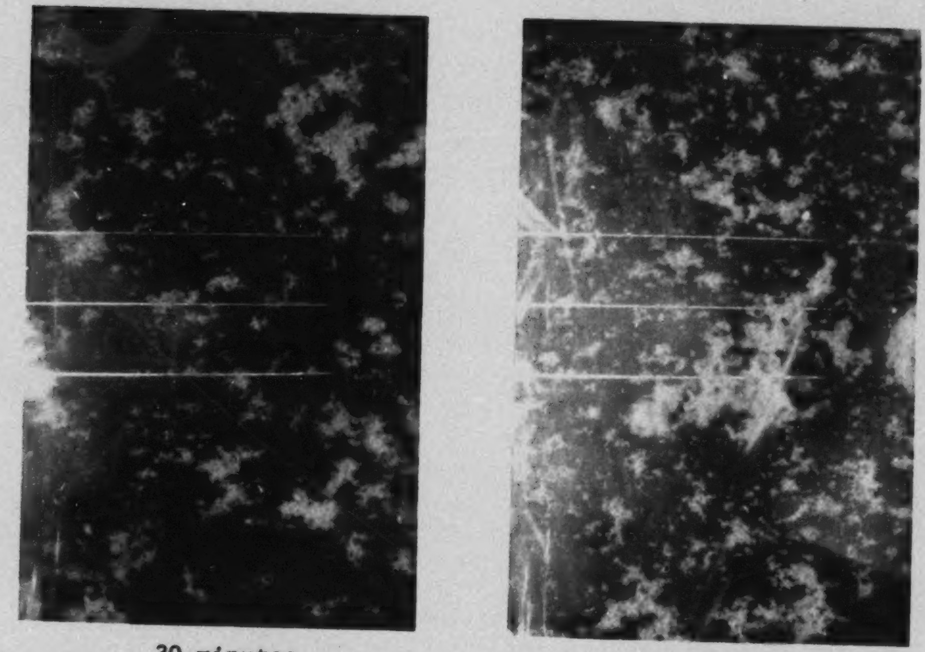

30 minutes

40 minutes

FIGURE 5-1. TYPICAL FLOC PICTURES. G=3.2 sec^{-1} $Fe_2(SO_4)_3$ = $1.6x10^{-4}$ mols/liter. Magnification ≑ 2x Flocculation time shown beneath each picture. Compare with Figures 5-5, 5-6, and 5-7.

Continued on next page

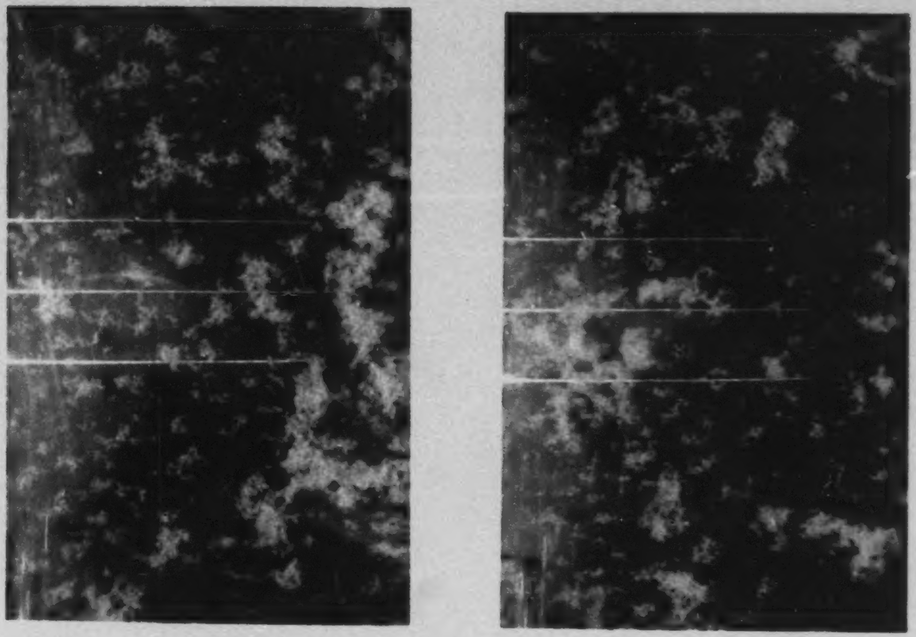

50 minutes

65 minutes

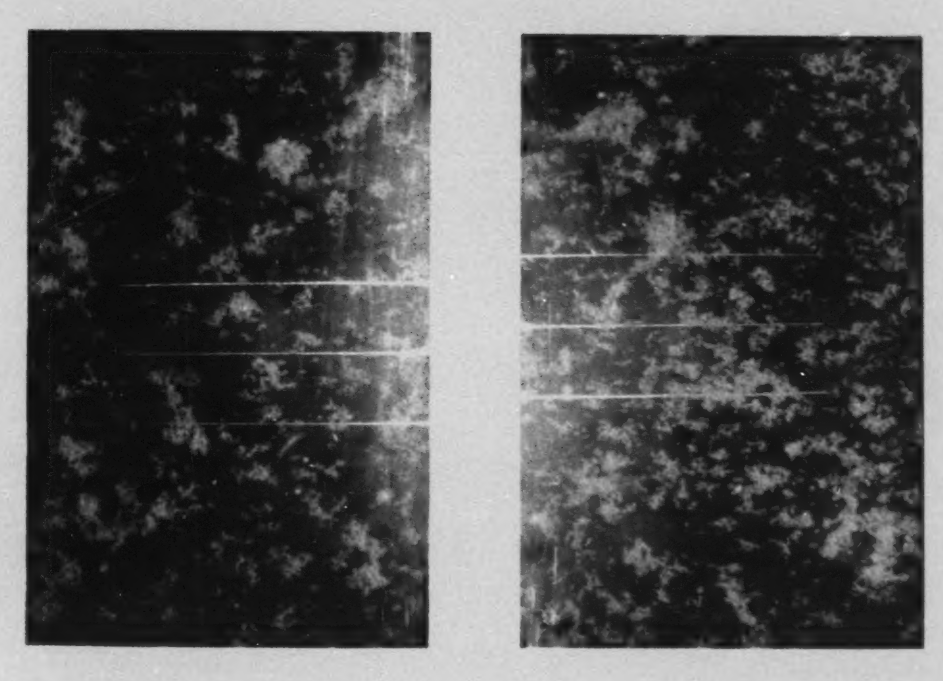

100 minutes

180 minutes

FIGURE 5-1 (continued)

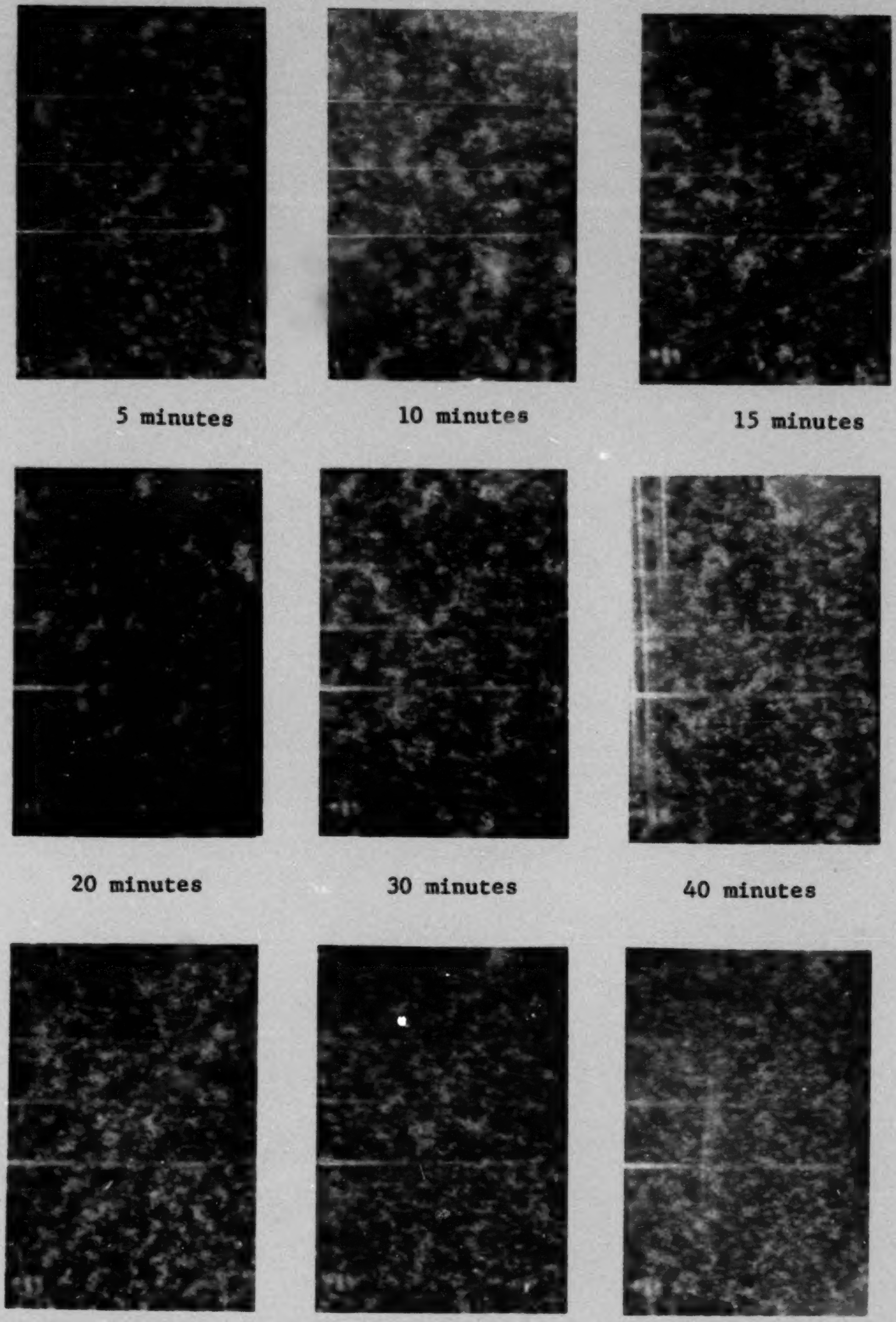

5 minutes

10 minutes

15 minutes

20 minutes

30 minutes

40 minutes

50 minutes

60 minutes

100 minutes

FIGURE 5-2. TYPICAL FLOC PICTURES. $G = 6.8\ \text{sec}^{-1}$. $Fe_2(SO_4)_3 = 1.6\text{x}10^{-4}$ mols/liter. Magnification ÷ 2x. Flocculation time shown beneath each picture. Compare with Figures 5-5, 5-6, and 5-7.

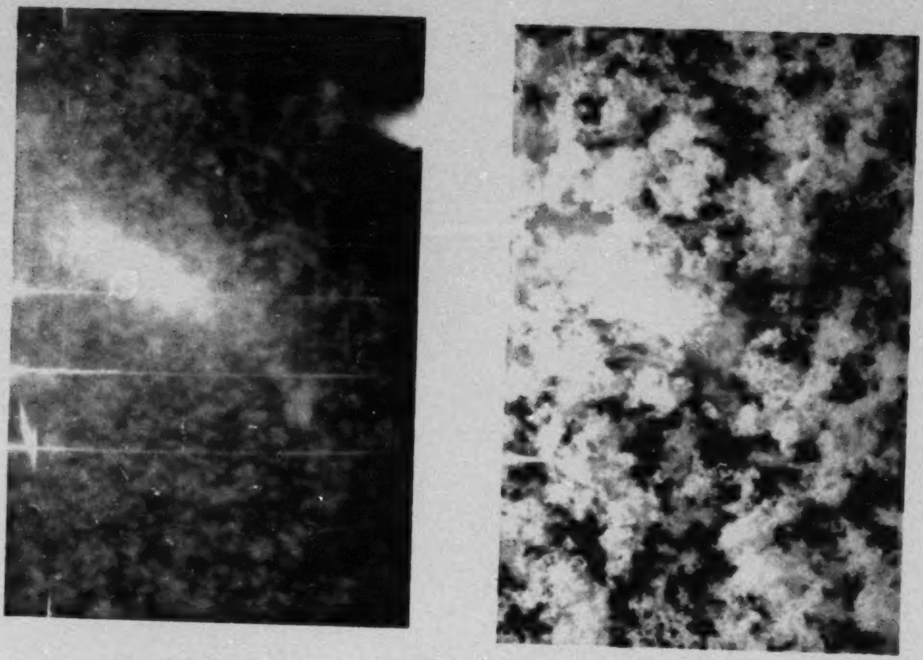

0 minutes

5 minutes

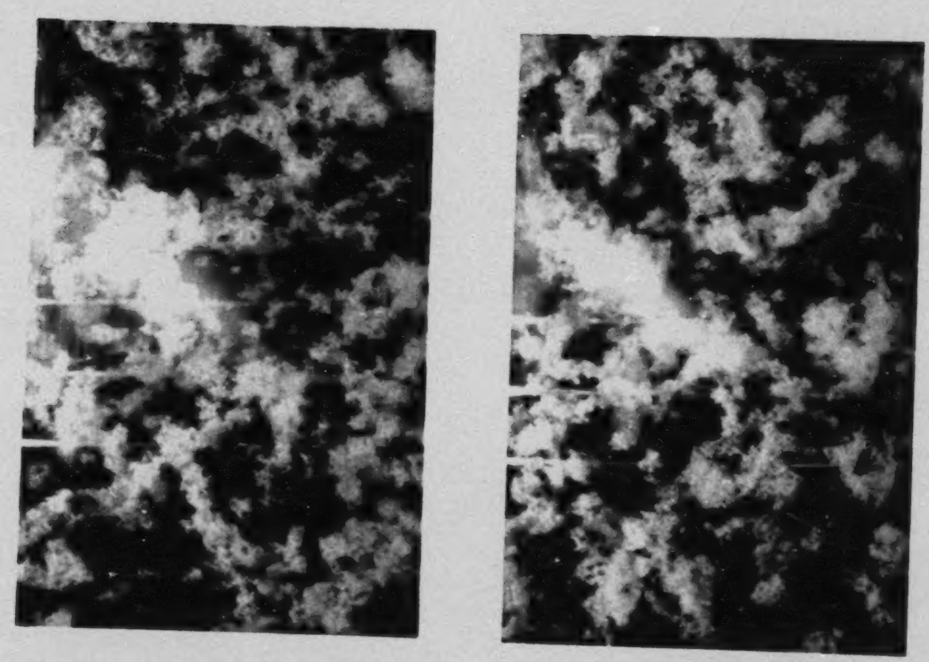

10 minutes

20 minutes

FIGURE 5-3. TYPICAL FLOC PICTURES. $G = 3.2\ sec^{-1}$. $Fe_2(SO_4)_3 = 6.4\times10^{-4}$ mols/liter. Magnification ≑ 2x. Flocculation time shown beneath each picture. Compare with Figure 5-14.

Continued on next page

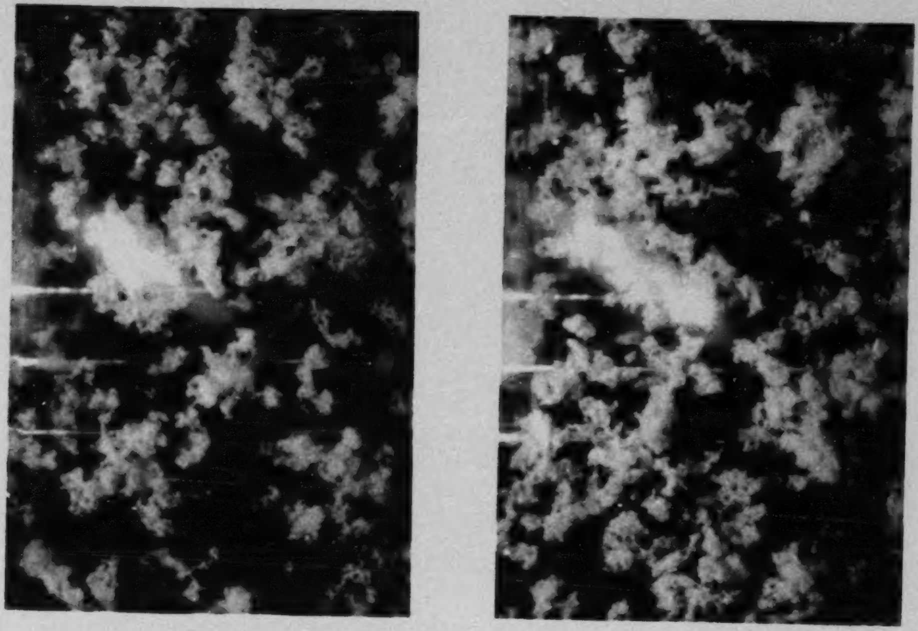

30 minutes

40 minutes

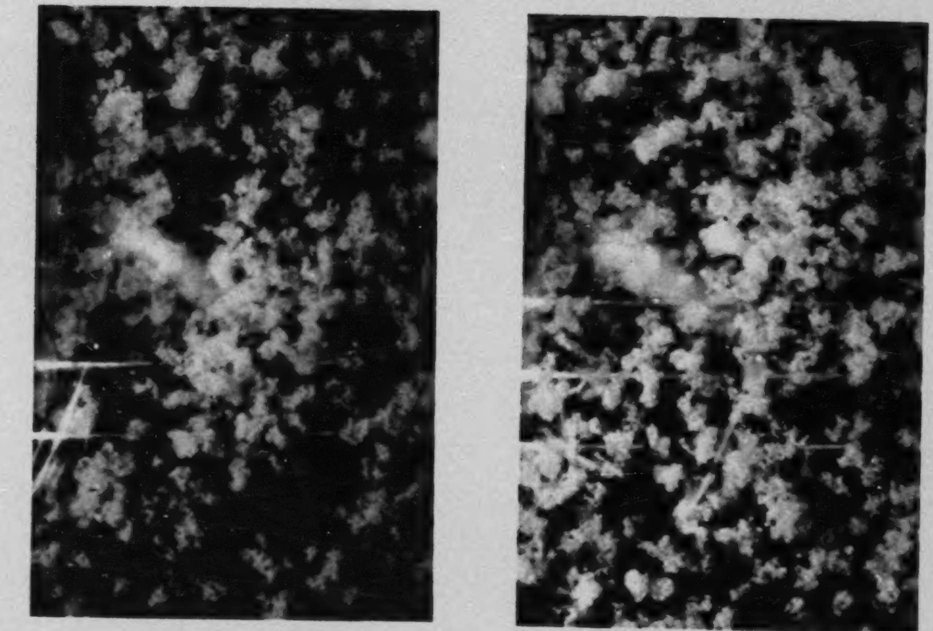

60 minutes

80 minutes

FIGURE 5-3 (continued)

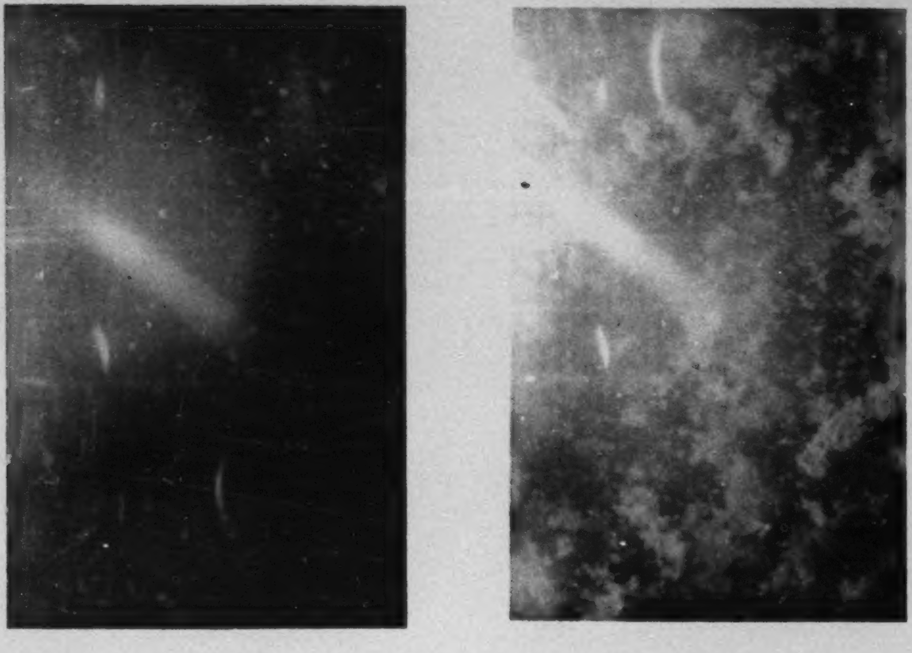

5 minutes 15 minutes

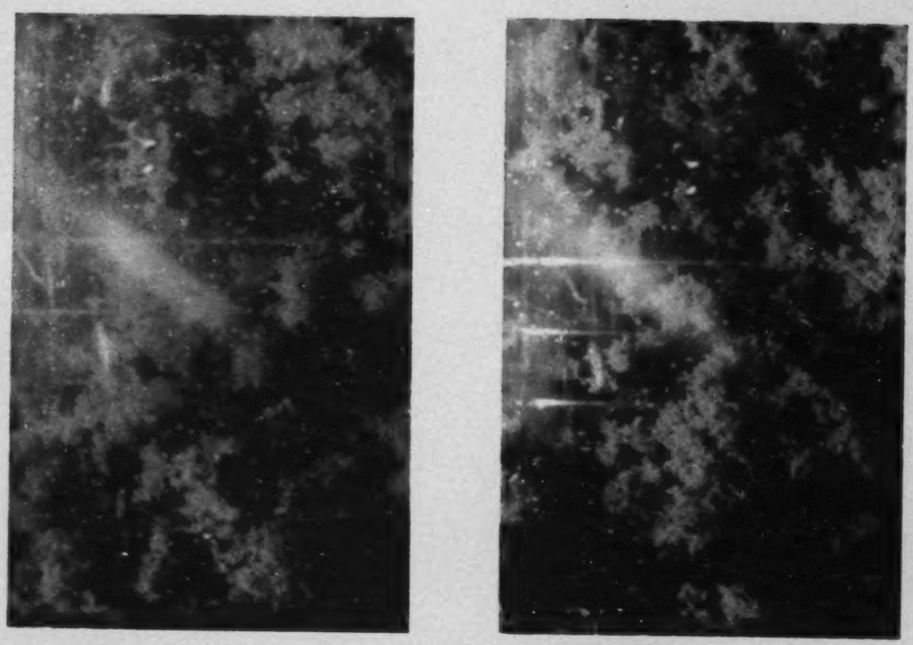

20 minutes 30 minutes

FIGURE 5-4. TYPICAL FLOC PICTURES. $G = 3.2\ sec^{-1}$. $Fe_2(SO_4)_3 = 7.5 \times 10^{-4}$ mols/liter. Coffee = 38 mg/liter. Magnification ÷ 2x. Flocculation time shown beneath each picture. Compare with Figure 5-15.

Continued on next page

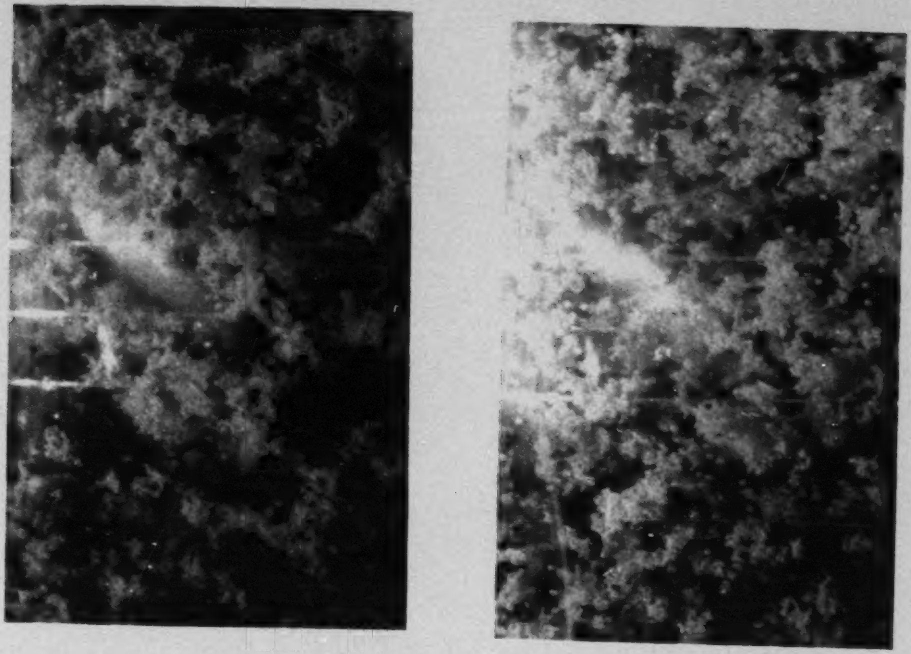

40 minutes

50 minutes

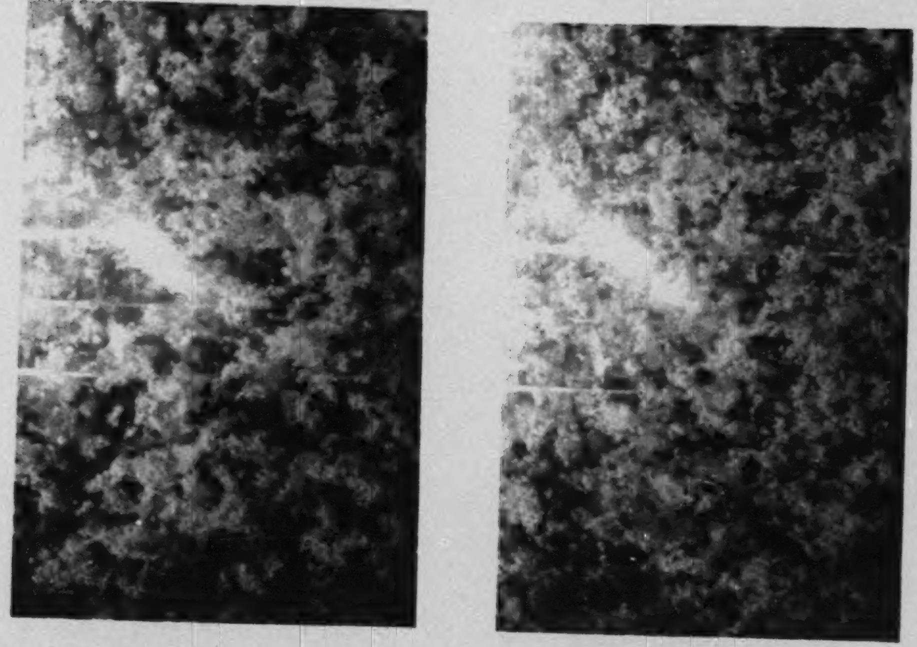

60 minutes

80 minutes

FIGURE 5-4 (continued)

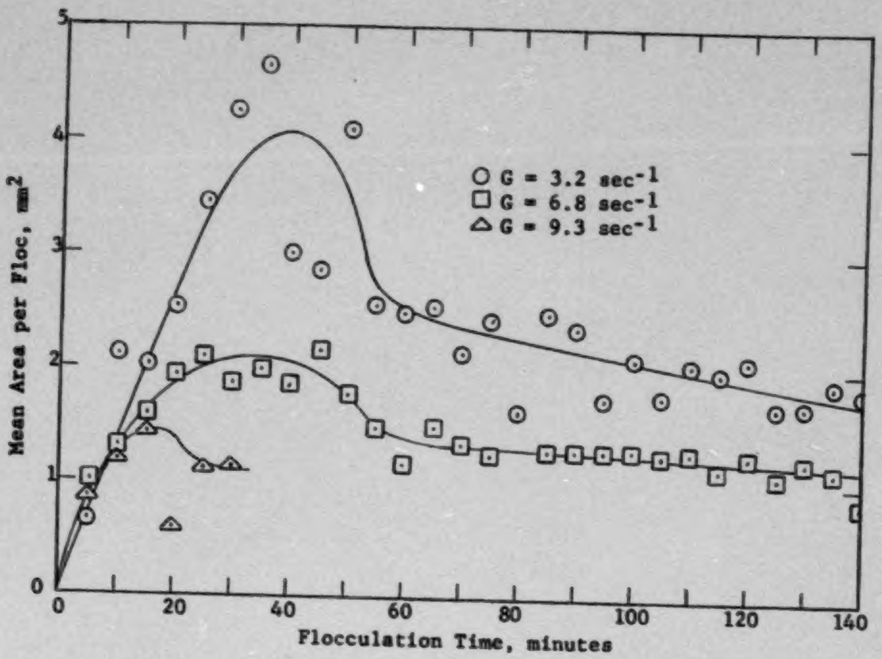

FIGURE 5-5. VARIATION IN MEAN FLOC SIZE DURING FLOCCULATION. $Fe_2(SO_4)_3 = 1.6 \times 10^{-4}$ mol/l . $NaHCO_3 = 1 \times 10^{-2}$ mols/l . pH = 6.8.

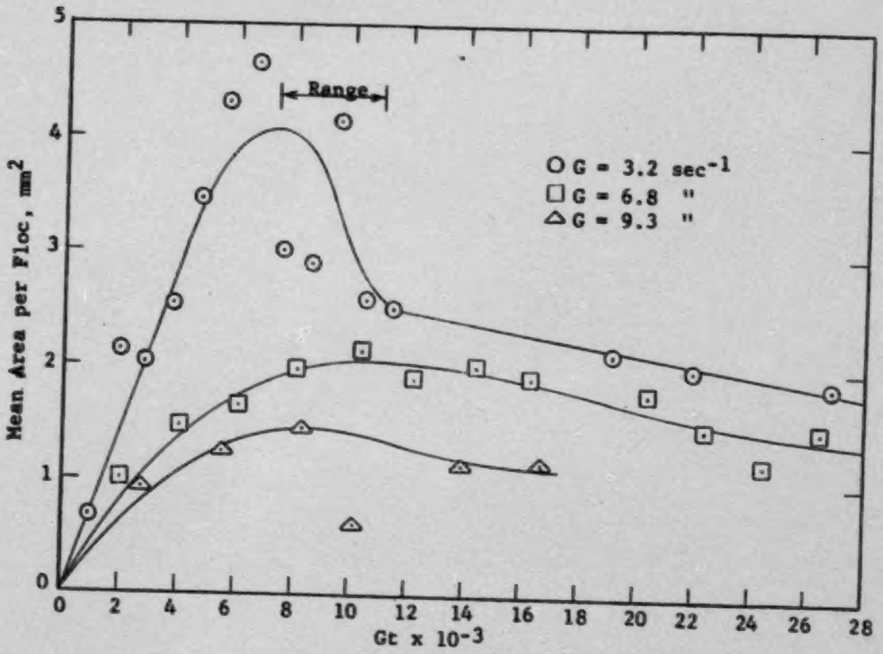

FIGURE 5-6. DEPENDENCE OF MEAN FLOC SIZE ON VALUE OF Gt.
$Fe_2(SO_4)_3 = 1.6 \times 10^{-4}$ mols/l
$NaHCO_3 = 1 \times 10^{-2}$ mols/l
pH = 6.8

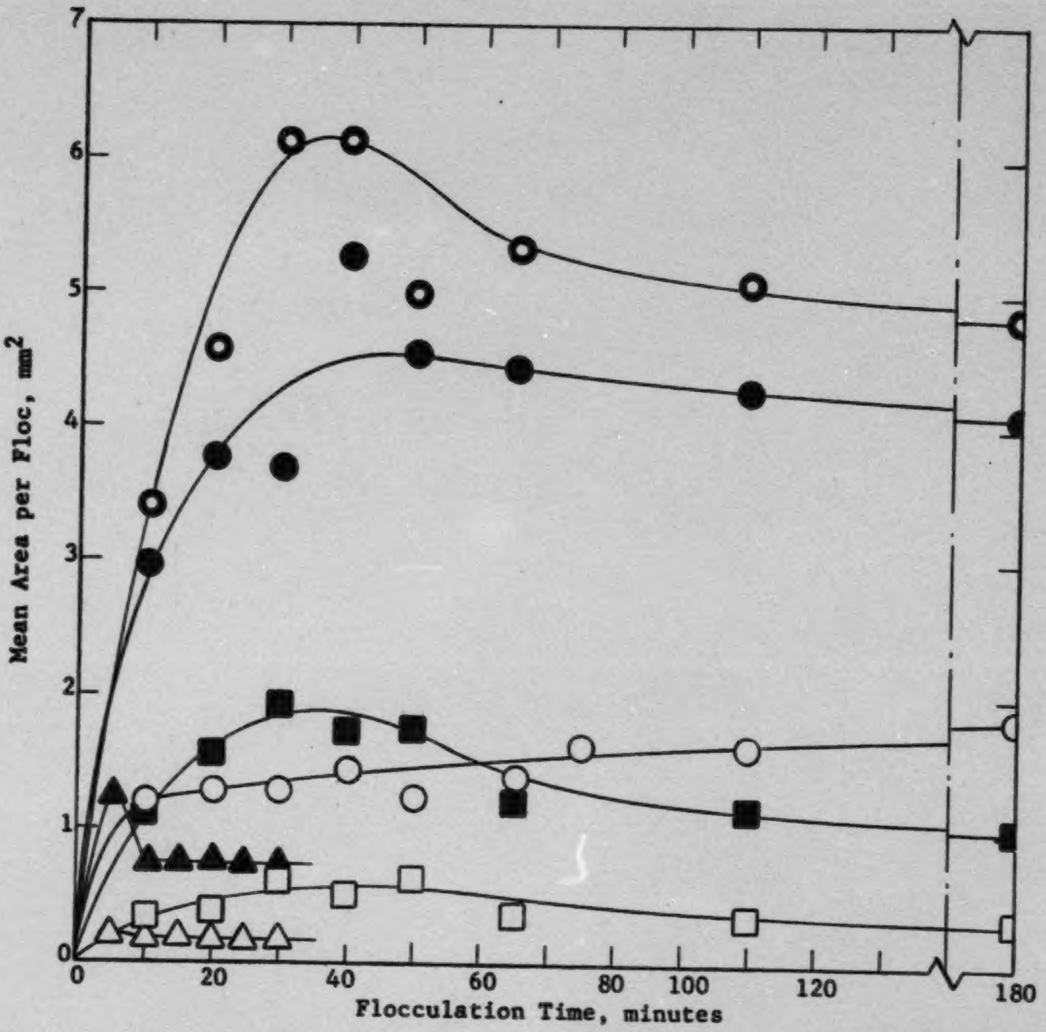

FIGURE 5-7. VARIATION IN MEAN FLOC SIZE DURING FLOCCULATION.

Mean of flocs larger than:	G=3.2 sec^{-1}	G=6.8 sec^{-1}	G=9.3 sec^{-1}
0.023 mm^2	○	□	△
0.5 mm^2	●	■	▲
1.0 mm^2	◎		

$Fe_2(SO_4)_3$ = 1.6x10^{-4} mols/l. $NaHCO_3$ = 1x10^{-2} mols/l. pH = 6.8

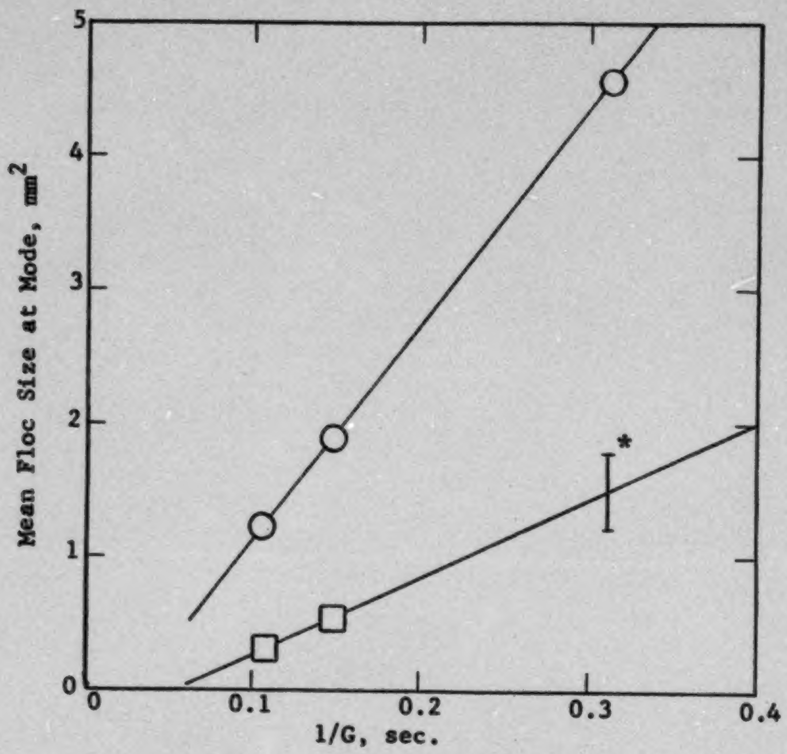

FIGURE 5-8. EFFECT OF MEAN VELOCITY GRADIENT ON SHEAR-CONTROLLED SIZING OF FLOC

Data taken from Figure 5-7:

○ All flocs larger than 0.5 mm^2
□ All flocs larger than 0.023 mm^2
* No mode occurred; range taken from steady-state portion of curve.

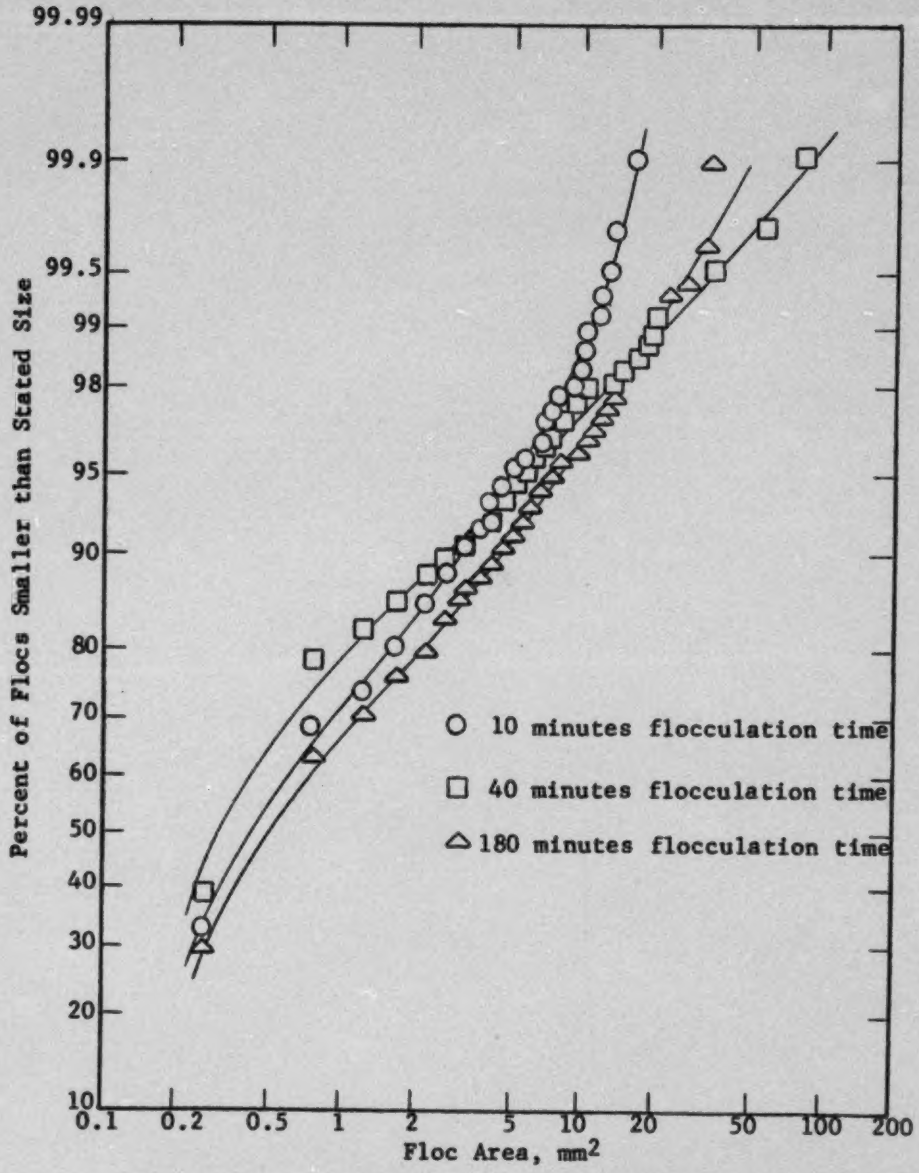

FIGURE 5-9. VARIATION IN FLOC SIZE DISTRIBUTION DURING FLOCCULATION.

$G=3.2\ \mathrm{sec}^{-1}$. $Fe_2(SO_4)_3 = 1.6\times10^{-4}$ mols/l .

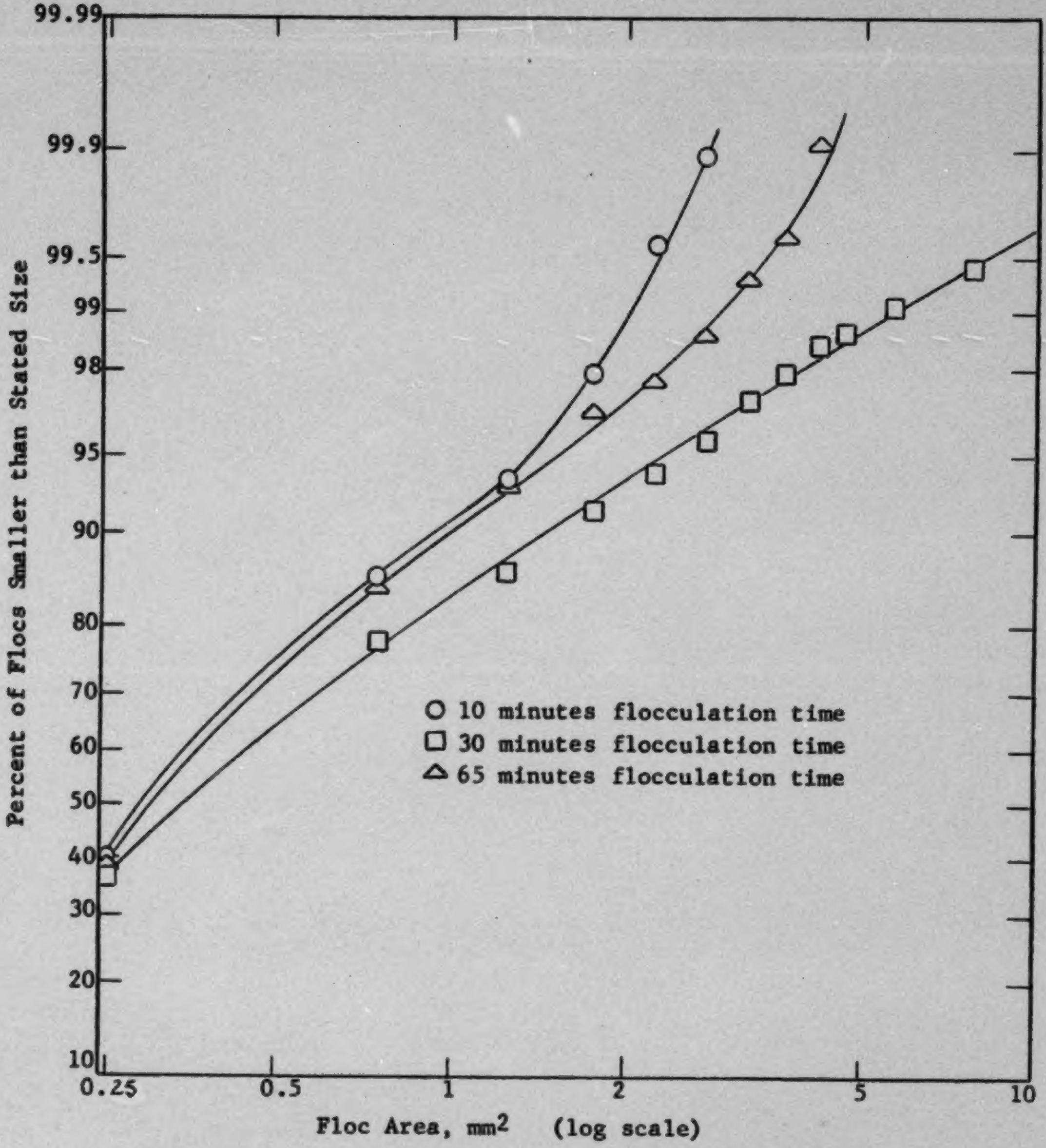

FIGURE 5-10. VARIATION IN PARTICLE SIZE DISTRIBUTION DURING FLOCCULATION.

$G=6.8\ sec^{-1}$. $Fe_2(SO_4)_3 = 1.6 \times 10^{-4}$ mols/l.

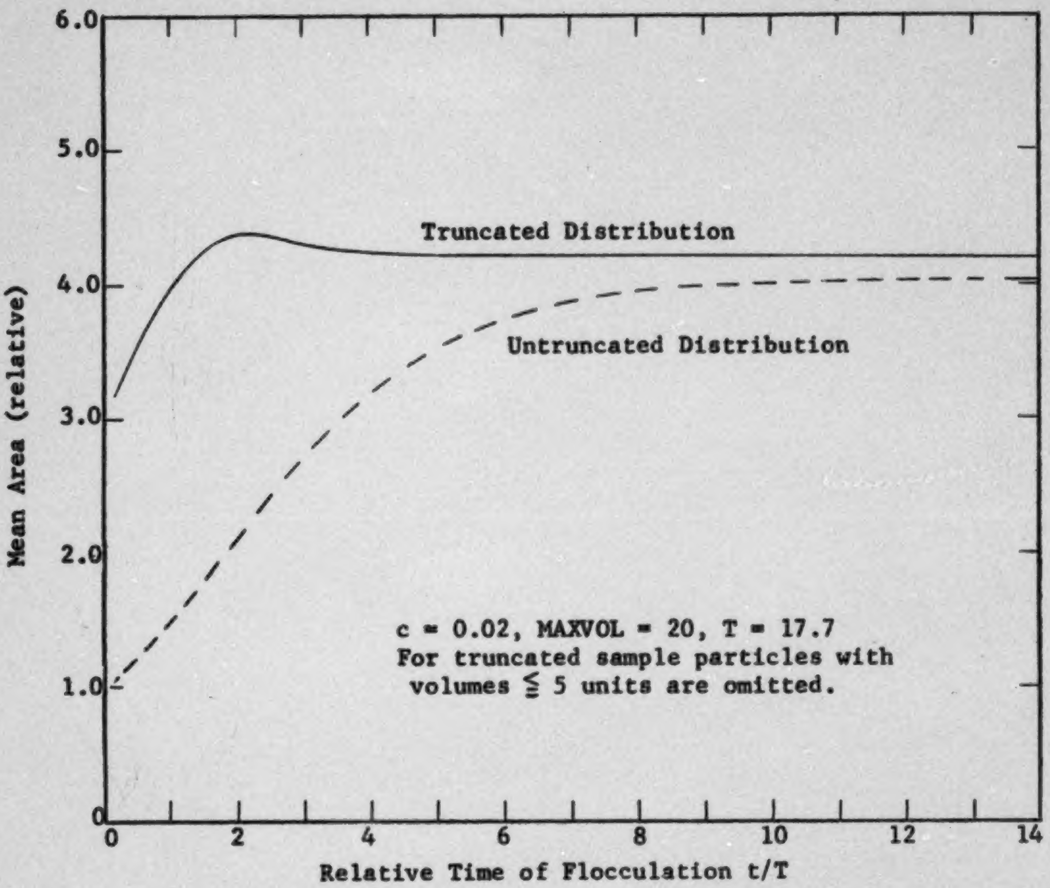

FIGURE 5-11. ORTHOKINETIC FLOCCULATION WITH BREAKUP 4: FLOC GROWTH FOR UNTRUNCATED AND TRUNCATED DISTRIBUTIONS

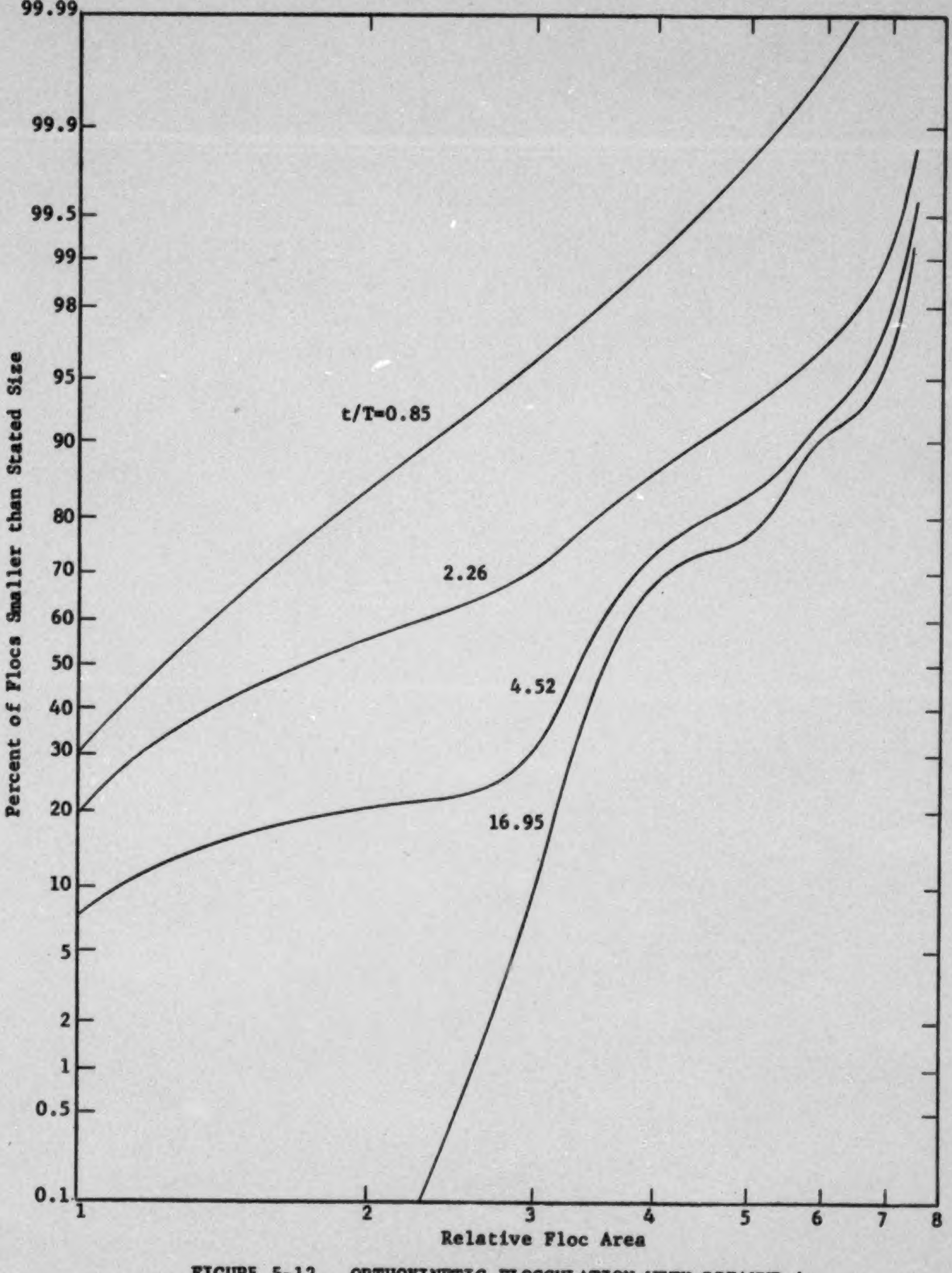

FIGURE 5-12. ORTHOKINETIC FLOCCULATION WITH BREAKUP 4:
VARIATION IN PARTICLE SIZE DISTRIBUTION
c = 0.02, MAXVOL = 20, T = 17.7
Complete (not truncated) distribution

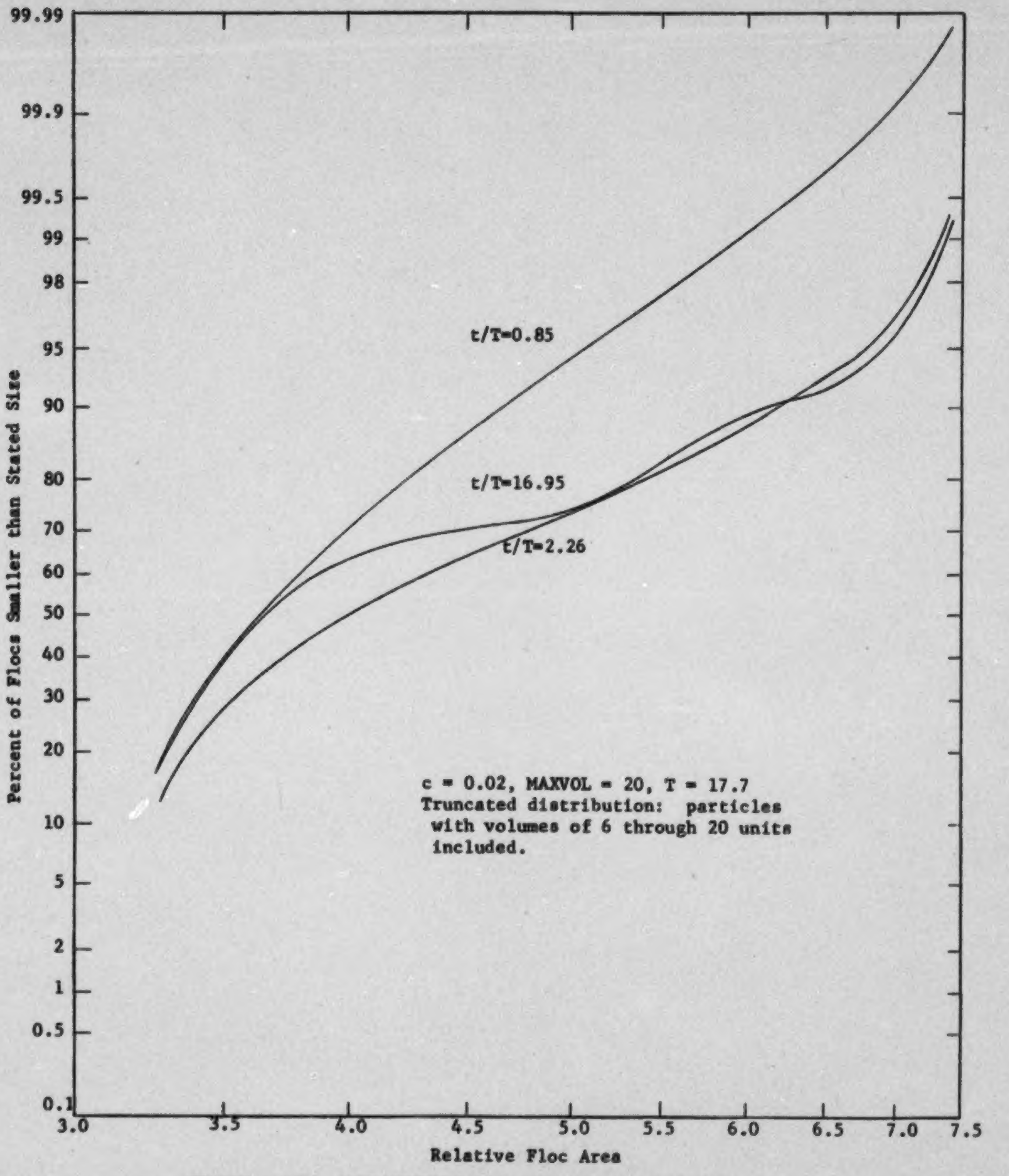

FIGURE 5-13. ORTHOKINETIC FLOCCULATION WITH BREAKUP 4: VARIATION IN PARTICLE SIZE DISTRIBUTION

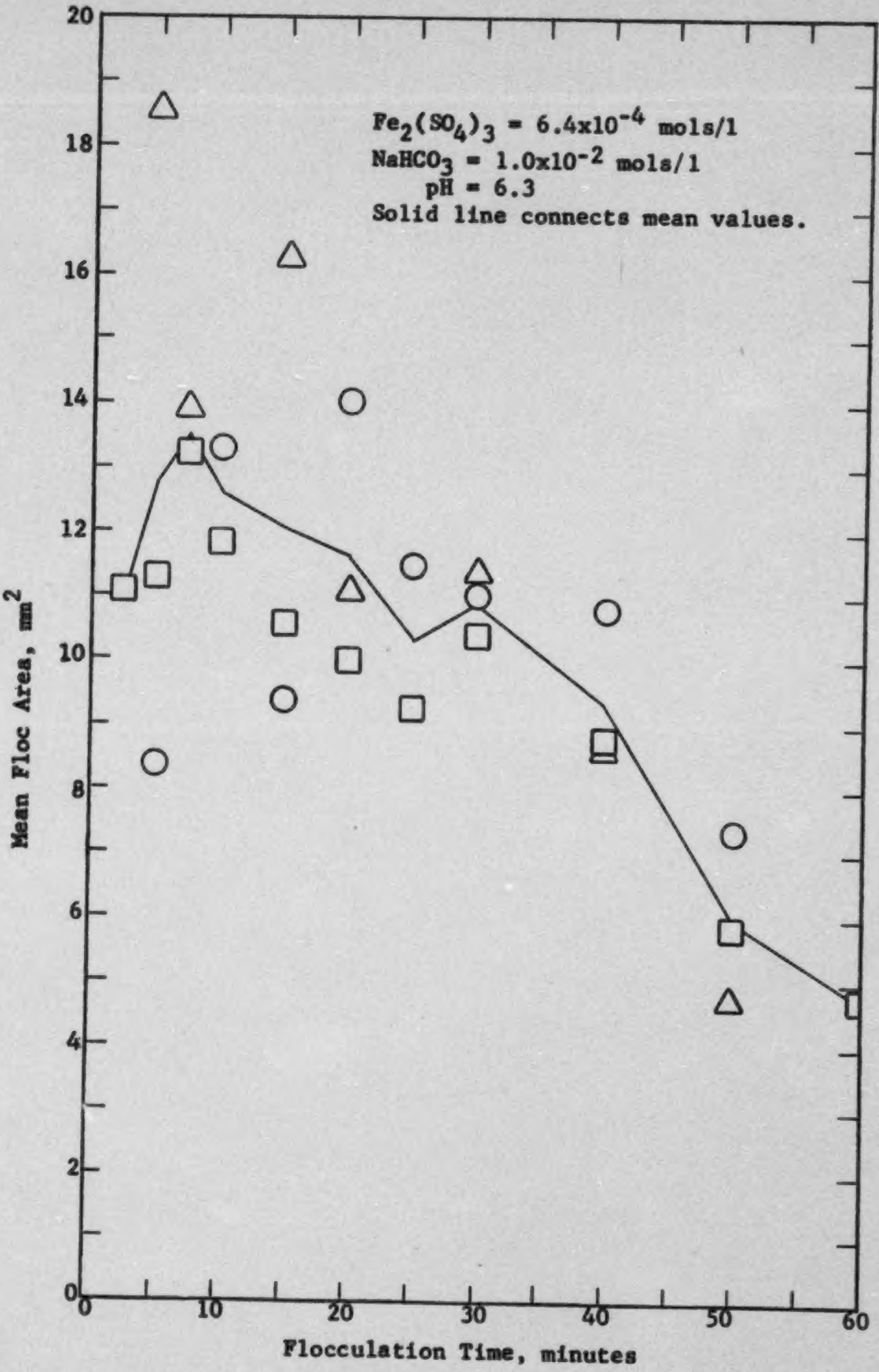

FIGURE 5-14. EFFECT OF HIGHER COAGULANT DOSE ON FLOC GROWTH AT G = 3.2 sec^{-1}

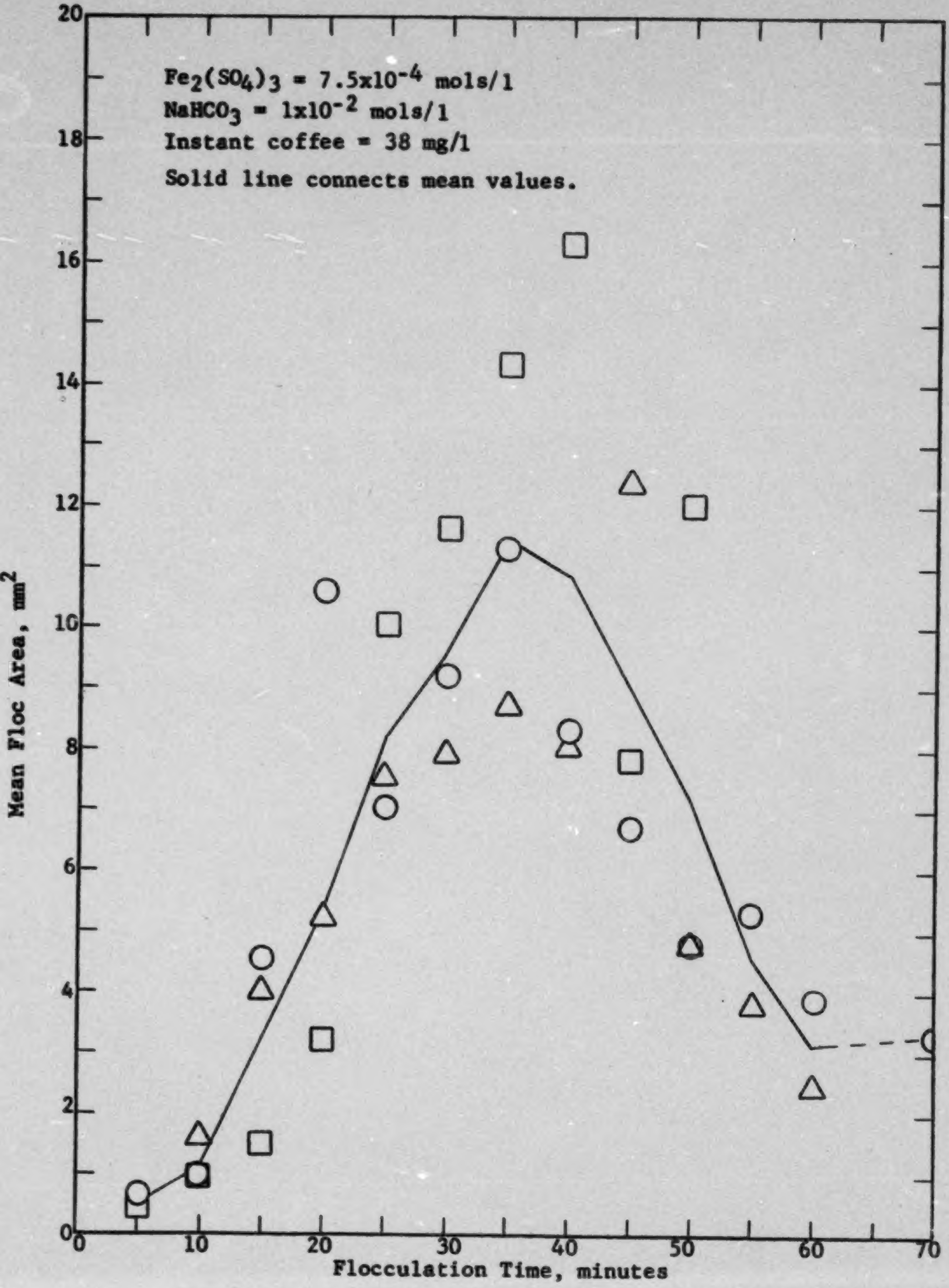

FIGURE 5-15. COAGULATION OF COLORED WATER:
VARIATION IN MEAN FLOC SIZE DURING FLOCCULATION AT G = 3.2 sec^{-1}

Chapter 6

REMOVAL OF COLOR BY COAGULATION

According to the idealized concept of coagulation introduced in Chapter 1, the primary function of flocculation is to condition the flocs in advance of phase separation, although the validity of this concept has not yet been demonstrated.

The only other major function of flocculation appears to be color and turbidity uptake by the floc as it is formed. In the idealized concept of coagulation, this function was assigned primarily to nucleation. Some insight into these matters was obtained in a series of color-removal experiments, and it is the purpose of the present chapter to examine the results obtained.

Experimental Procedures

Artificially Colored Water

Since experiments of this kind are necessarily repetitive, a standard colored water had to be found. Iron or aluminum ions could serve coagulants and bicarbonate could provide the necessary alkalinity, but a suitable coloring agent was harder to find. To become a simulant of natural color*, the agent had to be a material that imparted color of the hue commonly found in water and possessed the essential properties of the substances that impart natural color to water. Other considerations were ease of dispersion in water, reproducibility, availability, and cheapness. Several agents were considered; finally chosen was instant coffee. Chemically this soluble product contains a number of functional groups that occur in naturally colored water. A single, 6-oz. jar of a common brand of instant coffee (Maxwell House) was, therefore, employed in all color removal studies and eliminated possible variations in composition between different samples; day-to-day reproducibility of the color was indeed unquestionable.

---

* For a discussion of natural color, see Chemical and Biological Studies on the Yellow Organic Acids of Lake Water, J. Shapiro, *Limnology and Oceanography*, 2, 161 (1957).

As happens in natural colored waters, changes in acidic functional groups with increasing pH intensify the color of water containing coffee. This is shown in Figure 6-1 by the absorption spectra of instant coffee solution and of Charles River water for visible and ultraviolet wavelengths. At a pH of 10.2, the solution of coffee showed relative maximum absorbance at a wavelength of 365 mμ. About here, the absorbance of standard chloroplatinate solution, a color standard for natural color is also relatively constant. Accordingly, this wavelength was adopted for the tests to be reported. By contrast, there is seemingly no optimal wavelength for measuring the color of natural waters such as the Charles River water, shown for comparison in Figure 6-1.

Figure 6-2 shows that the coffee solution reached its maximum color intensity at a pH of 10.25. Accordingly, this became the pH for measurement and an ammonia buffer, one molar in the sum of ammonia species, was chosen to create it by the addition of 1 ml of buffer to 50 ml of sample.

Figure 6-3 shows that the intensity of instant-coffee color is also time-dependent. For this reason, colors were read 5 minutes after adding the buffer. This was long enough for adjusting the colorimeter.

The colorimeter was a Lumetron instrument equipped with 365 mμ absorption filter and 5 cm cells. A typical direct calibration curve is shown in Figure 6-4, together with a calibration curve for standard chloroplatinate solution. Cobalt chloride, which is commonly added to adjust the hue of chloroplatinate solution, shows no absorbance at the chosen wavelength. Most results are reported as percent color remaining after treatment without conversion to the chloroplatinate scale. Because the coffee calibration curve is linear, the percent color remaining could be computed more simply from the ratio of absorbance of the sample to absorbance of the control.

Experimental Technique

Batch rather than continuous-flow tests were normally carried out in 600 ml beakers with 500 ml of sample. The samples were stirred with rectangular blades attached to drive shafts. The blades were 1 in. high and 3 in. long. By assuming a coefficient of drag of 1.8 and a relative paddle velocity of half the paddle peripheral speed, the following approximate expression for G was developed from equation (2-29) for a water temperature of 20 C:

$$G = 0.16 N^{1.5} \tag{6-1}$$

where N is the paddle or shaft rotational speed in rpm.

To find the amount of color uptake by the floc as a function of time and stirring rate, the following procedure, which applies to all experiments unless otherwise noted, was most frequently used. For selected concentrations of bicarbonate and coffee in the water substrate, optimum coagulant dosage was determined by jar test. To begin with, different doses of coagulant were added without pH control. After the approximate optimal dosage had been found, pH values of the system were varied until dosage and pH were optimal. More often than not, the system was buffered enough by the bicarbonate alkalinity to bypass pH adjustment. At optimal dosage, first flocs generally became visible within one minute after adding the coagulant.

The water substrate was prepared as follows: enough bicarbonate solution was withdrawn from a bulk storage vessel into a test beaker to produce the desired alkalinity after ultimate dilution to 500 ml; an aliquot of coffee solution (prepared fresh daily in 1 gram per liter concentrations) was introduced to impart the necessary color; and sufficient distilled water was poured in to bring the total volume of the solution to 500 ml upon addition of the required amount of coagulant.

A separate sample was prepared for each flocculation time in the experiments together with a control made up to 500 ml with distilled water instead of coagulant solution. Needed amounts of coagulant were measured from a stock solution (prepared daily) into small beakers for substantially instantaneous addition at selected times. When intervals between samplings were small, as was true for a portion of most tests, the coagulants were added in staggered time sequence to give enough leeway for necessary sampling operations.

Initial rapid mixing, usually at 60 rpm for 30 seconds, was followed by the chosen conditions of stirring or flocculation. At each preselected time, a sample jar was removed from the gang-stirring apparatus, and a portion of the suspension was subjected to one of the following treatments: (1) centrifuging for 5 minutes at 12.4xg; (2) filtering through Whatman 40 paper; or (3) settling for one hour in the coagulation jar.

To find the residual color, the pH of a 50 ml aliquot of the sample supernatant or filtrate was adjusted to a value of 10.2 by the addition of ammonia buffer and the absorbance read exactly 5 minutes later.

The control solution was stirred continuously at flocculation speed, and at least two aliquots were withdrawn during the course of the experiment for measuring color in the same way as for the test samples. The percent color remaining was computed as the ratio of the sample absorbance to the absorbance of the control that had been stirred about as long as the sample. Changes in the color of the control were small.

Experimental Results

Coagulation with Iron

Ferric iron was chosen as the first coagulant. The results obtained with it are brought together in Figure 6-5 and 6-6. According to Figure 6-5 color uptake by the floc was relatively fast at the start for G values of both 15 and 76 sec^{-1}. For centrifuged samples, the initial rate was comparatively greater at the upper G value, but it became about equal to the rate for the lower G value after 70 percent of the color had been removed. For filtered samples, most of the color was removed within 30 seconds of the start of flocculation, and there was little further loss of color during the rest of the run. However, color not actually bound to the flocs at the start of filtration could have been removed in the floc mat on the filter. Centrifugation did not have this drawback.

Since iron itself exhibits some absorbance at 365 mμ, any iron remaining in the liquid after centrifuging (or filtering, for that matter) would be reported as color remaining. By keeping the coffee out of the synthetic water while adhering to the same coagulant concentration and testing procedure, it was shown, as in Figure 6-6, that a substantial proportion of the color remaining in the previous tests may indeed have come from residual dissolved or dispersed iron. At the two mean velocity gradients, the curves are seen to resemble those of earlier tests. Indeed, the differences in percent color remaining between the appropriate curves of Figures 6-5 and 6-6 are substantially alike over the entire range of flocculation times as shown by the dashed lines near the bottom of Figure 6-6. If these lines are representative of actual happenings, they say that after effecting a minimum color removal of 85 percent within two minutes, further flocculation has no measurable effect on color uptake.

Coagulation with Alum

Because iron coagulant has a color of its own, alum, which shows no absorbance at 365 mμ, was employed in a duplicating series of tests. The results are given in Figure 6-7. They indicate that approximately 85 to 90 percent of the color ultimately removed is taken out during the first two minutes of flocculation and that the rates of color removal at all G values employed become closely equal thereafter. Confining agitation to the 30 second rapid-mix phase gave erratic results, but the general trend of color removal remained nearly the same. The possibility that some of the color remaining in solution after flocculation is a soluble complex of the coagulant metal and the coffee was not examined experimentally.

Figure 6-8 records the findings of experiments in which an hour of settling took the place of centrifugation. Here the effect of mean temporal velocity gradient was more manifest during the early part of flocculation than in the preceding tests. More rapid sedimentation rather than more rapid color uptake may account for this, but such an explanation would be in conflict with the results presented in Chapter 5.

The small shear-gradient device described in Chapter 4 of this thesis was also tested for its ability to flocculate colored water. After rapid stirring in the conventional paddle apparatus for 30 seconds at 60 rpm, the liquid was transferred to the shear device and flocculated for the required length of time. Only one sample was collected in a given run, and the color control solution was left unagitated. Coagulation procedures were otherwise left unchanged. Alum was the coagulant, the initial concentrations of this substance and of bicarbonate and coffee being like those listed in Figure 6-7. Samples were centrifuged for color determination.

Although color removal was somewhat higher, the curves obtained (Figure 6-9) more or less follow the pattern of paddle flocculation (Figure 6-5). The G values of the paddle flocculators were not as well defined as those in the shear device, and any discrepancy in correlation of G value with color removal would have to be resolved in favor of the G value of the shear apparatus. However, delay in transfer and disturbance of the coagulating sol during transfer from the paddle stirrer to the cylinders may account for some of the discrepancies in results.

Color Removal by Preformed Floc

The hypothesis that color uptake by floc is confined principally to the nucleation phase was examined further by measuring the color removed by preformed floc. Experimental procedure remained much the same. Coagulant was added to the bicarbonate solution, and the mixture was stirred at 60 rpm for 30 sec. After that, the rate of stirring was lowered to the value at which the floc was to be preformed. Twenty minutes after beginning the test, the coffee solution was added to the preformed floc, and the suspension was stirred at the desired rate.

The results presented in Figure 6-10 tend to support the hypothesis tested. Within the first two minutes of contact, there was considerably less color uptake than in normal coagulation, and the rate of uptake lagged throughout the contact period. The effect of high G values was much more pronounced, presumably because of the smaller floc particles generated. Color uptake by floc formed at $G = 15\ sec^{-1}$ and exposed at $G = 76\ sec^{-1}$ was closely the same as color uptake by floc formed and exposed at $G = 76\ sec^{-1}$. Breakup of preformed floc at high rates of stirring could readily be seen. Because total surface area varies inversely with mean particle size, breakup must have enlarged the surface area available for adsorption, probably to a point at which the area was nearly the same in both instances. The slower uptake rate of floc formed at $G = 76\ sec^{-1}$ and exposed at $G = 15\ sec^{-1}$ may be accounted for by floc growth during the contact period.

Coagulation of Naturally Colored Water

The validity of results obtained with artificially colored water was confirmed in a small number of experiments with a naturally colored water taken from the Charles River near the Charles River Dam. This source was chosen because it was winter and most swamps and small streams were frozen over and carried little water. The color of the water varied with the degree of snow melt.

The natural color of the water collected was about 25 units (measured at pH 10.2), the natural alkalinity 10 mg/l as $CaCO_3$, and the pH about 6.8. In conformity with earlier experiments, the alkalinity was increased by the addition of 10 ml of an 0.1 molar bicarbonate solution to 450 ml river water. The resulting total alkalinity was approximately 109 mg/l as $CaCO_3$. The addition of coagulant and distilled water brought the total volume to 500 ml as before.

By measuring the absorbances of samples of diluted water at a wavelength of 365 mμ and a pH of 10.2, a calibration curve of relative color was established. Shown in Figure 6-11, this curve is linear in terms of relative color (or concentration of color). Accordingly, the ratios of absorbances were again used to compute the percent color remaining in solution after coagulation.

The experimental results obtained with natural waters proved to be more erratic than the results for artificially colored waters. However, the overall pattern of color removal agreed well with the earlier studies, thereby justifying the use of a synthetically colored water for the studies reported in this chapter.

Coagulation of Turbid Water

Success with color removal encouraged extension of the experimental program to coagulation of turbidity. A kaolin (Peerless[*] No. 2 clay) mined near Bath, South Carolina, provided the turbidity. It was selected because it was available through the Laboratory of Soil Mechanics in Harvard University.

The characteristics of the clay were obtained from studies made at Cornell University[**] on the same type of kaolin. The exchange capacity of the kaolin, determined by the ammonium acetate method, was 2.8 milliequivalents per 100 grams, with sodium, potassium, calcium, and magnesium ions accounting for about half the capacity. On a weight basis, the median particle size of the natural clay was 1.6 microns, with 80 percent of the particles smaller than 10 microns and 20 percent smaller than 0.1 micron. The 10-percent size was estimated, by extrapolation, as 0.4 micron.

A stock solution of turbidity was prepared by adding 0.2 gram of kaolin and a small quantity of dispersing agent (2×10^{-3} g/l Alconox) to 500 ml of distilled water in a blender. The mixture was agitated for one minute before being diluted to one liter. For most of the tests, the turbid mixture was allowed to settle for 18 hours before it was used, samples being carefully withdrawn to avoid resuspension of settled particles. Under these conditions, no particle larger than 1.8 microns and corresponding roughly in size to the 60-percent value of the original distribution would remain in suspension.

---

[*] Distributed by the R. T. Vanderbilt Co., Inc., 230 Park Avenue, New York, N. Y.

[**] Final Report, Soil Solidification Research, Vol. II, "Fundamental Properties, Clay-Water Systems," Cornell University, 1951.

Turbidity measurements were made with the Lumetron Colorimeter, a 429 mμ interference filter serving as the monochromator. The sample cells had nominal lightpaths of 5 cm. A typical calibration curve for the diluted stock solution is shown in Figure 6-13. The turbidity represents measurements of the same samples in a Jackson-Candle Turbidimeter. However, percent turbidity remaining was computed from absorbance ratios.

The experimental procedure remained essentially unchanged. Samples of turbid water were prepared by adding to 200 ml of stock kaolin suspension 100 ml of 0.01 molar bicarbonate solution and sufficient distilled water to bring the total volume to 500 ml after addition of the coagulant.

As shown in Figure 6-14, the pattern of the earlier studies appears once again. Removals were 90% or better within 10 minutes at all recorded G values. Ultimate removals approximated 97% within 40 minutes. Slightly greater initial uptake rates were associated with the larger G values.

Discussion of Results

The studies reported in this chapter have substantiated, in large measure, the hypothesis that uptake of color or turbidity by floc takes place predominantly within the first few minutes of the coagulation process. Average values for the results here reported indicate an overall removal efficiency of about 80 percent for 50 minutes of flocculation, of which about 85 percent occurs within the first 2 minutes of flocculation and about 95 percent within the first 10 minutes.

During the early stages of flocculation, the uptake rate seems to depend on the mean temporal velocity gradient in the liquid. Subsequently, this dependence appears to be lost, possibly because the nucleation rate is greater at high G values. However, this thought remains to be substantiated experimentally.

It seems reasonable to postulate, therefore, that the principal function of flocculation is the promotion of floc growth for "phase-separation" by sedimentation or filtration.

Color uptake, here ascribed to the nucleation of the floc, was not completed within the rapid-mix period employed in these studies. The nucleation step deserves more careful scrutiny. Of particular interest should be kinetic studies of nucleation both in the absence and presence of color and turbidity. They would be a logical extension of the particle-growth studies described in the previous chapter of this thesis.

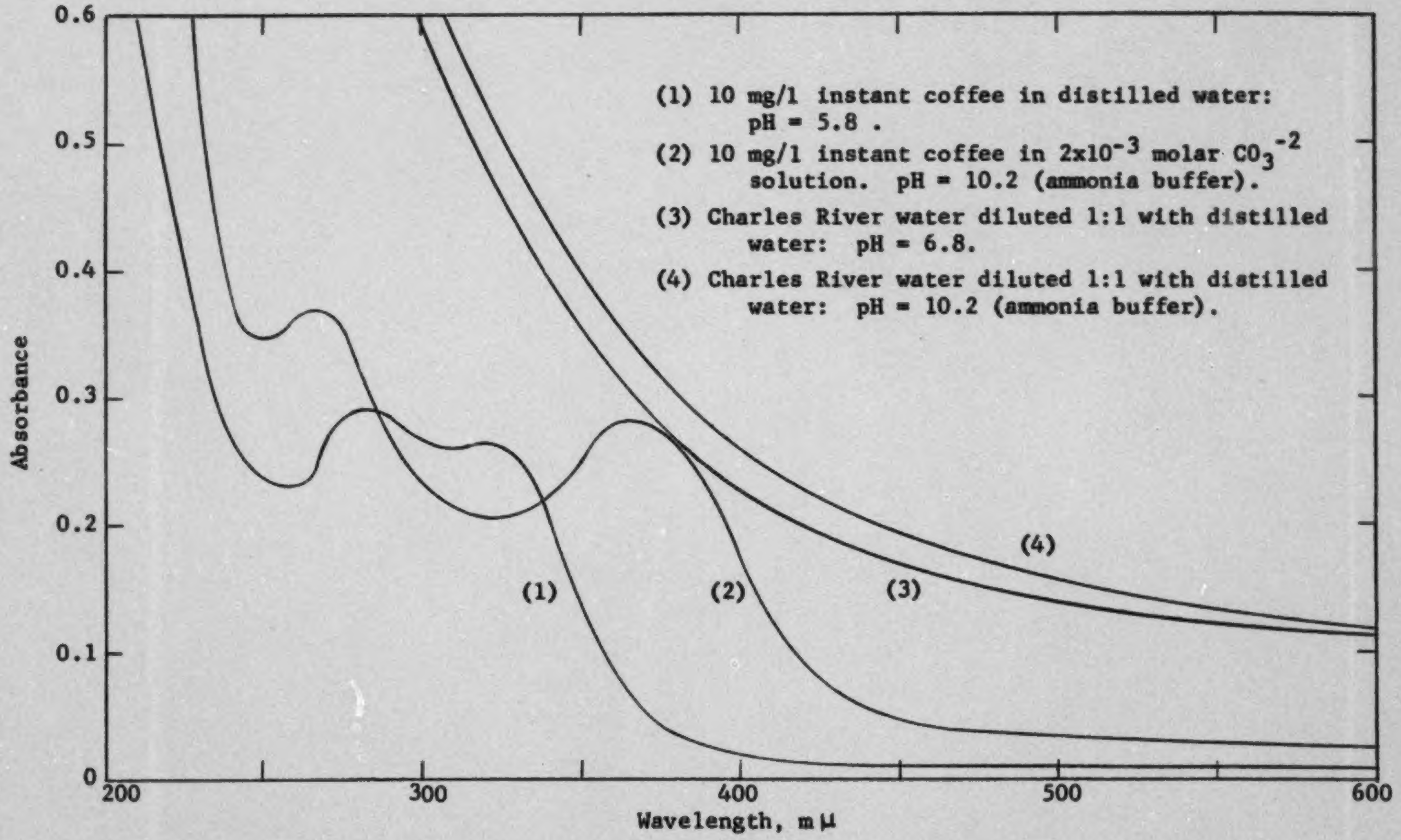

FIGURE 6-1. SPECTRA OF INSTANT COFFEE SOLUTION AND CHARLES RIVER WATER AT DIFFERENT pH VALUES

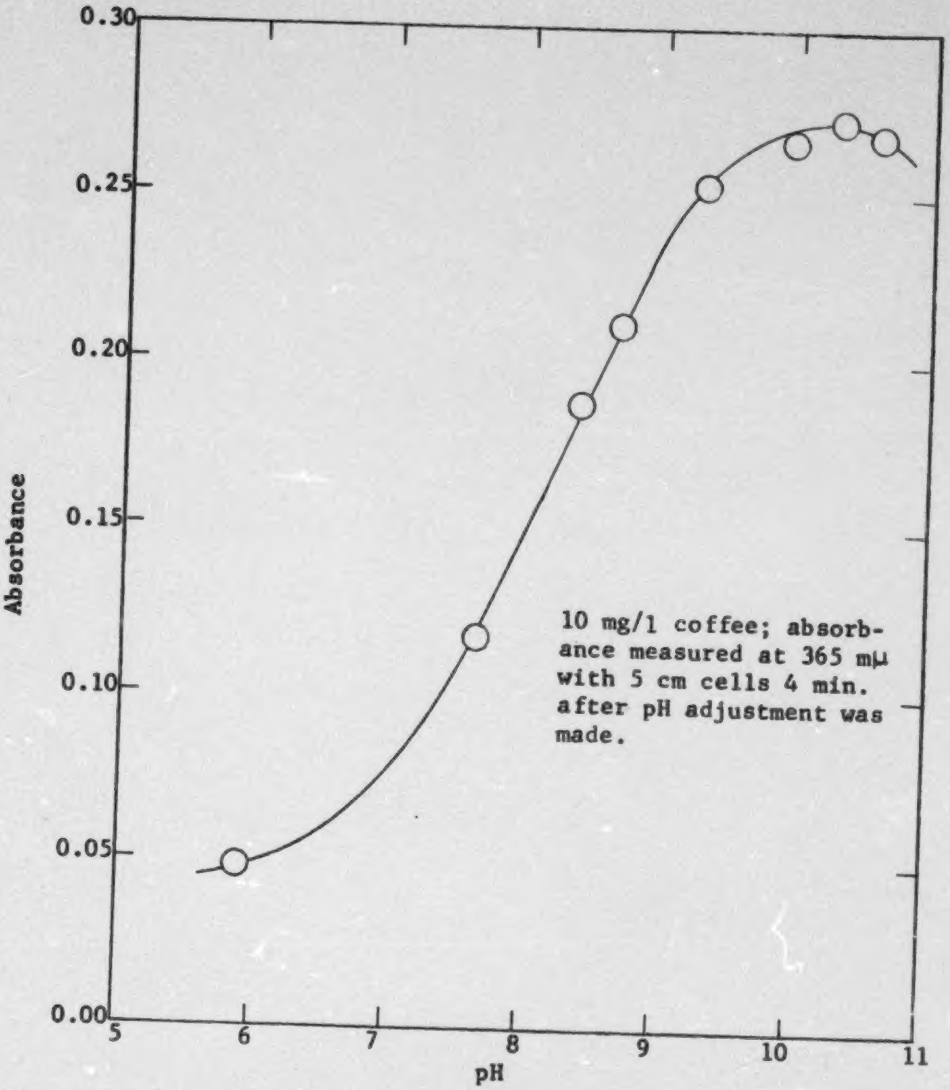

FIGURE 6-2. EFFECT OF pH ON ABSORBANCE OF INSTANT COFFEE SOLUTION.

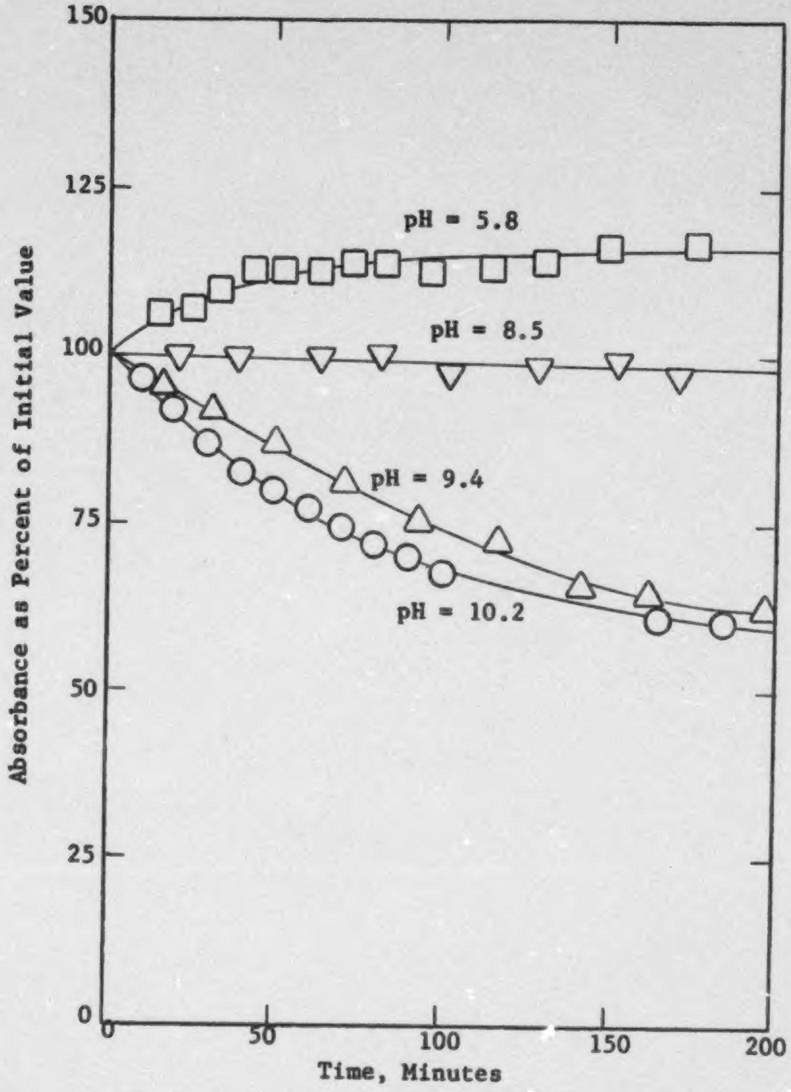

FIGURE 6-3. TIME STABILITY OF COFFEE COLOR AT DIFFERENT pH VALUES

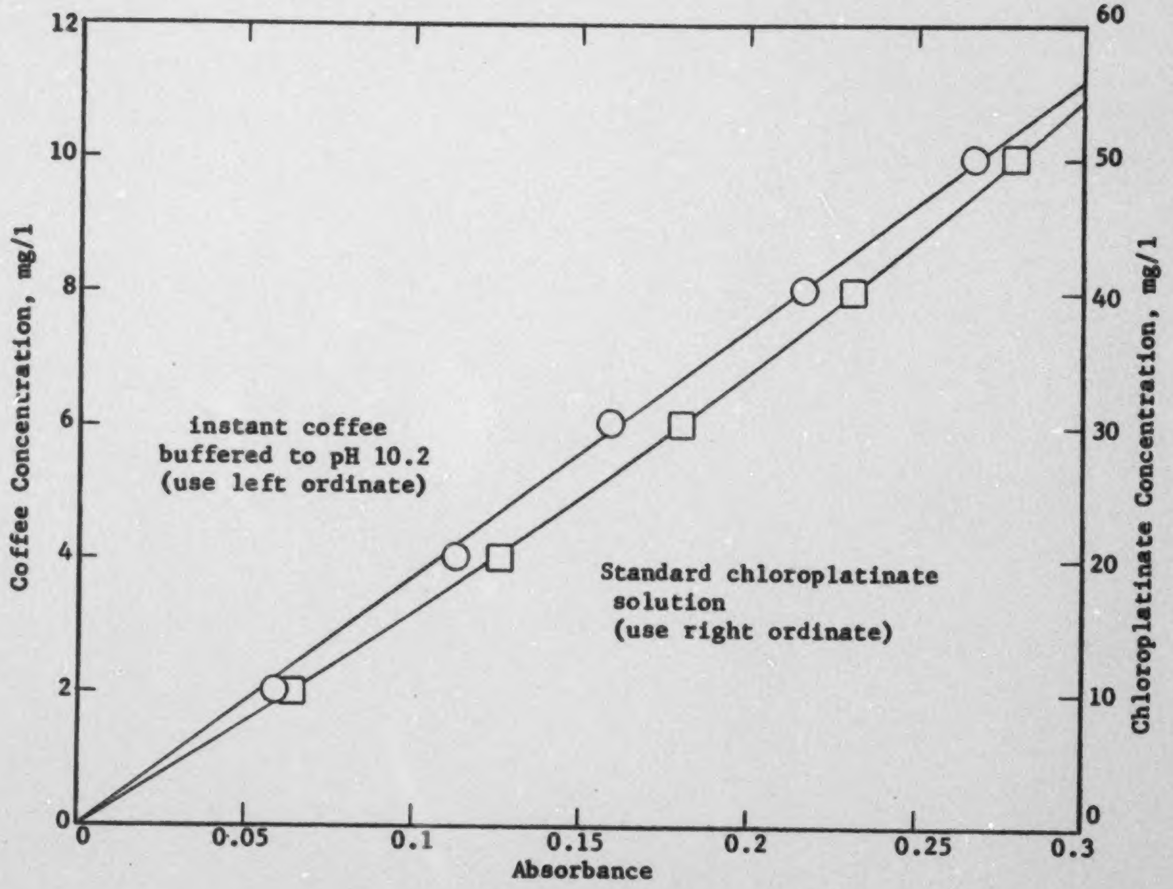

FIGURE 6-4. COLOR CALIBRATION CURVES FOR INSTANT COFFEE AT pH = 10.2 AND CHLOROPLATINATE SOLUTION (365 mμ wavelength, 5 cm cells)

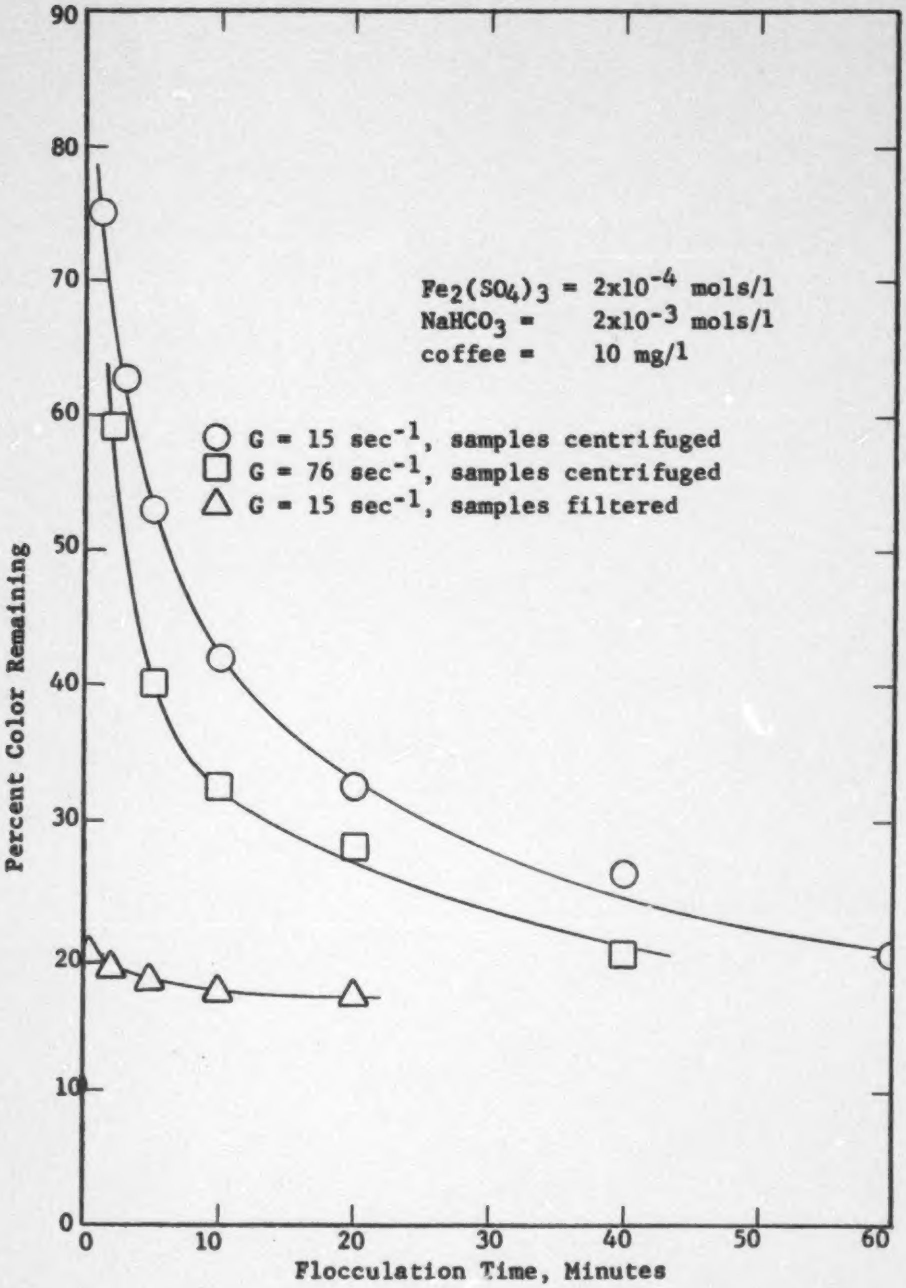

FIGURE 6-5. EFFECT OF G ON RATE OF COLOR REMOVAL. Coagulation of coffee with ferric sulfate.

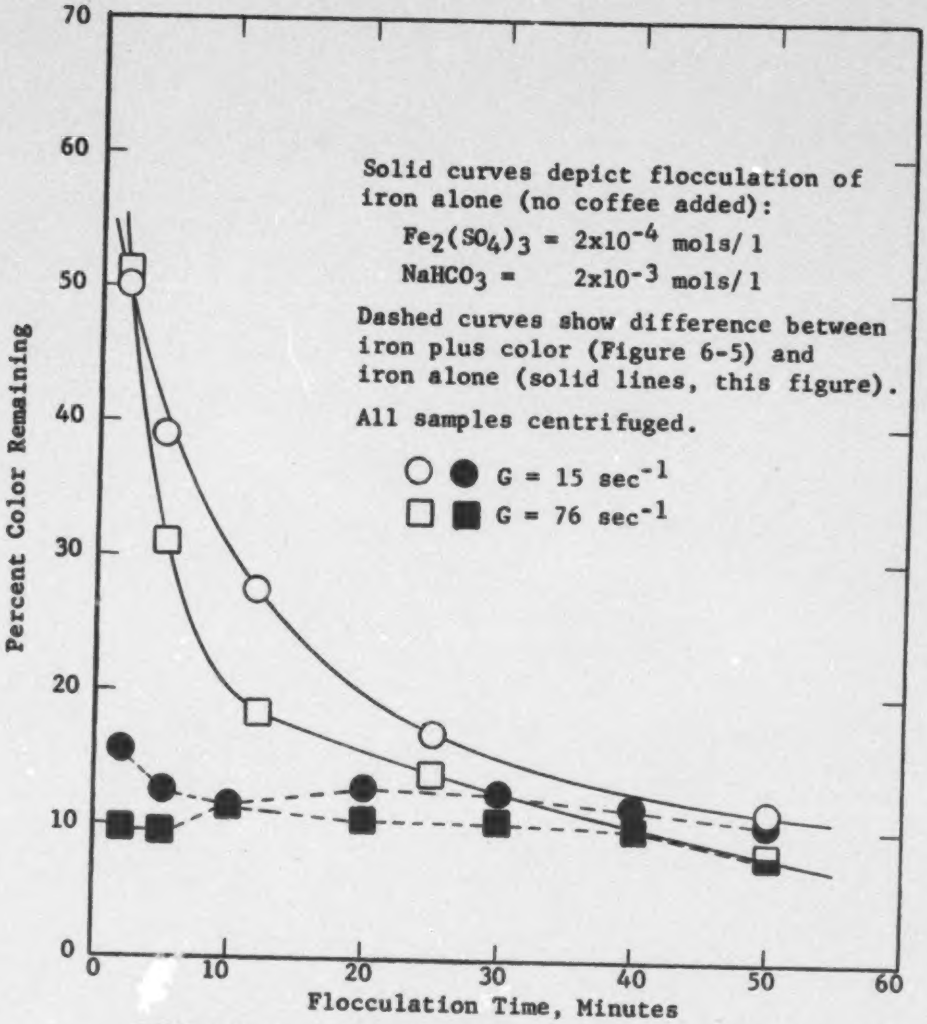

FIGURE 6-6. EFFECT OF G ON RATE OF COLOR REMOVAL.
Flocculation of ferric sulfate alone.

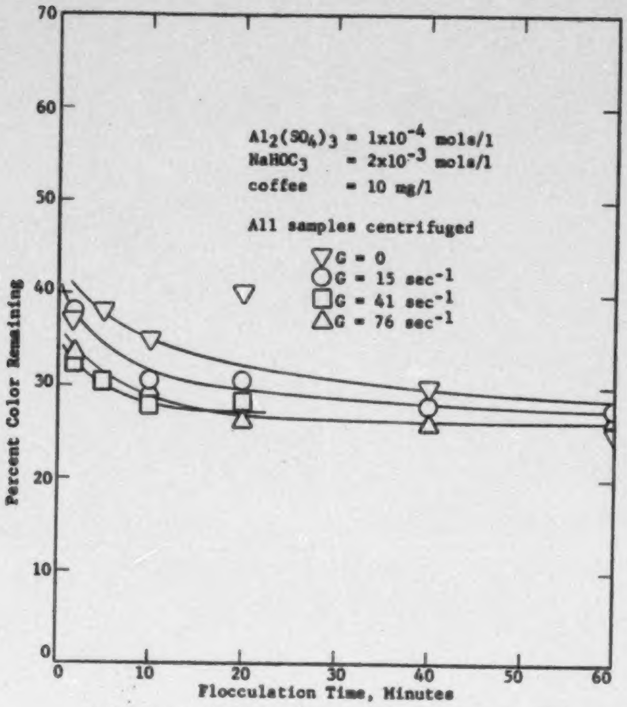

FIGURE 6-7. EFFECT OF G ON RATE OF COLOR REMOVAL. Coagulation of coffee with alum.

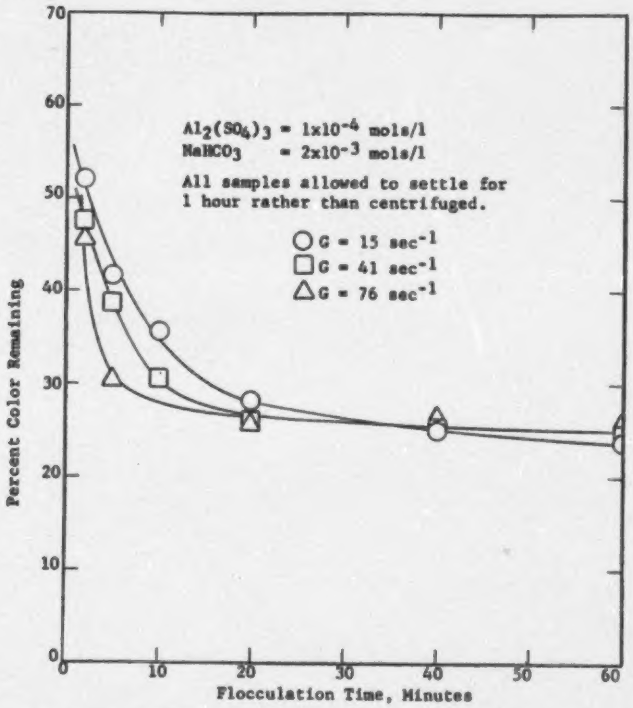

FIGURE 6-8. EFFECT OF G ON RATE OF COLOR REMOVAL. Coagulation of coffee with alum.

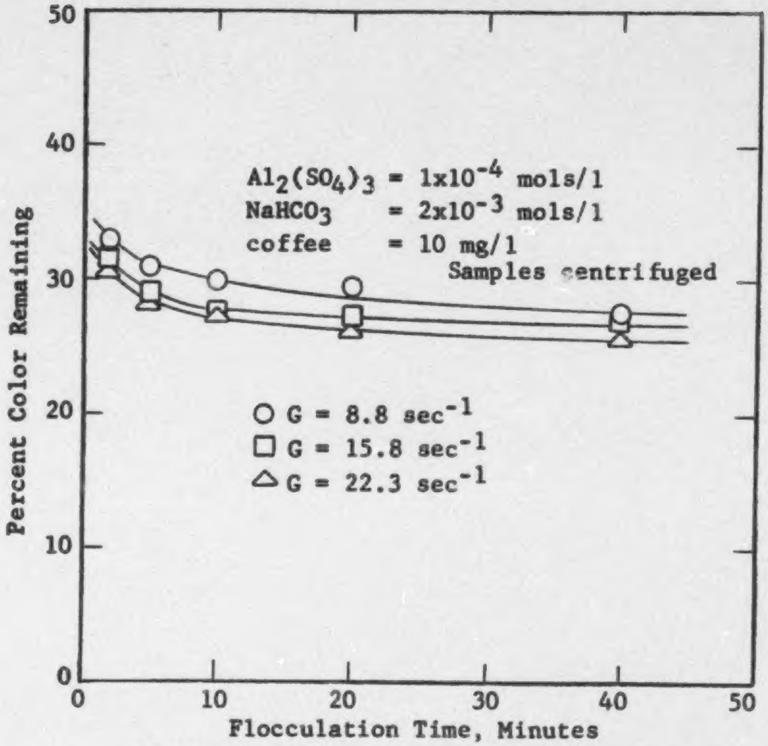

FIGURE 6-9. EFFECT OF G ON RATE OF COLOR REMOVAL.
Coagulation of coffee with alum using second shear gradient apparatus.

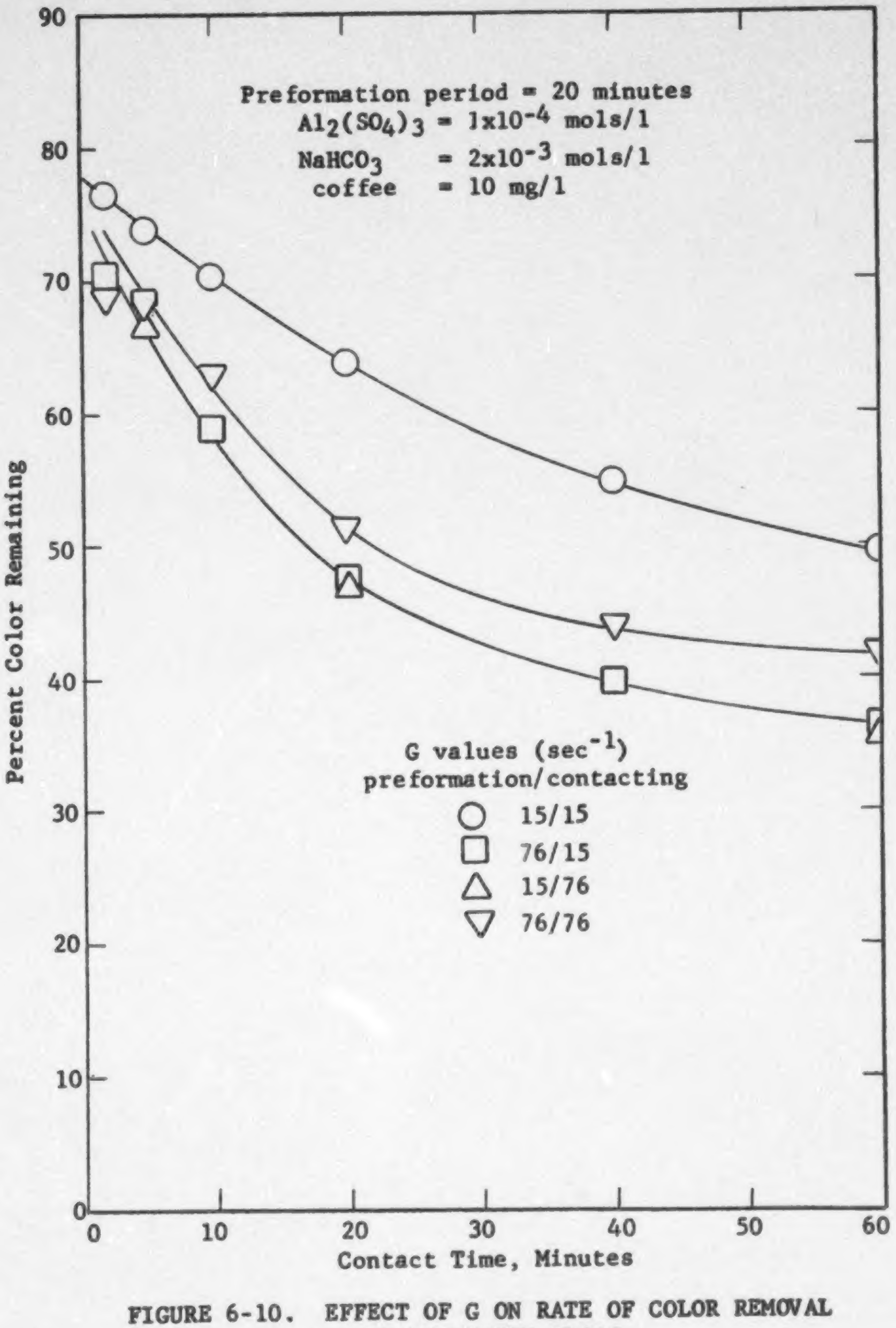

FIGURE 6-10. EFFECT OF G ON RATE OF COLOR REMOVAL BY PREFORMED FLOCS

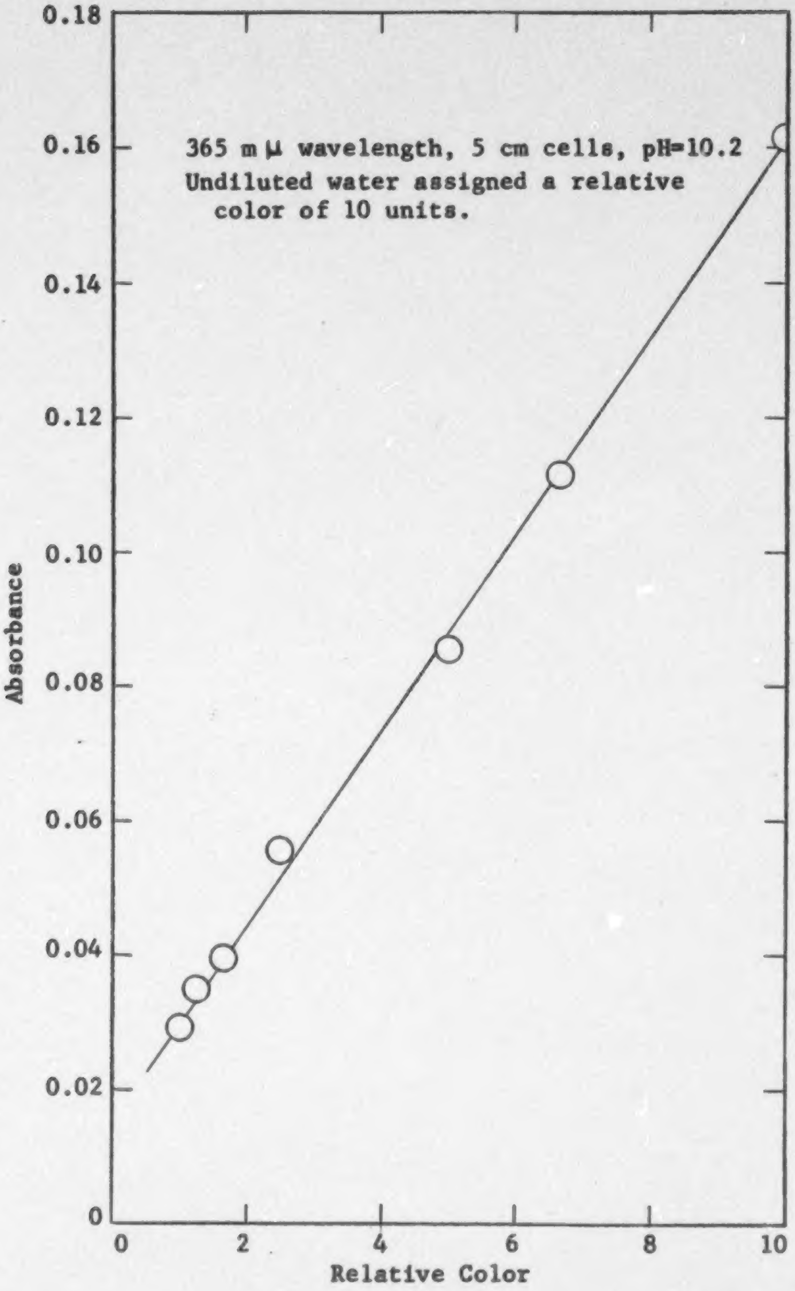

FIGURE 6-11. ABSORBANCE OF CHARLES RIVER WATER UPON DILUTION.

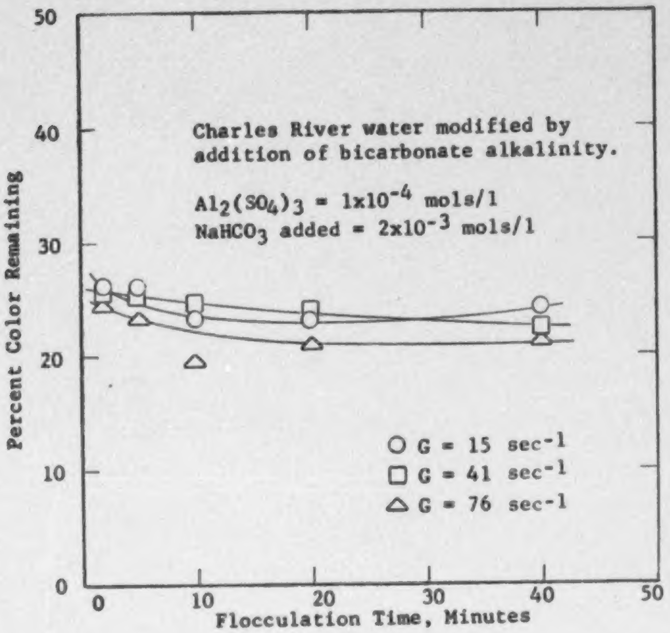

FIGURE 6-12. COAGULATION OF NATURALLY COLORED WATER

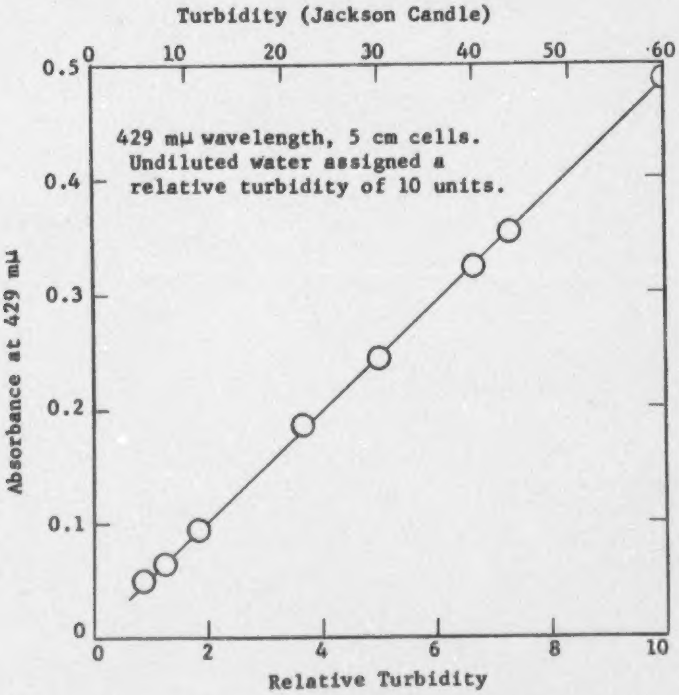

FIGURE 6-13. ABSORBANCE OF TURBID WATER UPON DILUTION.

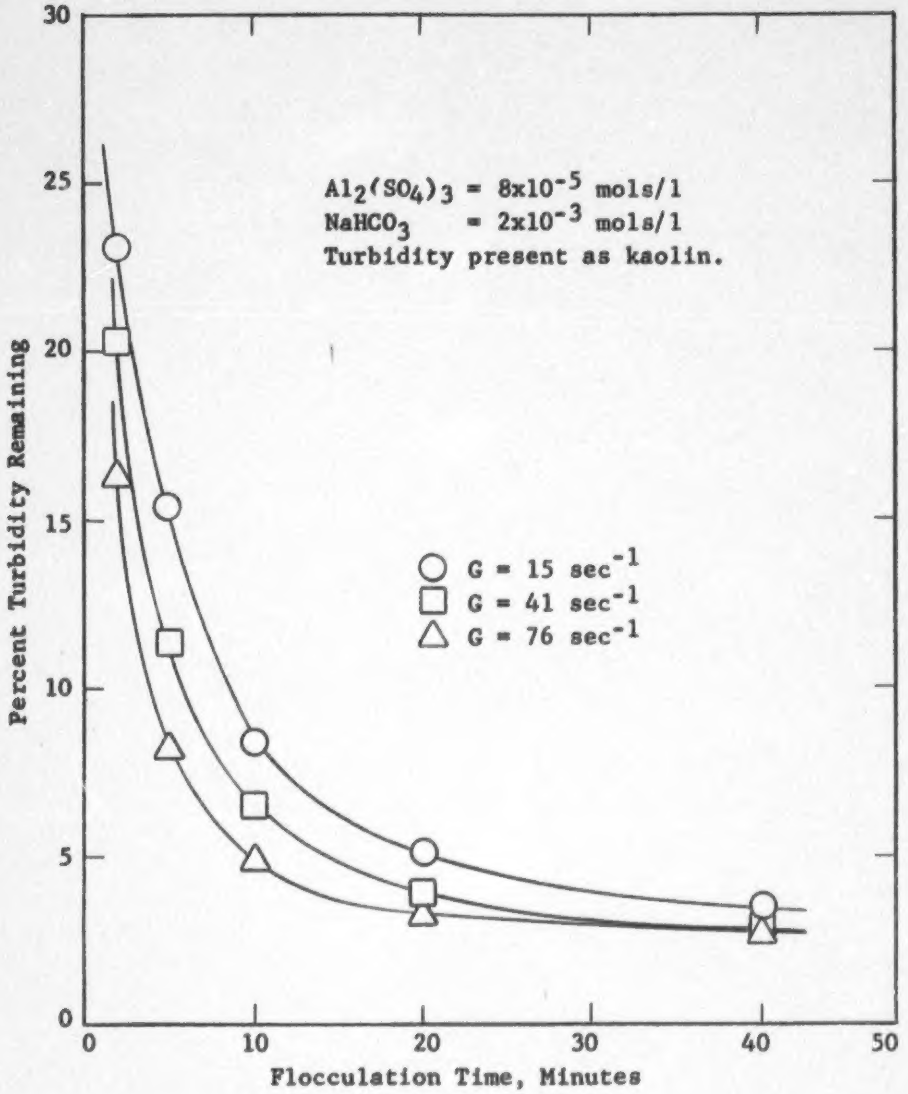

FIGURE 6-14. EFFECT OF G ON RATE OF TURBIDITY REMOVAL.

Chapter 7

SUMMARY AND RECOMMENDATIONS

The Smoluchowski Equation for Orthokinetic Flocculation

A theoretical base for the effect of fluid velocity gradients on rate of flocculation was laid in 1916 by von Smoluchowski(18) in the following equation for orthokinetic flocculation of colloids.

$$J_{ij} = \frac{4}{3} n_i n_j R_{ij}^3 \frac{du}{dz} \qquad (2\text{-}22)$$

Here J_{ij} is the rate of collision between particles of sizes i and j in a unit volume of flocculating liquid containing n_i and n_j particles of these respective sizes; R_{ij} is the radius of the sphere of influence of these particles, or the maximum separation of their centers at the time of conjunction; and du/dz is the local velocity gradient in the suspending liquid. Although lip service has been paid to this equation since the 1940's, it has not found as much use in the management of flocculation processes as it deserves. As shown in the body of this thesis, there are many reasons why this is so. Chief among them is the fact that there is no analytical solution for it.

A review of von Smoluchowski's work and that of his successors in this field does, indeed, lead to the conclusion that this equation of von Smoluchowski for number of contacts between particles suspended in moving fluids is an oversimplified mathematical model of flocculation. The deficiencies of the equation are many: the paths actually followed by the particles are more complex than assumed; the effects of surface charge and related phenomena are not accounted for in full; and the complexities of non-laminar flow are not considered at all. Nevertheless, the equation does give being to a number of parameters that are of major importance in flocculation performance. The relative simplicity of its form, unlike that of later modifications or alternative equations, was particularly useful in the studies reported in this thesis. For these, it could be incorporated readily in a preliminary mathematical model of the floc growth patterns that are traced by chemical coagulation of colored and turbid waters.

Results Obtained by a Computer Program

Since von Smoluchowski's equation cannot be solved analytically for the relationship between velocity gradient and rate of floc growth, it has been a purpose of this thesis to examine the equation by programming it for numerical solution with a high-speed digital computer. Within the frame of reference of the thesis and with computer capability in mind, von Smoluchowski's equation for orthokinetic flocculation was modified so as to narrow the range of particle sizes that had to be considered in the computer analysis. At the same time, a similar modification of von Smoluchowski's equation for perikinetic flocculation (equation 2-1) was also programmed. This was done primarily for the sake of comparing the results of the modified perikinetic equation with the results of its unmodified prototype for which there is an analytic solution (equations 2-9, 2-10, and 2-13). Agreement was good, but there was a steepening trend towards divergence as the flocculation period was lengthened. That divergence was not large, however, is shown by the fact that after 10 flocculation half-times, divergence was still under 3 percent.

The computer program was designed to provide information on mean floc size and floc size distribution at designated times in the course of flocculation. Based on the assumption that the particles were spherical, the size measures - diameter, area, and volume - were expressed in units of their respective values for a particle of unit volume, and the relative importance of the following groups of factors were determined by computer runs: (1) the variables in the von Smoluchowski equation; (2) the mechanism that establishes a floc-size maximum; (3) the restriction of particle contacts in ratio to floc size; and (4) the assumed initial distribution function of particle size.

For an initially monodisperse sol, it was found that the three-factor product of the number of particles at the start of flocculation, the constant proportional to the velocity gradient, and the half-time of flocculation T is essentially constant (see Table 3-1). For different floc-size limits, furthermore, growth patterns remained colinear during early flocculation and later departed thence only to become asymptotic to their imposed steady-state sizes (see Figure 3-10).

Four procedures of floc breakup or maximum-size control were examined. In the first, conjunctions larger than the prescribed maximum were automatically returned to their immediately preceding individuality. In the remaining three procedures, oversized conjunctions were split into two, three, or four substantially equi-sized components. Once again, floc growth patterns proved to be quite similar, except that the steady-state mean size was found to decrease in the order in which the procedures are listed (see Figure 3-6). The approach to steady-state size was most leisurely when conjunction and breakup neutralized each other. In all instances, sigmoidal curves terminated as asymptotes to the steady-state sizes, and particle size distributions showed that flocs accumulated at size levels that depended on the type of imposed breakup.

Kinetics of Flocculation*

The change in total number of particles during flocculation could not be represented satisfactorily by first- or second-order kinetic expressions. However, the near constancy of the product GTN_o did imply a certain kinship with second-order decrease. Moreover, the half-time of flocculation was inversely proportional to the initial number of particles present; in chemical coagulation, a corresponding determinant is the concentration of the coagulant applied.

Patterns of floc growth were affected only slightly by the form of the distribution graph for initial particle sizes. However, increased contact opportunity associated with polydispersion did enhance the rate at which flocculation proceeded.

An important conclusion to be drawn from the computer studies is that von Smoluchowski's equation can offer much help in flocculation analysis, and that until the dynamics of interparticle behavior have been better established, the use of more sophisticated expressions does not seem warranted.

Design Criteria

As a matter of experience, the chemical coagulation of water proceeds satisfactorily - with good floc formation, therefore - when the mean temporal velocity gradient G of the flocculation basin or device lies between 2 and 40 sec^{-1} and when the non-dimensional product Gt - where t is the duration of flocculation in seconds - lies between 5000 and 50,000. Although the water-purification literature is not always consistent in its support of these values and the values themselves range over at least one order of magnitude, it can be said with some assurance that the mean temporal velocity gradient imposed on flocculating suspensions is in fact a major determinant in flocculation operations.

---

* Based on the mathematical model

Shear Apparatus and Flocculation Measurement

For comparison of actual floc growth with growth predicted from theory, suitable apparatus and techniques for observing floc growth under controlled conditions were developed. The chosen test-cell design was patterned after the devices used earlier by Mason(41) and Ritchie(40). Analysis of the conditions of flow in cells of this kind laid down criteria for the design and operation of this type of cell to insure its satisfactory performance.

Progress of floc growth was recorded photographically; short-duration flash-lighting was used to "stop" floc motion; and size measurements were made on magnified images of the flocs. The measure of choice was the projected area of the floc. This was found by forming the product of the longest dimension of the floc and the greatest width of the floc perpendicular to the chosen axis. Although the calculated area is biased, it is a more reproducible concept of size than the estimated equivalent rectangle or equivalent circle.

Growth patterns of floc were recorded for constant G values of 3.2, 6.8, and 9.3 sec^{-1}. For measurement, floc images were either projected onto a screen from film negatives or transferred (with enlargement) onto a high-contrast photo paper. In projections, only flocs sharply in focus were measured; in prints, all visible flocs were examined.

In general, floc growth patterns at different G values were quite similar, but by no means equal. Observed mean floc size rose sharply at the beginning of flocculation, passed through a mode or maximum, and fell less sharply to an apparently steady-state value. The time for reaching the mode was such that, for the range of coagulant doses used, the product Gt ranged from 1,500 to 11,000 only. However, the prominence of the mode, or leptokurtosis, was shown to increase with truncation of the floc-size distribution as larger and larger flocs only were included in the mean. When smaller and smaller floc sizes were added, the curve flattened out. In one case, the mode vanished altogether. Measurement of all flocs in the sample would probably have raised the mean floc size monotonically during the course of flocculation, and a steady-state asymptote would have been approached. However, the larger flocs would still have undergone shear-induced rupture, and a modal growth pattern would still have applied to them.

Inverse proportionality between the modal mean floc size and the G value pointed to a reciprocal relationship between fluid shear and shear-controlled floc sizing. If the suggested relationship holds true, it will help to explain why the range of effective G values derived from inspection of design and operating data for treatment plants is so broad, for in traversing the upper region of the reported optimal range, mean floc size would be relatively insensitive to small differences in G values.

Comparison of Experiment and Mathematical Model

When the experimental results of this thesis were compared with the results synthesized by the mathematical models, it was discovered that the model in which the flocs are assumed to break up into four nearly equi-sized particles appears to simulate the experimental growth patterns with reasonable success. However, a maximum could not be created without truncating* the size distribution of the model. Moreover, the degree of truncation was found to determine the extent of the maximum. For successful simulation, the size distributions had to be truncated at the size of the smallest particle formed by breakup of conjunctions exceeding the allowable magnitude. Distributions with smaller particles failed to produce maxima; distributions truncated at larger sizes produced proportionally smaller or only relative maxima. The synthetic and experimental size distributions resembled one another and so gave added evidence of successful simulation.

Dosage and Color

In agreement with theory, bigger coagulant doses produced rates of floc growth more or less in keeping with the concentration of the coagulant. Moreover, flocs grew appreciably larger throughout most of the flocculation period. When bicarbonate water was colored with instant coffee, floc growth was retarded. However, the mean size of floc at the mode was left unchanged.

---

* Computations performed after this thesis was written indicate that truncation is not necessary if the breakup procedure and input variables are properly adjusted.

Most of the color ultimately removed by floc was bound to it within the first five or ten minutes of flocculation. Initial rates of color uptake were somewhat larger at high G values, but final differences in color removal were small.

A check of the usefulness of coffee as a coloring agent was obtained in experiments with turbid water prepared in the laboratory and with naturally colored water taken from the Charles River. Agreement with previous findings was good.

Although color uptake was not confined exclusively to a 30 sec rapid-mix period, the first few minutes of flocculation saw most of the "ultimate" binding of color to flocs. Hence, the conclusion is inescapable that the primary purpose of flocculation is to promote floc growth and thereby to facilitate sequent separation of flocs from the treated water.

Recommendations for Future Research

It is evident that flocculation is more than the agglomeration of small particles. Flocculation is not a static condition, but a state of equilibrium is generally reached. Flocs break up and recombine in merry roundelay. They are reduced into smaller components even when mean velocity gradients are low. This dynamic aspect of floc behavior should be studied further; the factors controlling floc destruction should be identified; and the inter-relationships of these factors within the flocculation process should be ascertained.

More fundamental would be an inquiry into the dynamics of particle interaction in a viscous fluid. Equations describing the motions of particles approaching one another lose their meaning when the particles are separated by only a few diameters, more particularly so, when particles do not move along an axis connecting their centers.

Before a fully satisfactory model of flocculation can be constructed, there must be much more general information about floc growth patterns and interparticle behavior. Of promise in computational research, such as that reported in this thesis, are the following inquiries: (1) widening the range of study of possible and useful floc sizes; (2) investigating other mechanisms by which maximum floc size may be limited; (3) revising the mathematical model for including the flocculation of non-spherical particles; and (4) solving the differential equations proposed by Fuchs(20) for perikinetic flocculation and by Müller(23) for orthokinetic flocculation.

The following comments upon these suggestions may be helpful. The maximum variation in diameter dealt with computationally in this thesis was somewhat less than fourfold and should be boosted substantially. It should be possible to reach a tenfold variation with present computer capacities and programming techniques. Floc growth has been limited in a few simple ways only. Other, more complex, ways should be introduced into the computer program. An example is the elaboration of the present forms of breakup to give the program a choice of breakup into two, three, or four particles, depending upon the size of unstable junctures. Moving to particle shape, it should be possible to select some useful single shape or to draw shapes, systematically or randomly, from a roster of possible constructions. A model of this kind is promising of considerably more sophisticated response than has been obtained so far.

Across the board comparisons of the successor equations of flocculation with von Smoluchowski's equations and with experimentally determined data should identify the relative importance of the newer parameters. In similar fashion, results obtained by von Smoluchowski's original differential equation for perikinetic flocculation might be compared with information derived from the analytic solution obtained by him through an approximation that is not valid for small flocculation times.

The kinetic aspects of color and turbidity uptake by chemically formed floc are also deserving of further study. If the results of such experiments are to be truly useful, the kinetics of nucleation or floc formation must first be known for the coagulant employed. There should be information on nucleation both in the presence and in the absence of color or turbidity. Description of the kinetics of nucleation is a logical extension of the description of floc growth patterns.

Once the properties of floc formed under careful control can be accurately predicted, attention should return to phase-separation. Inquiries into the settling of flocculent suspensions have been handicapped in two ways: (1) by inadequate characterization of the initial floc population and (2) by inadequate consideration of the flocculation that accompanies the settling process. There are similar inadequacies in the theory of filtration of flocculent suspensions.

The directions in which further investigation of orthokinetic flocculation can move are indeed many and so are the areas of interest.

APPENDIX A
NOTATION

Upper Case Roman

A	Area (general); Constant
A_p	Area of paddle blades in paddle flocculators
B	Constant
C	Centigrade
C_d	Coefficient of drag of paddles in paddle flocculator
D	Diffusion coefficient
E	Efficiency
G	Mean velocity gradient; Mean temporal velocity gradient; shear gradient
I_{ij}	Number of collisions per unit time and volume between particles of sizes i and j during perikinetic flocculation.
J_{ij}	Number of collisions per unit time and volume between particles of sizes i and j during orthokinetic flocculation.
K	Constant; A non-dimensional parameter used in the computation of critical Taylor number.
K_b	Boltzman Constant = 1.38×10^{-16} erg/degree Kelvin
L	Length
N	Concentration of particles (number per unit volume); Rotational speed of cylinders, revolutions per minute.
P	Power
R	Distance between centers of two particles forming a lasting contact; Radius of a collector particle; Radius of cylinder.
S	Shaft speed, revolutions per minute.

T	Half-time of flocculation, the time required for total number of particles to be reduced to half the initial number; Taylor Number.
T_c	Critical Taylor Number
Temp	Temperature in degrees Kelvin
U	Approach velocity of particle relative to a collector particle.
V	Velocity of paddle relative to the water in a paddle flocculator.
V	Volume

Lower Case Roman

a_n	centripetal (normal) acceleration
d	diameter
f	denotes functional relationship between parameters in equation
g	acceleration due to gravity
i	particle volume, often used as index or subscript
j	particle volume, often used as index or subscript
k	particle volume, often used as index or subscript; ratio of water speed to shaft speed in paddle flocculator
n_i	number of particles of size i per unit volume of flocculation liquid
q	volumetric rate of fluid flow
r	radius (general); ratio of particle length to particle diameter for rod-like particles; radius to areal centroid of individual paddle in paddle flocculators; space coordinate in cylindrical coordinates.
t	time (general)
u	fluid velocity in direction of increasing X in cartesian coordinates
v	fluid velocity in direction of increasing θ in cylindrical coordinates

x	cartesian coordinate axis; distance along this axis
y	cartesian coordinate axis; distance along this axis
z	cartesian coordinate axis; distance along this axis

Greek

α	The fraction of particle collisions leading to lasting combinations.
θ	Direction in cylindrical coordinate system; distance in this direction.
μ	Absolute viscosity of fluid; micron
ν	Kinematic viscosity of fluid
π	3.1416
ρ	Mass density
Σ	Summation
τ	Intensity of shear stress
Ω	Angular velocity

Miscellaneous Symbols

∂	Partial differential
$\doteqdot$	Approximate equality
∞	Infinity
$\int$	Integral

For a list of computer program input variables in Fortran mnemonics, see Appendix C.

APPENDIX B: BIBLIOGRAPHY

1. Fair, G.M., and Geyer, J.C., Water Supply and Waste Water Treatment. John Wiley & Sons, New York, 1954, Chapter 23, p. 617.
2. Kruyt, H.R., Editor, Colloid Science, Vol. 1, Elsevier Publishing Co., New York, 1952.
3. Mysels, K.J., Introduction to Colloid Chemistry, Interscience Publishers, Inc., New York, 1959.
4. Weiser, H.B., Colloid Chemistry, Second Ed., John Wiley & Sons, New York, 1948.
5. Tuorila, P., Über orthokinetische und perikinetische koagulation, Kolloidchem. Beihefte, 24, 1927, p. 1.
6. Langelier, W.F., and Ludwig, H.F., Mechanism of Flocculation in the Clarification of Turbid Waters, Jour. AWWA, 41, 1949, p. 163.
7. Peterson, B.H., and Bartow, E., Effect of Salts on the Rate of Coagulation and the Optimum Precipitation of Alum Floc, I. and E.C., 20, 1928, p. 51.
8. Bartow, E., Black, A.P., and Sansbury, W.E., Formation of Floc by Ferric Coagulants, I. and E.C., 25, 1933, p. 898.
9. Black, A.P., Rice, Owen, and Bartow, E., Formation of Floc by Aluminum Sulfate, I. and E.C., 25, 1933, p. 811.
10. Theriault, E.J., and Clark, W.M., An Experimental Study of the Relation of Hydrogen Ion Concentrations to the Formation of Floc in Alum Solutions, Pub. Health Rpts., 38, 1923, p. 181.
11. Miller, Lewis B., On the Composition of the Precipitate from Partially Alkalinized Alum Solutions, Pub. Health Rpts., 38, 1923, p. 1995.
12. Langelier, W.F., and Ludwig, H.F., Mechanism of Flocculation in the Clarification of Turbid Waters, Jour. AWWA, 41, 1949, p. 163.
13. Langelier, W.F., Ludwig, H.F., and Ludwig, R.G., Flocculation Phenomena in Turbid Water, Trans. ASCE, 118, 1953, p. 147.
14. Stumm, W., and Morgan, J.J., Chemical Aspects of Coagulation, Jour. AWWA, 54, 1962, p. 971.
15. Turkevich, John, The World of Fine Particles, American Scientist, 47, 1959, p. 57.

16. Baylis, J.R., Electron Microscope Methods, Proceedings, Rudolfs Research Conference, pp. 337, 338, June 1961. (Rutgers, The State University of New Jersey)

17. Overbeek, J.Th.B., Kinetics of Flocculation, Chapter 7, *Colloid Science*, *Vol.1*, edited by H.R.Kruyt; Elsevier Publishing Co., New York, 1952.

18. von Smoluchowski, M., Drei Vorträge über Diffusion, Brownsche Molekularbewegung und Koagulation von Kolloidteilchen, *Physik. Z.*, *17*, 1916, p. 557.

19. von Smoluchowski, M., Versuch einer mathematischen Theorie der Koagulationskinetik kolloider Losungen, *Z. Physik. Chem.*, *92*, 1917, pp. 129 and 155.

20. Fuchs, N., Über die Stabilität und Aufladung der Aerosole, *Z.Physik.*, *89*, 1934, p. 736.

21. Müller, H., Die Theorie der Koagulation polydisperser Systeme, *Kolloid-Z.*, *38*, 1926, p. 1

22. Müller, H., Zur Theorie der electrischen Ladung und der Koagulation der Kolloide, *Kolloidchem. Beihefte*, *26*, 1928, p. 257.

23. Müller, H., Zur allgemeinen Theorie der raschen Koagulation, *Kolloidchem. Beihefte*, *27*, 1928, p. 223.

24. Fair, G.M., and Geyer, J.C., *Water and Waste Water Treatment*, John Wiley & Sons, New York, 1954, Chapter 22, pp. 597 and 608.

25. Langelier, W.F., Coagulation of Water with Alum by Prolonged Agitation, *Eng'g News Record*, *86*, June 1921, p. 924.

26. Black, A.P., Buswell, A.M., Eidsness, F.A., and Black, A.L., Review of the Jar Test, *Jour. AWWA*, *49*, 1957, p. 1414.

27. Hyde, C.G., and Ludwig, H.F., Some New Features in the Design of Vertical Flocculation Units, *Jour. AWWA*, *36*, 1944, p. 151.

28. Fleming, J.D., The Purification of Highly Turbid Waters, *Jour.AWWA*, *22*, 1930, p. 1559.

29. Willcomb, G.E., Floc Formation and Mixing Basin Practice, *Jour. AWWA*, *24*, 1932, p. 1416.

30. Nolte, A.G., and Kramer, W.A., Coagulation with Aluminum Sulfate, *Jour. AWWA*, *25*, 1933, p. 1263.

31. Leipold, C., Mechanical Agitation and Alum Floc Formation, Jour. AWWA, 26, 1934, p. 1070.

32. Dempster, A.T., An Experimental Study of Stilling Walls for Sedimentation Basins, M.S. Thesis, M.I.T., 1934.

33. Dennis, A.P., Experimental Studies of the Shearing Strength of Floc Particles, M.S. Thesis, M.I.T., 1939.

34. Camp, T.R., Root, D.A., and Bhoota, B.V., Effects of Temperature on Rate of Floc Formation, Jour. AWWA, 32, 1940, p. 1913.

35. Camp, T.R., and Stein, P.C., Velocity Gradients and Internal Work in Fluid Motion, Jour. Bos.Soc.Civil Engrs., 30, 1943, p. 219.

36. Camp, T.R., Sedimentation and the Design of Settling Tanks, Trans. ASCE,111, 1946, pp. 921-22 and 929-30.

37. Camp, T.R., Flocculation and Flocculation Basins, Trans. ASCE, 120, 1955, p. 1.

38. Bean, E.L., Study of Physical Factors Affecting Flocculation, Water Works Engin., 106, 1953, p. 33.

39. Hudson, H.E., Jr., Flocculation and Flocculation Aids, Jour. AWWA, 49, 1957, p. 242.

40. Ritchie, A.R., Certain Aspects of Flocculation as Applied to Water and Sewage Purification, Doctoral Thesis, University of London, 1955.

41. Mason, S.G., and Bartok, W., The Behavior of Suspended Particles in Laminar Shear, Chapter 2, Rheology of Disperse Systems, Pergamon Press, New York, 1959.

42. Richardson, E.G., Editor, Aerodynamic Capture of Particles, Pergamon Press, New York, 1960.

43. Couette,E., Etudes sur le frottement des liquides, Ann. d. Chim. et Phys., 21, 1890, p. 433.

44. Rouse, H., Advanced Mechanics of Fluids, John Wiley & Sons, New York, 1959, p. 218.

45. Schlicting, Boundary Layer Theory, Pergamon Press, London, 1955, p.64.

46. Townsend, A., The Structure of Turbulent Shear Flow, Cambridge University Press, 1956, p. 294.

47. Taylor, G.I., Stability of a Viscous Liquid Contained between Two Rotating Cylinders, Phil. Trans. Royal Soc. (London), Series A, 223, 1923.

48. Taylor, G.I., Distribution of Velocity and Temperature between Concentric Cylinders, Proc. Royal Soc. (London), Series A, 151, 1935, p. 494.

49. Taylor, G.I., Fluid Friction between Rotating Cylinders, Proc. Royal Soc. (London), Series A, 157, December 1936, p. 546.

50. Wendt, F., Turbulente Strömungen zwischen zwei rotierenden koaxialen Cylindern, Ing. Archiv., IX, No. 6, 1933, p. 577.

51. Lord Rayleigh, On the Dynamics of Revolving Fluids, Proc. Royal Soc. (London), Series A, 93, 1917-1918, p. 148.

52. Chandrasekhar, S., The Stability of Flow between Rotating Cylinders, Proc. Royal Soc. (London), Series A, 246, 1958, p. 301.

53. Donnelly, R.J., Experiments on the Stability of Viscous Flow between Rotating Cylinders, I. Proc. Royal Soc. (London), Series A, 246, 1958, p. 312.

54. Donnelly, R.J., and Fultz, D., Experiments on the Stability of Viscous Flow between Rotating Cylinders, II. Proc. Royal Soc. (London), Series A, 258, 1960, p. 101.

C-1

APPENDIX C

COMPUTER PROGRAM

FOR

FLOCCULATION EQUATIONS

Contents

1. Program Flow Sheet
    a. main program
    b. subroutines
2. List of Input Variables
    a. Fortran mnemonic for variable
    b. common value of variable
    c. meaning or significance of variable
3. Actual Program in Fortran Mnemonics
4. Sample of Program Output

FLOCCULATION PROGRAM: MAIN ROUTINE

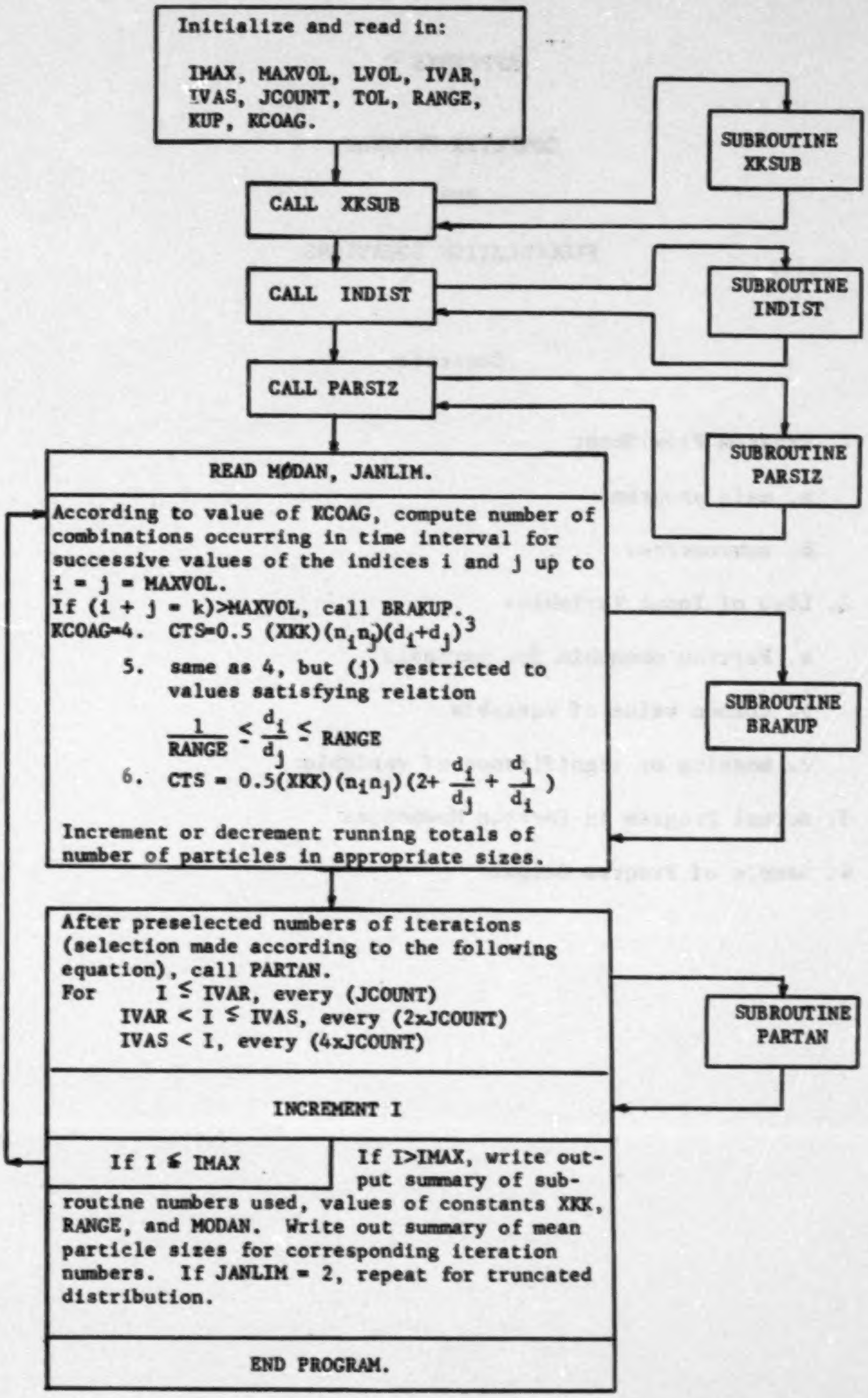

Initialize and read in:

IMAX, MAXVOL, LVOL, IVAR, IVAS, JCOUNT, TOL, RANGE, KUP, KCOAG.

CALL XKSUB
SUBROUTINE XKSUB
CALL INDIST
SUBROUTINE INDIST
CALL PARSIZ
SUBROUTINE PARSIZ

READ MØDAN, JANLIM.

According to value of KCOAG, compute number of combinations occurring in time interval for successive values of the indices i and j up to i = j = MAXVOL.

If (i + j = k)>MAXVOL, call BRAKUP.

KCOAG=4. $CTS=0.5\,(XKK)(n_i n_j)(d_i+d_j)^3$

5. same as 4, but (j) restricted to values satisfying relation

$$\frac{1}{RANGE} \le \frac{d_i}{d_j} \le RANGE$$

6. $CTS = 0.5(XKK)(n_i n_j)(2+ \frac{d_i}{d_j} + \frac{d_j}{d_i})$

Increment or decrement running totals of number of particles in appropriate sizes.

SUBROUTINE BRAKUP

After preselected numbers of iterations (selection made according to the following equation), call PARTAN.

For $I \le IVAR$, every (JCOUNT)

$IVAR < I \le IVAS$, every (2xJCOUNT)

$IVAS < I$, every (4xJCOUNT)

SUBROUTINE PARTAN

INCREMENT I

If $I \le IMAX$

If I>IMAX, write output summary of subroutine numbers used, values of constants XKK, RANGE, and MODAN. Write out summary of mean particle sizes for corresponding iteration numbers. If JANLIM = 2, repeat for truncated distribution.

END PROGRAM.

FLOCCULATION PROGRAM: SUBROUTINES

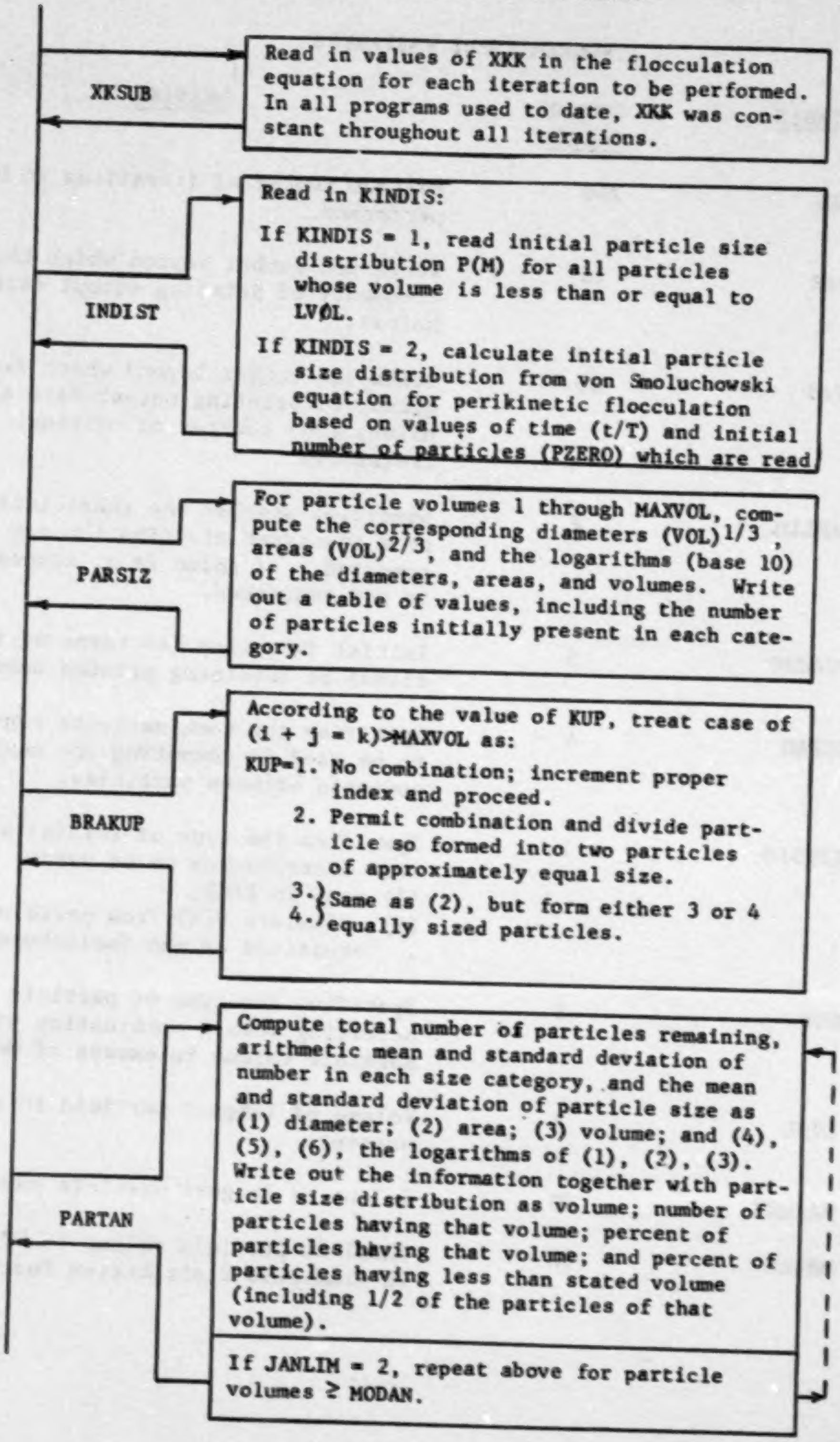

XKSUB

Read in values of XKK in the flocculation equation for each iteration to be performed. In all programs used to date, XKK was constant throughout all iterations.

INDIST

Read in KINDIS:

If KINDIS = 1, read initial particle size distribution P(M) for all particles whose volume is less than or equal to LVØL.

If KINDIS = 2, calculate initial particle size distribution from von Smoluchowski equation for perikinetic flocculation based on values of time (t/T) and initial number of particles (PZERO) which are read

PARSIZ

For particle volumes 1 through MAXVOL, compute the corresponding diameters $(VOL)^{1/3}$, areas $(VOL)^{2/3}$, and the logarithms (base 10) of the diameters, areas, and volumes. Write out a table of values, including the number of particles initially present in each category.

BRAKUP

According to the value of KUP, treat case of $(i + j = k) > MAXVOL$ as:

KUP=1. No combination; increment proper index and proceed.
2. Permit combination and divide particle so formed into two particles of approximately equal size.
3.} 4.} Same as (2), but form either 3 or 4 equally sized particles.

PARTAN

Compute total number of particles remaining, arithmetic mean and standard deviation of number in each size category, and the mean and standard deviation of particle size as (1) diameter; (2) area; (3) volume; and (4), (5), (6), the logarithms of (1), (2), (3). Write out the information together with particle size distribution as volume; number of particles having that volume; percent of particles having that volume; and percent of particles having less than stated volume (including 1/2 of the particles of that volume).

If JANLIM = 2, repeat above for particle volumes ≥ MODAN.

PROGRAM INPUT VARIABLES

VARIABLE	COMMON VALUE	MEANING
IMAX	200	Maximum number of iterations to be performed.
IVAR	20	Iteration number beyond which the frequency of printing output data halves.
IVAS	60	Iteration number beyond which frequency of printing output data again halves (one quarter of original frequency).
JANLIM	2	Specifies whether the characteristics of a truncated distribution are to be computed: if value is 1, truncation is not requested.
JCØUNT	5	Initial frequency (in terms of iterations) of obtaining printed output.
KCØAG	4	Specifies the combinational equation to be used in computing the number of contacts between particles.
KINDIS	1	Specifies the type of initial particle size distribution to be used: (1) read in P(M); (2) calculate P(M) from perikinetic equations of von Smoluchowski.
KUP	3	Specifies the type of particle breakup occurring when a combination yields a particle volume in excess of MAXVØL.
LVØL	1	Volume of largest particle initially present.
MAXVØL	20	Volume of largest particle permitted.
MØDAN	11	Smallest particle volume to be included in truncated distribution (output).

VARIABLE	COMMON VALUE	MEANING
* P(M); M=1, LVØL	$P_{(1)}$ = 1000.0	Initial number of particles of size M.
** PZERØ	1000.0	Initial number of particles to be used in computation of initial particle size distribution for orthokinetic flocculation.
RANGE	2.0	Limitation on permissible particle combinations based on relative particle sizes. Only two particles whose diameter ratio satisfies the relation $\left(\frac{1}{RANGE} \leq \frac{d_i}{d_j} \leq RANGE \right)$ may combine.
TØL	0.001	Tolerance placed on conservation of mass (volume) throughout run (a fraction of initial total volume).
** TRATIØ	1.0	Specifies value of t/T to be used in von Smoluchowski equation for perikinetic flocculation to compute the initial P(M) for orthokinetic flocculation.
XKK	0.00001	Parameter in coagulation equation which (for orthokinetic flocculation) reflects: (1) mean temporal velocity gradient; (2) particle size factor; (3) time factor.

---

*,** Alternative sets of variables: if KINDIS = 1, P(M) is used; if KINDIS - 2, TRATIØ and PZERØ are used.

```
*     FORTRAN
*     LIST8
*     LABEL
C COAG
      COMMON ALGBAR,ALGSUM,ALOG,ANOSUM,AREA,AREBAR,CTS,DIA,DIABAR,DLGBAR
     1,DLGSUM,DLOG,DNOSUM,I,IMAX,     IPSUM,IVAR,IVAS,J,JCOUNT,L,LINE,LL,
     2      LSAVE,LVOL,M,MAXVOL,N,P,PARSUM,PC,PCC,PLESS,PP,PRCNT,PSUM,PV
     3OL,R,RR,TCRIT,TOL,TVOL,VLGBAR,VLGSUM,VLOG,VNOSUM,VOLBAR,XK,XKK,IND
     4EX,LLINE,SAVEMN,B,MM,NN,NNN,MMM,KCOAG,KPRTN,KPSIZ,KROUT,KUP
     5,JAN,MOD,MODAN,SVPART,JANLIM,TRATIO,PZERO,KINDIS,RANGE,J1,J2
     6,PNOMN,PSQSM,ASQSM,VSQSM,DLSQSM,ALSQSM,VLSQSM,SDPNO,SDDIA,SDAREA,
     7 SDVOL,SDDIAL,SDAREL,SDVOLL,VOLMAX,DSQSM
      DIMENSION ALOG(100),AREA(100),DIA(100),DLOG(100),P(100),PLESS(100)
     1,PP(100),PRCNT(100),PSUM(100),PVOL(100),SAVEMN(8,1000),VLOG(100),
     2XK(1000),SVPART(8,1000)
      READ INPUT TAPE 4, 120,IMAX, MAXVOL, LVOL, IVAR, IVAS, JCOUNT, TOL
     1 ,RANGE,KUP,KCOAG
  120 FORMAT(6I5,F10.7,F10.4,2I5)
      CALL XKSUB
      J=1
      I=1
      INDEX=0
      DO 122 M=1,MAXVOL
      P(M)=0.0
  122 CONTINUE
      CALL INDIST
      CALL PARSIZ
      TCRIT=0.0
      READ INPUT TAPE 4, 123, MODAN, JANLIM
  123 FORMAT(I5,I5)
  124 DO 180 M=1, MAXVOL
      PP(M)=P(M)
      TCRIT=TCRIT+PVOL(M)*P(M)
  180 CONTINUE
  106 DO 100 M=1, LVOL
      IF(KCOAG-5) 191,192,191
  191 J1=1
      J2=LVOL
      GO TO 1910
  192 J1=PVOL(M)/(RANGE**3)+0.5
      J2= PVOL(M)*(RANGE**3)+0.5
 1910 DO 101 N=J1, J2
      IF (N-1) 101,190,190
  190 CONTINUE
      L=M+N
      PC=P(M)
      IF(M-N) 102, 103, 102
  103 PCC=P(N)-1.0
      B=0.5
      GO TO 1020
  102 PCC=P(N)
      B=0.5
 1020 IF (MAXVOL-L) 105, 104, 104
  105 CALL BRAKUP
      GO TO 101
  104 IF (KCOAG-5) 1042,1042,1040
 1042 CTS= B *XKK  *PC*PCC*(DIA(M)+DIA(N))**3
      GO TO 1041
 104C CTS=B*XKK*(2.0+(DIA(M)/DIA(N))+(DIA(N)/DIA(M)))*PC*PCC
 1041 CONTINUE
      PP(M)=PP(M)-CTS
      PP(N)=PP(N)-CTS
      PP(L)=PP(L)+CTS
      LSAVE=L
  101 CONTINUE
      LL=LSAVE
  100 CONTINUE
      TVOL=0.0
      DO150 M=1, MAXVOL
      TVOL=TVOL+PVOL(M)*PP(M)
  150 CONTINUE
      R=ABSF(TVOL-TCRIT)
      RR=TOL*TCRIT
      IF(R-RR) 151, 151, 152
  152 CALL DUMP
  151 LVOL=LL
      IF(JCOUNT-J) 110, 110, 111
  110 CALL PARTAN
      IF (I-IVAR) 111, 154, 155
  155 IF(I-IVAS) 111, 154, 111
  154 JCOUNT=JCOUNT*2
  111 J=J+1
      IF(IMAX-I) 114, 114, 115
  115 I=I+1
      DO 112 M=1, LVOL
      P(M)=PP(M)
  112 CONTINUE
      GO TO 106
  114 WRITE OUTPUT TAPE 2, 130
  13C FORMAT(1H155X10HTEST  DATA)
      WRITE OUTPUT TAPE 2, 131
  131 FORMAT(1H0 5X4HCOAG 9X5HXKSUB 9X3HXKK 8X6HINDIST 7X6HPARSIZ7X6HBRA
     1KUP 7X6HPARTAN8X5HRANGE 8X5HMODAN)
      WRITE OUTPUT TAPE 2, 132, KCOAG, KROUT, XKK, KINDIS, KPSIZ, KUP,
     1 KPRTN, RANGE, MODAN
  132 FORMAT(I8,I14,F17.8,I9,3I13,F16.4,I10)
      IF(INDEX) 170,170,171
  171 WRITE OUTPUT TAPE 2, 172
  172 FORMAT(1H033X54HMEAN  PARTICLE  SIZE  SUMMARY,  COMPLETE  DISTRIBU
     1TION)
      WRITE OUTPUT TAPE 2, 4070
 4070 FORMAT(1H 5X5HITER. 8X9HNO. PARTS 9X4HDIA. 11X4HAREA 10X4HVOL. 9X8
     1HLOG DIA. 7X8HLOG AREA 7X8HLOG VOL.//)
      WRITE OUTPUT TAPE 2,4080, ((SAVEMN(K1,K2),K1=1,8),K2=1,INDEX)
 4080 FORMAT(1H F9.1,F15.1,F18.4,2F15.4,3F15.6)
      IF (JANLIM-1) 170,170,174
  174 WRITE OUTPUT TAPE 2, 173
  173 FORMAT(1H133X55HMEAN  PARTICLE  SIZE  SUMMARY,  TRUNCATED  DISTRIB
     1UTION)
      WRITE OUTPUT TAPE 2, 4070
      WRITE OUTPUT TAPE 2, 4080,((SVPART(K1,K2),K1=1,8),K2=1,INDEX)
  170 CONTIMUE
      CALL EXIT
      END
```

```
*     FORTRAN
*     LIST8
*     LABEL
CXKSUB
      SUBROUTINE XKSUB
      COMMON ALGBAR,ALGSUM,ALOG,ANOSUM,AREA,AREBAR,CTS,DIA,DIABAR,DLGBAR
     1,DLGSUM,DLOG,DNOSUM,I,IMAX,     IPSUM,IVAR,IVAS,J,JCOUNT,L,LINE,LL,
     2      LSAVE,LVOL,M,MAXVOL,N,P,PARSUM,PC,PCC,PLESS,PP,PRCNT,PSUM,PV
     3OL,R,RR,TCRIT,TOL,TVOL,VLGBAR,VLGSUM,VLOG,VNOSUM,VOLBAR,XK,XKK,IND
     4EX,LLINE,SAVEMN,B,MM,NN,NNN,MMM,KCOAG,KPRTN,KPSIZ,KROUT,KUP
     5,JAN,MOD,MODAN,SVPART,JANLIM,TRATIO,PZERO,KINDIS,RANGE,J1,J2
     6,PNOMN,PSQSM,ASQSM,VSQSM,DLSQSM,ALSQSM,VLSQSM,SDPNO,SDDIA,SDAREA,
     7 SDVOL,SDDIAL,SDAREL,SDVOLL,VOLMAX,DSQSM
      DIMENSION ALOG(100),AREA(100),DIA(100),DLOG(100),P(100),PLESS(100)
     1,PP(100),PRCNT(100),PSUM(100),PVOL(100),SAVEMN(8,1000),VLOG(100),
     2XK(1000),SVPART(8,1000)
      KROUT=1
      READ INPUT TAPE 4, 200, XKK
  200 FORMAT (F10.6)
      DO 210 I=1, IMAX
      XK(I)=XKK
  210 CONTINUE
      RETURN
      END
```

```
*     FORTRAN
*     LIST8
*     LABEL
CINDIST
      SUBROUTINE INDIST
      COMMON ALGBAR,ALGSUM,ALOG,ANOSUM,AREA,AREBAR,CTS,DIA,DIABAR,DLGBAR
     1,DLGSUM,DLOG,DNOSUM,I,IMAX,     IPSUM,IVAR,IVAS,J,JCOUNT,L,LINE,LL,
     2      LSAVE,LVOL,M,MAXVOL,N,P,PARSUM,PC,PCC,PLESS,PP,PRCNT,PSUM,PV
     3OL,R,RR,TCRIT,TOL,TVOL,VLGBAR,VLGSUM,VLOG,VNOSUM,VOLBAR,XK,XKK,IND
     4EX,LLINE,SAVEMN,B,MM,NN,NNN,MMM,KCOAG,KPRTN,KPSIZ,KROUT,KUP
     5,JAN,MOD,MODAN,SVPART,JANLIM,TRATIO,PZERO,KINDIS,RANGE,J1,J2
     6,PNOMN,PSQSM,ASQSM,VSQSM,DLSQSM,ALSQSM,VLSQSM,SDPNO,SDDIA,SDAREA,
     7 SDVOL,SDDIAL,SDAREL,SDVOLL,VOLMAX,DSQSM
      DIMENSION ALOG(100),AREA(100),DIA(100),DLOG(100),P(100),PLESS(100)
     1,PP(100),PRCNT(100),PSUM(100),PVOL(100),SAVEMN(8,1000),VLOG(100),
     2XK(1000),SVPART(8,1000)
      READ INPUT TAPE 4, 500, KINDIS
  500 FORMAT(I5)
      IF (KINDIS-2) 505, 506, 507
  505 READ INPUT TAPE 4, 501, (P(M), M=I, LVOL)
  501 FORMAT(7F10.4)
      GO TO 508
  506 READ INPUT TAPE 4, 501, TRATIO, PZERO
      DENOM= 1.0 + TRATIO
      DO 502 M=1, LVOL
      P(M)=(PZERO*TRATIO**(M-1))/(DENOM**(M+1))
  502 CONTINUE
      GO TO 508
  507 CONTINUE
  508 RETURN
      END
```

C-9

```
*     FORTRAN
*     LISTB
*     LABEL
CPARSIZ
      SUBROUTINE PARSIZ
      COMMON ALGBAR,ALGSUM,ALOG,ANOSUM,AREA,AREBAR,CTS,DIA,DIABAR,DLGBAR
     1,DLGSUM,DLOG,DNOSUM,I,IMAX,     IPSUM,IVAR,IVAS,J,JCOUNT,L,LINE,LL,
     2      LSAVE,LVOL,M,MAXVOL,N,P,PARSUM,PC,PCC,PLESS,PP,PRCNT,PSUM,PV
     3OL,R,RR,TCRIT,TOL,TVOL,VLGBAR,VLGSUM,VLOG,VNOSUM,VOLBAR,XK,XKK,IND
     4EX,LLINE,SAVEMN,B,MM,NN,NNN,MMM,KCOAG,KPRTN,KPSIZ,KROUT,KUP
     5,JAN,MOD,MODAN,SVPART,JANLIM,TRATIO,PZERO,KINDIS,RANGE,J1,J2
     6,PNOMN,PSQSM,ASQSM,VSQSM,DLSQSM,ALSQSM,VLSQSM,SDPNO,SDDIA,SDAREA,
     7 SDVOL,SDDIAL,SDAREL,SDVOLL,VOLMAX,DSQSM
      DIMENSION ALOG(100),AREA(100),DIA(100),DLOG(100),P(100),PLESS(100)
     1,PP(100),PRCNT(100),PSUM(100),PVOL(100),SAVEMN(8,1000),VLOG(100),
     2XK(1000),SVPART(8,1000)
      KPSIZ=2
      LINE=0
      WRITE OUTPUT TAPE 2, 302
  302 FORMAT(1H145X31HPARTICLE  SIZE  CHARACTERISTICS)
      WRITE OUTPUT TAPE 2, 303
  303 FORMAT (1H06X6HVOLUME 11X8HDIAMETER 11X4HAREA  9X12HLOG DIAMETER
     17X8HLOG AREA  8X10HLOG VOLUME 7X9HINIT. NO.//)
      DO 300 M=1,MAXVOL
      LINE=LINE+1
      PVOL(M)=M
      DIA(M)=PVOL(M)**0.33333
      AREA(M)=PVOL(M)**0.66667
      DLOG(M)=LOGF(DIA(M))/2.30259
      ALOG(M)=LOGF(AREA(M))/2.30259
      VLOG(M)=LOGF(PVOL(M))/2.30259
      IF (LINE-50) 304, 304, 305
  305 LINE=0
      WRITE OUTPUT TAPE 2, 302
      WRITE OUTPUT TAPE 2, 303
  304 WRITE OUTPUT TAPE 2, 301, PVOL(M),DIA(M),AREA(M),DLOG(M),ALOG(M),V
     1LOG(M),P(M)
  301 FORMAT(1H F12.3,F18.4,F16.4,F18.5,F19.5,F17.5,F16.3)
  300 CONTINUE
      RETURN
      END
```

```
*      FORTRAN
*      LIST8
*      LABEL
CBRAKUP
       SUBROUTINE BRAKUP
       COMMON ALGBAR,ALGSUM,ALOG,ANOSUM,AREA,AREBAR,CTS,DIA,DIABAR,DLGBAR
      1,DLGSUM,DLOG,DNOSUM,I,IMAX,     IPSUM,IVAR,IVAS,J,JCOUNT,L,LINE,LL,
      2      LSAVE,LVOL,M,MAXVOL,N,P,PARSUM,PC,PCC,PLESS,PP,PRCNT,PSUM,PV
      3OL,R,RR,TCRIT,TOL,TVOL,VLGBAR,VLGSUM,VLOG,VNOSUM,VOLBAR,XK,XKK,IND
      4EX,LLINE,SAVEMN,B,MM,NN,NNN,MMM,KCOAG,KPRTN,KPSIZ,KROUT,KUP
      5,JAN,MOD,MODAN,SVPART,JANLIM,TRATIO,PZERO,KINDIS,RANGE,J1,J2
      6,PNOMN,PSQSM,ASQSM,VSQSM,DLSQSM,ALSQSM,VLSQSM,SDPNO,SDDIA,SDAREA,
      7 SDVOL,SDDIAL,SDAREL,SDVOLL,VOLMAX,DSQSM
       DIMENSION ALOG(100),AREA(100),DIA(100),DLOG(100),P(100),PLESS(100)
      1,PP(100),PRCNT(100),PSUM(100),PVOL(100),SAVEMN(8,1000),VLOG(100),
      2XK(1000),SVPART(8,1000)
       IF(KUP-2) 601, 602, 603
   603 IF (KUP-4) 604, 605, 606
   606 CONTINUE
       GO TO 601
   605 CTS= B*XKK*PC*PCC*(DIA(M)+DIA(N))**3
       MM=L/4
       NN=(L-MM)/3
       MMM=(L-(MM+NN))/2
       NNN=L-(MM+NN+MMM)
       PP(M)=PP(M)-CTS
       PP(N)=PP(N)-CTS
       PP(MM)=PP(MM)+CTS
       PP(NN)=PP(NN)+CTS
       PP(NNN)=PP(NNN)+CTS
       PP(MMM)=PP(MMM)+CTS
       GO TO 601
   604 CTS= B*XKK*PC*PCC*(DIA(M)+DIA(N))**3
       MM=L/3
       NN=(L-MM)/2
       NNN=L-(MM+NN)
       PP(M)=PP(M)-CTS
       PP(N)=PP(N)-CTS
       PP(MM)=PP(MM)+CTS
       PP(NN)=PP(NN)+CTS
       PP(NNN)=PP(NNN)+CTS
       GO TO 601
   602 CTS= B*XKK*PC*PCC*(DIA(M)+DIA(N))**3
       MM=L/2
       NN=L-MM
       PP(M)=PP(M)-CTS
       PP(N)=PP(N)-CTS
       PP(MM)=PP(MM)+CTS
       PP(NN)=PP(NN)+CTS
   601 RETURN
       END
```

```
*     FORTRAN
*     LIST8
*     LABEL
CPARTAN
      SUBROUTINE PARTAN
      COMMON ALGBAR,ALGSUM,ALOG,ANOSUM,AREA,AREBAR,CTS,DIA,DIABAR,DLGBAR
     1,DLGSUM,DLOG,DNOSUM,I,IMAX,     IPSUM,IVAR,IVAS,J,JCOUNT,L,LINE,LL,
     2      LSAVE,LVOL,M,MAXVOL,N,P,PARSUM,PC,PCC,PLESS,PP,PRCNT,PSUM,PV
     3OL,R,RR,TCRIT,TOL,TVOL,VLGBAR,VLGSUM,VLOG,VNOSUM,VOLBAR,XK,XKK,IND
     4EX,LLINE,SAVEMN,B,MM,NN,NNN,MMM,KCOAG,KPRTN,KPSIZ,KROUT,KUP
     5,JAN,MOD,MODAN,SVPART,JANLIM,TRATIO,PZERO,KINDIS,RANGE,J1,J2
     6,PNOMN,PSQSM,ASQSM,VSQSM,DLSQSM,ALSQSM,VLSQSM,SDPNO,SDDIA,SDAREA,
     7 SDVOL,SDDIAL,SDAREL,SDVOLL,VOLMAX,DSQSM
      DIMENSION ALOG(100),AREA(100),DIA(100),DLOG(100),P(100),PLESS(100)
     1,PP(100),PRCNT(100),PSUM(100),PVOL(100),SAVEMN(8,1000),VLOG(100),
     2XK(1000),SVPART(8,1000)
      KPRTN=4
      JAN=1
      MOD=1
      INDEX=INDEX+1
  443 ALGSUM=0.0
      ANOSUM=0.0
      DLGSUM=0.0
      DNOSUM=0.0
      PARSUM=0.0
      VLGSUM=0.0
      VNOSUM=0.0
      PSQSM=0.0
      DSQSM=0.0
      ASQSM=0.0
      VSQSM=0.0
      DLSQSM=0.0
      ALSQSM=0.0
      VLSQSM=0.0
      DO 420 M=MOD, MAXVOL
      PARSUM=PARSUM+PP(M)
      PSUM(M)=PARSUM-PP(M)/2.0
  420 CONTINUE
      IPSUM=PARSUM+0.5
      DO 400 M=MOD,MAXVOL
      PRCNT(M)=100.0*PP(M)/PARSUM
      PLESS(M)=100.0*PSUM(M)/PARSUM
      DNOSUM=DNOSUM+DIA(M)*PP(M)
      ANOSUM=ANOSUM+AREA(M)*PP(M)
       VNOSUM=VNOSUM+PVOL(M)*PP(M)
      DLGSUM=DLGSUM+DLOG(M)*PP(M)
      ALGSUM=ALGSUM+ALOG(M)*PP(M)
      VLGSUM=VLGSUM+VLOG(M)*PP(M)
  400 CONTINUE
      DIABAR=DNOSUM/PARSUM
      AREBAR=ANOSUM/PARSUM
      VOLBAR=VNOSUM/PARSUM
      DLGBAR=DLGSUM/PARSUM
      ALGBAR=ALGSUM/PARSUM
      VLGBAR=VLGSUM/PARSUM
      IF(JAN-1) 482,482,483
  482 VOLMAX=MAXVOL
      GO TO 484
  483 VOLMAX=MAXVOL-MODAN+1
  484 PNOMN= PARSUM/VOLMAX
      DO 480 M=MOD, MAXVOL
      PAB= ABSF(PP(M))
      PSQSM=PSQSM+(PP(M)-PNOMN)**2
      DSQSM= DSQSM+((DIA(M)-DIABAR)**2)*PAB
      ASQSM=ASQSM+((AREA(M)-AREBAR)**2)*PAB
      VSQSM=VSQSM+((PVOL(M)-VOLBAR)**2)*PAB
      DLSQSM=DLSQSM+((DLOG(M)-DLGBAR)**2)*PAB
      ALSQSM=ALSQSM+((ALOG(M)-ALGBAR)**2)*PAB
      VLSQSM=VLSQSM+((VLOG(M)-VLGBAR)**2)*PAB
  480 CONTINUE
      IF (PARSUM-1.0) 488,488,487
  488 SDPNO=0.0
      SDDIA=0.0
      SDAREA=0.0
      SDVOL=0.0
      SDDIAL=0.0
      SDAREL=0.0
      SDVOLL=0.0
      GO TO 489
  487 SDPNO= SQRTF(PSQSM/(PARSUM-1.0))
      SDDIA= SQRTF(DSQSM/(PARSUM-1.0))
      SDAREA= SQRTF(ASQSM/(PARSUM-1.0))
      SDVOL= SQRTF(VSQSM/(PARSUM-1.0))
      SDDIAL= SQRTF(DLSQSM/(PARSUM-1.0))
      SDAREL= SQRTF(ALSQSM/(PARSUM-1.0))
      SDVOLL= SQRTF(VLSQSM/(PARSUM-1.0))
  489 IF (JAN-1) 470,470,471
  470 WRITE OUTPUT TAPE 2, 405
  405 FORMAT(1H138X43HITERATION  RESULTS,  COMPLETE  DISTRIBUTION)
      GO TO 4060
  471 WRITE OUTPUT TAPE 2, 472
  472 FORMAT(1H137X44HITERATION  RESULTS,  TRUNCATED  DISTRIBUTION)
 4060 WRITE OUTPUT TAPE 2, 406
  406 FORMAT(1H050X20HMEAN  PARTICLE  SIZE)
      WRITE OUTPUT TAPE 2, 407
  407 FORMAT(1H 4X5HITER. 6X9HNO. PARTS 5X8HMEAN NO.  7X4HDIA. 9X4HAREA
     1 9X4HVOL. 8X8HLOG DIA. 5X8HLOG AREA 5X8HLOG VOL.)
      WRITE OUTPUT TAPE 2,408,I,PARSUM,PNOMN,DIABAR,AREBAR,VOLBAR,DLGBAR
     1,ALGBAR,VLGBAR
  408 FORMAT(1H I9, F16.4, 4F13.4, 3F13.6)
      WRITE OUTPUT TAPE 2,485
  485 FORMAT(1H 50X19HSTANDARD  DEVIATION)
      WRITE OUTPUT TAPE 2, 486, SDPNO,SDDIA, SDAREA,SDVOL,SDDIAL,SDAREL,
     I SDVOLL
  486 FORMAT(1H F38.4, 3F13.4, 3F13.6)
      IF(JAN-1) 450, 450, 451
  450 SAVEMN(1,INDEX)=I
      SAVEMN(2,INDEX)=IPSUM
      SAVEMN(3,INDEX)=DIABAR
      SAVEMN(4,INDEX)=AREBAR
      SAVEMN(5,INDEX)=VOLBAR
      SAVEMN(6,INDEX)=DLGBAR
      SAVEMN(7,INDEX)=ALGBAR
      SAVEMN(8,INDEX)=VLGBAR
      GO TO 460
  451 SVPART(1,INDEX)=I
```

```
      SVPART(2,INDEX)=IPSUM
      SVPART(3,INDEX)=DIABAR
      SVPART(4,INDEX)=AREBAR
      SVPART(5,INDEX)=VOLBAR
      SVPART(6,INDEX)=DLGBAR
      SVPART(7,INDEX)=ALGBAR
      SVPART(8,INDEX)=VLGBAR
  460 WRITE OUTPUT TAPE 2, 409
  409 FORMAT(1H046X28HPARTICLE  SIZE  DISTRIBUTION)
      WRITE OUTPUT TAPE 2, 410
  410 FORMAT(1H034X6HVOLUME 9X6HNUMBER 9X7HPERCENT 6X13HPCT LESS THAN//)
      LLINE=0
      DO 412 M=MOD, MAXVOL
      LLINE=LLINE+1
      IF (LLINE-50) 430,430,431
  431 IF(JAN-1) 433, 433, 434
  433 WRITE OUTPUT TAPE 2, 405
      GO TO 439
  434 WRITE OUTPUT TAPE 2, 472
  439 LLINE=0
      WRITE OUTPUT TAPE 2, 409
      WRITE OUTPUT TAPE 2, 410
  430 CONTINUE
      WRITE OUTPUT TAPE 2, 411, PVOL(M), PP(M),PRCNT(M),PLESS(M)
  411 FORMAT(1H F40.2,F16.4,F15.4,F17.5)
  412 CONTINUE
      JAN=JAN+1
      IF(JAN-JANLIM) 440,440,415
  440 MOD=MODAN
      GO TO 443
  415 J=0
      RETURM
      END
```

PARTICLE SIZE CHARACTERISTICS

VOLUME	DIAMETER	AREA	LOG DIAMETER	LOG AREA	LOG VOLUME	INIT. NO.
1.000	1.0000	1.0000	-0.	-0.	-0.	1000.000
2.000	1.2599	1.5874	0.10034	0.20069	0.30103	0.
3.000	1.4422	2.0801	0.15904	0.31808	0.47712	0.
4.000	1.5874	2.5199	0.20068	0.40137	0.60206	0.
5.000	1.7100	2.9240	0.23299	0.46598	0.69897	0.
6.000	1.8171	3.3019	0.25938	0.51877	0.77815	0.
7.000	1.9129	3.6593	0.28170	0.56340	0.84510	0.
8.000	2.0000	4.0000	0.30103	0.60206	0.90309	0.
9.000	2.0801	4.3268	0.31808	0.63616	0.95424	0.
10.000	2.1544	4.6416	0.33333	0.66667	1.00000	0.
11.000	2.2240	4.9461	0.34713	0.69426	1.04139	0.
12.000	2.2894	5.2415	0.35972	0.71946	1.07918	0.
13.000	2.3513	5.5288	0.37131	0.74263	1.11394	0.
14.000	2.4101	5.8088	0.38204	0.76409	1.14613	0.
15.000	2.4662	6.0823	0.39203	0.78406	1.17609	0.
16.000	2.5198	6.3497	0.40137	0.80275	1.20412	0.
17.000	2.5713	6.6116	0.41014	0.82030	1.23045	0.
18.000	2.6207	6.8684	0.41842	0.83685	1.25527	0.
19.000	2.6684	7.1204	0.42625	0.85250	1.27875	0.
20.000	2.7144	7.3681	0.43367	0.86736	1.30103	0.

```
                              ITERATION  RESULTS,  COMPLETE  DISTRIBUTION
                                               MEAN  PARTICLE  SIZE
ITER.      NO. PARTS      MEAN NO.       DIA.         AREA          VOL.        LOG DIA.       LOG AREA       LOG VOL.
  5         817.0581      40.8529       1.0542       1.1266        1.2239      0.020363       0.040727       0.061091
                                                STANDARD  DEVIATION
                          23.0041       0.1234       0.2948        0.5385      0.045560       0.091121       0.136680
                                           PARTICLE  SIZE  DISTRIBUTION
                            VOLUME         NUMBER         PERCENT       PCT LESS THAN
                              1.00       671.8279         82.2252         41.11262
                              2.00       115.2580         14.1065         89.27846
                              3.00        23.7630          2.9084         97.78587
                              4.00         4.9634          0.6075         99.54379
                              5.00         1.0114          0.1238         99.90942
                              6.00         0.1925          0.0236         99.98309
                              7.00         0.0355          0.0043         99.99704
                              8.00         0.0055          0.0007         99.99955
                              9.00         0.0009          0.0001         99.99994
                             10.00         0.0000          0.0000        100.00000
                             11.00         0.0000          0.0000        100.00000
                             12.00        -0.0000         -0.0000        100.00000
                             13.00         0.0000          0.0000        100.00000
                             14.00        -0.0000         -0.0000        100.00000
                             15.00        -0.0000         -0.0000        100.00000
                             16.00        -0.0000         -0.0000        100.00000
                             17.00        -0.0000         -0.0000        100.00000
                             18.00        -0.0000         -0.0000        100.00000
                             19.00         0.0000          0.0000        100.00000
                             20.00         0.0000          0.0000        100.00000
```

```
                                   ITERATION  RESULTS,  TRUNCATED  DISTRIBUTION
                                                  MEAN  PARTICLE  SIZE
ITER.       NO. PARTS      MEAN NO.       DIA.        AREA          VOL.           LOG DIA.       LOG AREA       LOG VOL.
  5           0.0000        0.0000       2.0294      4.0593        7.9675         0.310020       0.620049       0.930069
                                                STANDARD  DEVIATION
                              0.           0.          0.            0.             0.             0.             0.
                                                PARTICLE  SIZE  DISTRIBUTION

                           VOLUME          NUMBER            PERCENT         PCT LESS THAN

                            11.00          0.0000            333.7701         166.88503
                            12.00         -0.0000           -203.2252         232.15744
                            13.00          0.0000              3.2047         132.14720
                            14.00         -0.0000            -31.1733         118.16289
                            15.00         -0.0000             -0.1578         102.49732
                            16.00         -0.0000             -2.2203         101.30824
                            17.00         -0.0000             -0.0127         100.19172
                            18.00         -0.0000             -0.2844         100.04316
                            19.00          0.0000              0.0009          99.90139
                            20.00          0.0000              0.0982          99.95091
```

```
                                 ITERATION  RESULTS,  COMPLETE  DISTRIBUTION

                                           MEAN  PARTICLE  SIZE
 ITER.     NO. PARTS      MEAN NO.      DIA.        AREA          VOL.        LOG DIA.      LOG AREA      LOG VOL.
   60       180.2805       9.0140      1.5441      2.7529        5.5469      0.157405      0.314815      0.472220
                                           STANDARD  DEVIATION
                           5.2540      0.6089      2.1558        6.1595      0.162152      0.324309      0.486461
                                          PARTICLE  SIZE  DISTRIBUTION

                          VOLUME          NUMBER          PERCENT       PCT LESS THAN
                            1.00          75.2355         41.7324         20.86622
                            2.00          21.1085         11.7087         47.58678
                            3.00          11.4111          6.3296         56.60595
                            4.00           7.7459          4.2966         61.91905
                            5.00           5.8765          3.2597         65.69717
                            6.00           4.7258          2.6214         68.63768
                            7.00           4.0299          2.2353         71.06605
                            8.00           3.5203          1.9527         73.16007
                            9.00           4.1534          2.3039         75.28835
                           10.00           3.1507          1.7477         77.31413
                           11.00           2.9753          1.6504         79.01315
                           12.00           3.8584          2.1402         80.90844
                           13.00           2.8053          1.5561         82.75659
                           14.00           3.0319          1.6818         84.37549
                           15.00           3.0699          1.7028         86.06779
                           16.00           3.2448          1.7998         87.81914
                           17.00           4.2495          2.3572         89.89764
                           18.00           5.0840          2.8200         92.48623
                           19.00           5.4140          3.0031         95.39780
                           20.00           5.5899          3.1007         98.44967
                          ITERATION  RESULTS,  TRUNCATED  DISTRIBUTION
                                                MEAN  PARTICLE  SIZE
ITER.        NO. PARTS      MEAN NO.      DIA.         AREA          VOL.        LOG DIA.      LOG AREA      LOG VOL.
  60           39.3228       3.9323      2.5169        6.3599       16.1312      0.399984      0.799980      1.199964
                                                 STANDARD  DEVIATION
                             0.5256      0.1602        0.7957        2.9726      0.028116      0.056233      0.084349
                                          PARTICLE  SIZE  DISTRIBUTION
                            VOLUME          NUMBER         PERCENT       PCT LESS THAN
                             11.00          2.9753          7.5663          3.78313
                             12.00          3.8584          9.8122         12.47234
                             13.00          2.8053          7.1339         20.94540
                             14.00          3.0319          7.7102         28.36749
                             15.00          3.0699          7.8069         36.12604
                             16.00          3.2448          8.2516         44.15529
                             17.00          4.2495         10.8067         53.68445
                             18.00          5.0840         12.9288         65.55219
                             19.00          5.4140         13.7681         78.90062
                             20.00          5.5899         14.2153         92.89233
```

```
                                              TEST  DATA
 COAG        XKSUB         XKK          INDIST        PARSIZ       BRAKUP        PARTAN        RANGE        MODAN
  5            1       0.00001000         1             2            1             4          2.0000        11

                         MEAN  PARTICLE  SIZE  SUMMARY,  COMPLETE  DISTRIBUTION
 ITER.        NO. PARTS      DIA.           AREA          VOL.        LOG DIA.       LOG AREA       LOG VOL.

   5.0          817.0        1.0542         1.1266        1.2239      0.020363       0.040727       0.061091
  10.0          671.0        1.1085         1.2639        1.4908      0.039395       0.078790       0.118185
  15.0          554.0        1.1623         1.4115        1.8054      0.056995       0.113992       0.170987
  20.0          461.0        1.2145         1.5666        2.1677      0.072972       0.145947       0.218920
  30.0          333.0        1.3114         1.8858        2.9999      0.100025       0.200054       0.300079
  40.0          257.0        1.3980         2.1976        3.8868      0.122137       0.244277       0.366414
  50.0          211.0        1.4752         2.4883        4.7479      0.140978       0.281961       0.422939
  60.0          180.0        1.5441         2.7529        5.5469      0.157405       0.314815       0.472220
  80.0          144.0        1.6601         3.2049        6.9287      0.184741       0.369488       0.554229
 100.0          124.0        1.7530         3.5687        8.0488      0.206504       0.413015       0.619519


                         MEAN  PARTICLE  SIZE  SUMMARY,  TRUNCATED  DISTRIBUTION
 ITER.        NO. PARTS      DIA.           AREA          VOL.        LOG DIA.       LOG AREA       LOG VOL.

   5.0            0.         2.0294         4.0593        7.9675      0.310020       0.620049       0.930069
  10.0            0.         2.2666         5.1415       11.6721      0.355208       0.710426       1.065634
  15.0            1.0        2.3099         5.3462       12.3988      0.363184       0.726379       1.089563
  20.0            5.0        2.3528         5.5527       13.1460      0.370945       0.741902       1.112847
  30.0           17.0        2.4217         5.8889       14.3795      0.383230       0.766471       1.149700
  40.0           28.0        2.4666         6.1105       15.2008      0.391170       0.782351       1.173520
  50.0           35.0        2.4963         6.2574       15.7481      0.396376       0.792764       1.189140
  60.0           39.0        2.5169         6.3599       16.1312      0.399984       0.799980       1.199964
  80.0           45.0        2.5434         6.4922       16.6275      0.404613       0.809238       1.213851
 100.0           48.0        2.5597         6.5735       16.9334      0.407442       0.814897       1.222339
```